

A PARAMETRIC STUDY ON HYDROTHERMAL SYNTHESIS OF  
ZINC OXIDE NANOWIRES WITH VARIOUS ZINC SALTS

A THESIS SUBMITTED TO  
THE GRADUATE SCHOOL OF NATURAL AND APPLIED  
SCIENCES  
OF  
MIDDLE EAST TECHNICAL UNIVERSITY

BY

MEHMET CAN AKGÜN

IN PARTIAL FULFILLMENT OF THE REQUIREMENTS  
FOR  
THE DEGREE OF MASTER OF SCIENCE  
IN  
MICRO AND NANOTECHNOLOGY

FEBRUARY 2012

Approval of the thesis:

**A PARAMETRIC STUDY ON HYDROTHERMAL SYNTHESIS OF  
ZINC OXIDE NANOWIRES WITH VARIOUS ZINC SALTS**

submitted by **MEHMET CAN AKGÜN** in partial fulfillment of the requirements  
for the degree of **Master of Science in Micro and Nanotechnology Program,**  
**Middle East Technical University** by,

Prof. Dr. Canan Özgen \_\_\_\_\_  
Dean, Graduate School of **Natural and Applied Sciences**

Prof. Dr. Mürvet Volkan \_\_\_\_\_  
Head of Program, **Micro and Nanotechnology**

Assist. Prof. Dr. Hüsnü Emrah Ünal \_\_\_\_\_  
Supervisor, **Metallurgical and Materials Eng. Dept., METU**

Prof. Dr. Raşit Turan \_\_\_\_\_  
Co-Supervisor, **Physics Dept., METU**

**Examining Committee Members:**

Prof. Dr. İshak Karakaya \_\_\_\_\_  
Department of Metallurgical and Materials Engineering, METU

Assist. Prof. Dr. Hüsnü Emrah Ünal \_\_\_\_\_  
Department of Metallurgical and Materials Engineering, METU

Prof. Dr. Raşit Turan \_\_\_\_\_  
Department of Physics, METU

Assoc. Prof. Dr. Caner Durucan \_\_\_\_\_  
Department of Metallurgical and Materials Engineering, METU

Assist. Prof. Dr. Eren Kalay \_\_\_\_\_  
Department of Metallurgical and Materials Engineering, METU

Date: \_\_\_\_\_

**I hereby declare that all information in this document has been obtained and presented in accordance with academic rules and ethical conduct. I also declare that, as required by these rules and conduct, I have fully cited and referenced all material and results that are not original to this work.**

Name, Last name: Mehmet Can AKGÜN  
Signature :

## **ABSTRACT**

# **A PARAMETRIC STUDY ON HYDROTHERMAL SYNTHESIS OF ZINC OXIDE NANOWIRES WITH VARIOUS ZINC SALTS**

AKGÜN, Mehmet Can

Master of Science, Micro and Nanotechnology Program

Supervisor: Assist. Prof. Dr. Hüsnü Emrah ÜNALAN

Co-Supervisor: Prof. Dr. Raşit TURAN

February 2012, 74 Pages

ZnO is a promising semiconducting material for manufacturing optoelectronic devices. Its most important properties are its wide and direct band gap and its high electron-hole binding energy. Synthesis of ZnO in bulk and thin film form has been investigated intensively over recent decades. Likewise, nanomaterials have been in the point of focus for their different properties compared to their bulk form. The vastly increased ratio of surface area to volume and change in electronic properties with great reduction in particle size enable improved performance in conventional applications where their bulk counterparts have been used for decades. As a result of this trend, research on synthesis of ZnO nanowires and their incorporation in prototype optoelectronic devices has been intensive in recent years. Therefore, synthesis of ZnO nanowires in a cost effective way and understanding the factors influencing the ZnO nanowire growth is essential for contribution to ongoing research.

In this thesis, hydrothermal synthesis of ZnO nanowires, which is a solution based method enabling vertically aligned ZnO nanowire array fabrication over large areas, is investigated. In the first part of this thesis, the effect of using various zinc salts as zinc sources on ZnO nanowires is investigated by monitoring pH, temperature and light transmittance of growth solutions. In the second part, a detailed parametric study on the use of zinc acetate dihydrate salt is provided with regard to the existence of its unique properties compared to other two zinc salts. The effect of growth time, temperature, ratio of concentration of precursor chemicals and precursor chemical concentrations is investigated. The results show that hydrothermal synthesis method could replace the conventional ZnO nanowire fabrication methods. It was shown that specific nanowire lengths for any application can be obtained simply by adjusting the parameters of hydrothermal growth system.

**Keywords:** Hydrothermal synthesis, ZnO nanowires

## ÖZ

# ÇİNKO OKSİT NANOTELLERİN ÇEŞİTLİ TUZLAR İLE SENTEZLENMESİ ÜZERİNE PARAMETRİK ÇALIŞMA

AKGÜN, Mehmet Can

Master of Science, Micro and Nanotechnology Program

Tez Yöneticisi: Yrd. Doç. Dr. Hüsnü Emrah ÜNALAN

Ortak-Tez Yöneticisi: Prof. Dr. Raşit TURAN

Şubat 2012, 74 Sayfa

Çinko oksit optoelektronik cihazların üretilmesi için gelecek vadede bir yarıiletken malzemedir. En önemli özellikleri arasında geniş ve doğrudan bant aralığı ve yüksek elektron-boşluk çifti bağlanma enerjisi yer alır. Çinko oksitin yığın ve ince film halinde sentezi son yıllarda yoğun bir şekilde araştırılmıştır. Buna benzer olarak, nanomalzemelerde yığın durumundaki hallerinden farklı olan özellikleri ile araştırmaların odak noktasında bulunmaktadır. Yüzey alanlarının hacimlerine olan oranlarının yüksek olması ve elektronik özelliklerindeki değişim, yıllardır yığın hallerinin kullanıldığı uygulamalara kıyasla yüksek performansa olanak vermektedir. Bunun sonucu olarak, çinko oksit nanotellerin üretimi ve prototip optoelektronik aygıtlara dahil edilmesi ile ilgili araştırmalar son yıllarda yoğunlaşmıştır. Bundan dolayı, çinko oksit nanotellerin düşük maliyetli bir yolla üretilmesi ve çinko oksit nanotellerin büyümesini etkileyen faktörlerin anlaşılması devam eden araştırmalara katkı sağlanması açısından önemlidir.

Bu tezde, dikey olarak yönelmiş çinko oksit nanotel dizilerinin geniş alanlar üzerinde üretilmesine olanak sağlayan, çözelti bazlı bir yöntem olan çinko oksit nanotellerin hidrotermal metod yöntemiyle üretilmesi incelenmiştir. Tezin ilk kısmında, farklı çinko tuzlarının çinko kaynakları olarak kullanımının çinko oksit nanoteller

zerindeki etkisi; bytme zeltilerinin pH, scaklık ve k geirgenlięinin izlenmesi ile incelenmitir. İkinci kısımda, dięer tuzlara kıyasla kendine zg zelliklerinin bulunmasından dolayı inko asetat dihidrat tuzunun kullanımının etkisi ile ilgili parametrik bir alıma yapılmıtır. Bytme sresi, scaklık, ncl kimyasalların deriimlerinin oranları ve ncl kimyasal deriimlerinin etkisi incelenmitir. Sonular, hidrotermal retim ynteminin konvansiyonel inko oksit nanotel retim yntemlerinin yerine geebileceęini gstermitir. Hidrotermal bytme sisteminin parametrelerinin ayarlanmasıyla herhangi bir uygulama iin belirli nanotel uzunluklarının elde edilebileceęi gsterilmitir.

***Anahtar Kelimeler:*** Hidrotermal retim, inko oksit nanoteller

*To My Family...*



## ACKNOWLEDGEMENTS

This thesis is an interdisciplinary work between Micro and Nanotechnology and Metallurgical and Materials Engineering in METU, and financed by Scientific and Technological Research Council of Turkey (TUBITAK) under Grant No. 109M084 and the Distinguished Young Scientist Award of the Turkish Academy of Sciences (TUBA).

I would like to thank my advisor Assist. Prof. Dr. Hüsnu Emrah Ünalan for his support and guidance throughout the whole time I have worked on this project. I would like to thank Hülya Yalçın, Serkan Yılmaz, Saffet Ayık and Assist. Prof. Dr. Eren Kalay for spending infinite hours of SEM / TEM sessions and Hakan Yavaş and Tümerkan Kesim for their help in UV-VIS measurement sessions.

I owe my deepest gratitude to my lab-mates and dearest friends Şahin Coşkun, Ayşegül Afal, Elif Selen Ateş, Burcu Aksoy and Şeyda Küçükyıldız for their infinite support, patience and kindness. I also appreciate the great moral support from Mustafa Kulakçı, Aytaç Çelik, Halil İbrahim Yavuz, Murat Güneş, İsmail Seçkin Çardaklı, Ali Arda Özkenter and all my friends in my department who have helped and supported me all along.

## TABLE OF CONTENTS

ABSTRACT .....	IV
ÖZ .....	VI
ACKNOWLEDGEMENTS .....	IX
LIST OF FIGURES .....	XII

### CHAPTERS

1. INTRODUCTION.....	1
2. ZnO NANOWIRES; THEIR PROPERTIES, USES AND SYNTHESIS METHODS .....	3
2.1. Current Status of Zinc Oxide.....	3
2.2. Features of Nanomaterials .....	3
2.3. Properties of ZnO Nanowires .....	5
2.4. Uses of ZnO Nanowires .....	6
2.4.1. Light Emitting Diodes (LEDs) .....	6
2.4.2. Nanolasers.....	8
2.4.3. Hydrophobic Surfaces .....	10
2.4.4. Solar Cells.....	10
2.4.5. Field Effect Transistors.....	13
2.4.6. Gas Sensors.....	14
2.4.7. Piezoelectrics .....	16
2.5. Conventional Synthesis Methods for ZnO Structures .....	17
2.5.1. Synthesis of Bulk ZnO Crystals .....	17
2.5.2. Deposition of ZnO Thin-Films .....	18
2.6. Synthesis Methods of ZnO Nanowires.....	18
2.6.1. Vapor Deposition Methods.....	19
2.6.2. Vapor-Liquid-Solid (VLS) Mechanism.....	20
2.6.3. Template Assisted Fabrication .....	21
2.6.4. Solution Based Synthesis.....	23

3. HYDROTHERMAL SYNTHESIS OF ZnO NANOWIRES WITH THREE COMMON ZINC SALTS.....	25
3.1. History and Development of Hydrothermal Synthesis of ZnO Nanowires.....	25
3.2. ZnO Nanowire Growth Reactions and Mechanism.....	26
3.3. Experimental Details .....	28
3.4. ZnO Nanowire Characterization Methods.....	32
3.4.1. Scanning Electron Microscopy (SEM).....	32
3.4.2. Transmission Electron Microscopy (TEM) .....	32
3.4.3 XRD Measurements.....	32
3.4.4. UV-VIS Spectroscopy .....	32
3.4.5. Photoluminescence Measurements .....	33
3.4.6. Thermogravimetric Analysis (TGA) .....	34
3.5. Hydrothermal Synthesis of ZnO Nanowires with Conventional Heating .....	35
3.5.1. Zinc Acetate Dihydrate as Zinc Source .....	35
3.5.2. Zinc Nitrate Hexahydrate as Zinc Source.....	37
3.5.3 Zinc Chloride as Zinc Source .....	40
3.5.4 Comparison of Zinc Salts Used in Hydrothermal Method .....	44
3.6. Hydrothermal Synthesis of ZnO Nanowires with Microwave Heating .....	47
3.6.1. Microwave Heating with Annealed Substrates.....	47
3.6.2. Microwave Heating with Non-annealed Substrates .....	49
3.6.3. Comparison of Microwave Heating with Conventional Heating .....	51
4. DETERMINATION of HYDROTHERMAL GROWTH PARAMETERS USING ZINC ACETATE DIHYDRATE SALT .....	52
4.1. Introduction .....	52
4.2. Experimental Details .....	52
4.3. Characterization of Nanowires .....	53
4.4. Investigation of ZnO Nanowire Hydrothermal Growth Parameters .....	57
4.4.1. Effect of the Time .....	57
4.4.2. Effect of the Temperature .....	59
4.4.3. Effect of the Concentration Ratios on the Growth Process .....	61
4.4.4. Effect of the Solution Concentration on the Growth Process.....	64
5. CONCLUSIONS AND FUTURE RECOMMENDATIONS .....	67
5.1. Conclusions .....	67
5.2. Future Work.....	68
REFERENCES.....	69

## LIST OF FIGURES

Figure 1.1. Fluorescence emission in different colors with UV illumination (top row) and ambient illumination (bottom row) with respect to the variation in the size of cadmium selenide quantum dots [2]... ..	4
Figure 1.2. Stick and ball representation of ZnO structures. The shaded gray and black spheres denote Zn and O atoms, respectively. ....	5
Figure 1.3. A schema the showing operating principle of a LED.....	7
Figure 1.4. Schematics of (a) ZnO nanowire LEDs with heterojunctions (the interface that occurs between dissimilar semiconductors) and (b) ZnO nanowire LEDs with homojunctions (a semiconductor interface that occurs between layers of similar semiconductor material which are doped with different elements). ....	8
Figure 1.5. (a) Emission spectra from nanowire arrays below (line a) and above (line b and inset) the lasing threshold. The pump power for these spectra are 20, 100, and 150 kW/cm <sup>2</sup> , respectively. The spectra are offset for easy comparison. (b) Integrated emission intensity from nanowires as a function of optical pumping energy intensity. (c) Schematic illustration of a nanowire as a resonance cavity with two naturally faceted hexagonal end faces acting as reflecting mirrors [12].....	9
Figure 1.6. Hydrophobic behavior of cotton fabric with ZnO nanowires. [13]. ....	10
Figure 1.7. (a) Schematic of a dye-sensitized solar cell with ZnO nanowires. (b) Comparative performance of nanowire and nanoparticle cells. [16] .....	12
Figure 1.8. 45° tilted SEM image of fabricated ZnO nanowire FET with self-aligned gate electrodes and nanosize air gaps. Scale bar is 2.5 μm. [17].....	13
Figure 1.9. (a) Output characteristics of ZnO nanowire FET. The gate voltage range is from -2 to 1.0 V. (b) Transfer characteristic of the device with 0.8 V of source-	

drain voltage. Insert is transconductance curve of the device. The saturation value is 3.06 $\mu$ S. [17].....	14
Figure 1.10. (a) Cross-sectional view of the ultrathin (5 $\mu$ m) silicon on insulator (SOI) micro-hotplate and the ceramic metal oxide semiconductor (CMOS) electronic cells. (b) An optical microscope picture of the fabricated micro hotplate with interdigitated electrode. (c) Response of the ZnO NWs measured at different humidities (3000 ppm, 4500 ppm, 6570ppm and 9853 ppm). [19]. .....	15
Figure 1.11. Schematic of a piezoelectric nanogenerator made of a ZnO nanowire working with vibrations caused by atomic force microscope tip [23]. .....	16
Figure 1.12. Corresponding output voltage image of the ZnO NW arrays. Most of the voltage peaks are ~6 to 9 mV in height [22]. .....	17
Figure 1.13. ZnO nanowire fabrication methods. ....	19
Figure 1.14. Schematic sketch of a CVD apparatus used for ZnO nanowire synthesis [28]. .....	20
Figure 1.15. Schematic diagram of the VLS mechanism [28]. .....	21
Figure 1.16. (a) Thermal Silicon dioxide(SiO <sub>2</sub> ) deposition, (b) SiO <sub>2</sub> patterned and etched using reactive ion etching (RIE), (c) ZnO deposition with filtered cathodic vacuum arc (FCVA) method, (d) ZnO nanowire formed at the spacer after RIE etch, (e) Optical image of ZnO nanowires formed at the SiO <sub>2</sub> spacer and (f) optical image of array of ZnO nanowires [51]. .....	22
Figure 1.17. SEM images of ZnO nanowire arrays deposited on silicon substrate with applied potentials of 0 V for 8 h (a) and -1.2 V for 2 h. (b) ZnO nanocrystals which have a diameter of 10 nm were used as seeds for (a); the growth in (b) was unseeded [48]. .....	24
Figure 2.1. Schematic representation of an individual ZnO nanowire with Zn-terminated surface. ....	28
Figure 2.2. Photograph of the hydrothermal growth setup used in experiments. ....	30

Figure 2.3. Change of the weight of zinc acetate dihydrate compound temperature obtained from thermogravimetric analysis. ....	31
Figure 2.4. Schematic of UV-VIS spectroscopy system.....	33
Figure 2.5. Schematic of photoluminescence measurement system.....	34
Figure 2.6. X-Ray diffraction pattern for ZnO nanowires grown on silicon substrate in an equimolar 0.02M solution of zinc acetate dihydrate and HMTA for 120 minutes. ....	35
Figure 2.7. Cross-sectional SEM images of ZnO nanowires that are grown for (a) 30, (b) 60, (d) 120, (e) 150 and (f)180 minutes. All scales are the same. Magnifications are 40000x.....	36
Figure 2.8. Variation of diameter and length of nanowires with growth time using zinc acetate dihydrate salt. Lines are for visual aid. ....	37
Figure 2.9. X-Ray diffraction pattern for ZnO nanowires grown on silicon substrates within an equimolar 0.02 M zinc nitrate hexahydrate and HMTA solution for 120 minutes. ....	38
Figure 2.10. Cross-sectional SEM images of ZnO nanowires that are grown for (a) 30, (b) 60, (c) 90, (d) 120, (e) 150 and (f) 180 minutes. All scales are the same. Magnifications are 40000x.....	39
Figure 2.11. Variation of diameter and length of nanowires with growth time using zinc nitrate hexahydrate salt. Lines are for visual aid.....	40
Figure 2.12. X-Ray diffraction pattern for ZnO nanowires grown on silicon substrate in an equimolar 0.02M zinc chloride and HMTA solution for 120 minutes. ....	41
Figure 2.13. Cross-sectional SEM images of ZnO nanowires that are grown for (a) 30, (b) 60, (c) 90, (d) 120, (e) 150 and (f) 180 minutes. All scales are the same. Magnifications are 40000x.....	42

Figure 2.14. Variation of diameter and length of nanowires with growth time using zinc chloride salt. Bar charts for 30, 60 and 180 minutes have not been drawn since nanowire features have not been observed.....	43
Figure 2.15. Variation of the temperature of the growth solutions with time.....	44
Figure 2.16. Variation of the pH of the growth solutions with time.....	45
Figure 2.17. Variation of the transmittance of each growth solution with time containing different zinc salts. ....	46
Figure 2.17. Variation of length and diameter of ZnO nanowires grown with different zinc salts.....	47
Figure 2.18. Cross-sectional SEM images of the annealed samples grown with (a) zinc acetate dihydrate salt, (c) zinc chloride salt, (e) zinc nitrate hexahydrate salt. Top view SEM images of the samples grown with (b) zinc acetate dihydrate salt, (d) zinc chloride salt and (f) zinc nitrate hexahydrate salt. Magnifications are 40000x..	48
Figure 2.19. Variation of length and diameter of ZnO nanowires grown with different salts using non-annealed substrates.....	49
Figure 2.20. Cross-sectional SEM images of the non-annealed samples grown with (a) zinc acetate dihydrate, (c) zinc chloride and (e) zinc nitrate hexahydrate salt. Top view SEM images of the samples grown with (b) zinc acetate dihydrate (d) zinc chloride and (f) zinc nitrate hexahydrate salt. Magnifications are 40000x.....	50
Figure 3.1. XRD spectrum from ZnO nanowires grown on silicon substrates.....	54
Figure 3.2. UV-VIS transmission pattern of ZnO nanowires grown on quartz substrates. Inset shows the Tauc plot showing the change in $(\alpha h\nu)^2$ with respect to energy.....	54
Figure 3.3. Photoluminescence spectra from ZnO nanowires grown on silicon substrates.....	55
Figure 3.4. Bright Field TEM image showing a group of ZnO nanowires at relatively low magnification. ....	55

Figure 3.5. Bright field TEM image and corresponding SAED pattern (inset) taken from single ZnO nanowire. ....	56
Figure 3.6. High resolution TEM image of a single ZnO nanowire showing the lattice fringes along the [0001] growth direction.....	56
Figure 3.7. Cross-sectional SEM images of ZnO nanowires that are grown for (a) 40, (b) 80, (c) 160 and (d) 180 minutes. Magnifications are 40000x. ....	58
Figure 3.8. Variation of the diameter and length of ZnO nanowires with reaction time. Inset shows the variation of aspect ratio of the same samples. Lines are for visual aid. ....	59
Figure 3.9 Cross-sectional SEM images of ZnO nanowires that are grown at (a) 50°C, (b) 60°C, (c) 70°C, (d) 80°C, (e) 90°C and (f) 100°C. Magnifications are 40000x.....	60
Figure 3.10. Variation of diameter and length of ZnO nanowires with temperature. Inset shows the aspect ratio of the samples. Lines are for visual aid.....	61
Figure 3.11. Graph showing the effect of different solution concentration ratios of HMTA and zinc acetate hexahydrate on the diameter and length of ZnO nanowires. Lines are for visual aid.....	62
Figure 3.12. Cross-sectional SEM images of ZnO nanowires grown with solution concentration ratios of ([HMTA]/[Zinc Acetate Dihydrate]) (a) 3:1, (b) 2:1, (c) 1:1, (d) 1:2 and (e) 1:3. Magnifications are 40000x.....	63
Figure 3.13. Cross-sectional SEM images of ZnO nanowires grown in solutions for 180 minutes containing (a) 0.01 M, (b) 0.02 M, (c) 0.03 M, (d) 0.04 M, (e) 0.05 M, and (f) 0.1 M. Inset shows top view SEM images of the samples grown at indicated concentrations. Magnifications are 40000x. ....	65
Figure 3.14. Graph showing the effect of different equimolar solution concentrations of HMTA and zinc acetate hexahydrate on the diameter and length of ZnO nanowires. Lines are for visual aid. ....	66



# CHAPTER 1

## INTRODUCTION

Nanomaterials have been the point of interest for their novel properties over their bulk form. The vastly increased ratio of surface area to volume and change in electronic properties with great reduction in particle size enable improved performance in conventional applications where their bulk counterparts have been used for decades. Recent applications of these materials in prototypes of solar cells, transistors, sensors, batteries and catalyzers have brought great performance to these devices so that they are expected to be widely available in the market in the future with advancements in their production thanks to progress in synthesis of these nanomaterials and they are expected to dominate the market over their counterparts made of materials in bulk form.

Nanomaterials have tremendous economic potential; so great emphasis has been given to research in their synthesis, characterization and applications. In our country, a great portion of academic research has been done in these fields recently and utilization of these materials in industry has just begun and it's expected to rise in the coming years. ZnO is a semiconducting material with a wide band gap and high electron mobility. Recently, nanowire form of ZnO has drawn great attention to be embedded in prototype light emitting diodes, solar cells and piezoelectric devices. As a result; improving synthesis methods and understanding the factors that influence the properties of ZnO during the synthesis has drawn a lot of attention. In this thesis, the effect of the use of different zinc sources in hydrothermal method has been studied and ZnO nanowires were characterized with different instruments available in METU. With this thesis, our aims were;

- a) Understand the factors influencing the growth of ZnO nanowires through hydrothermal method.
- b) Gain experience about production and characterization of ZnO nanowires.

This thesis is composed of five chapters. First chapter gives an introduction about the thesis.

Second one gives an explanation on the general properties of ZnO nanowires, their uses in emerging applications and their synthesis methods.

Third chapter consists of a detailed study on the hydrothermal synthesis of ZnO nanowires with three different zinc salts. Two different heating methods have been explored. Nanowire characterization has been made.

Fourth chapter consists of a parametric study for hydrothermal synthesis of ZnO nanowires with zinc acetate dihydrate salt as zinc source. Nanowire characterization has also been made.

Fifth chapter includes conclusions of is thesis and future work.

## **CHAPTER 2**

### **ZnO NANOWIRES; THEIR PROPERTIES, USES AND SYNTHESIS METHODS**

#### **2.1. Current Status of Zinc Oxide**

ZnO is a material in high demand, which is used in many products as an additive. Its powder is widely used as an additive into the plastics, ceramics, glass, cement, rubber, lubricants, paints, ointments, adhesives, sealants, pigments, foods, batteries, ferrites, fire retardants, and first aid tapes.

Due to its distinctive properties such like good transparency, high electron mobility, wide bandgap and strong room-temperature luminescence, its use in optoelectronic applications is also gaining momentum. Energy saving or heat protecting windows, transparent electrodes in liquid-crystal displays and applications of ZnO as active component in light emitting diodes (LEDs) component and thin film transistors (TFTs) are only a few applications where it is used either in thin film or bulk form.

#### **2.2. Features of Nanomaterials**

Nanomaterials have enhanced properties compared to their bulk counterparts. Conventional materials have grain sizes ranging from few microns to several millimeters and contain several billion atoms each. Nanometer sized grains contain only about 900 atoms each. As the grain size decreases, there is a significant increase in the volume fraction of grain boundaries or interfaces. This characteristic strongly influence the chemical and physical properties of the material. As an example, nanostructured ceramics are tougher and stronger than the coarse grained ceramics. Additionally, nanophase metals exhibit significant increases in yield strength and

elastic modulus. It has also been shown that other properties (such as electrical, optical, magnetic) are influenced by the fine grained structure of these materials. The enhanced optical and electrical properties of nanomaterials emerge from the quantum confinement effect. Quantum confinement is the trapping of charge carriers in a small enough space, so that their quantum (wave-like) behavior dominates over their classical (particle-like) behavior. For a semiconducting material, the effective band gap of nanomaterials increases with decreasing particle size due to quantization of discrete electronic states. For instance, different colors can be seen depending on the size of the gold nanoparticles. Likewise, cadmium selenide quantum dots have fluorescence emission of light in different colors depending on their particle size, as shown in Figure 1.1.

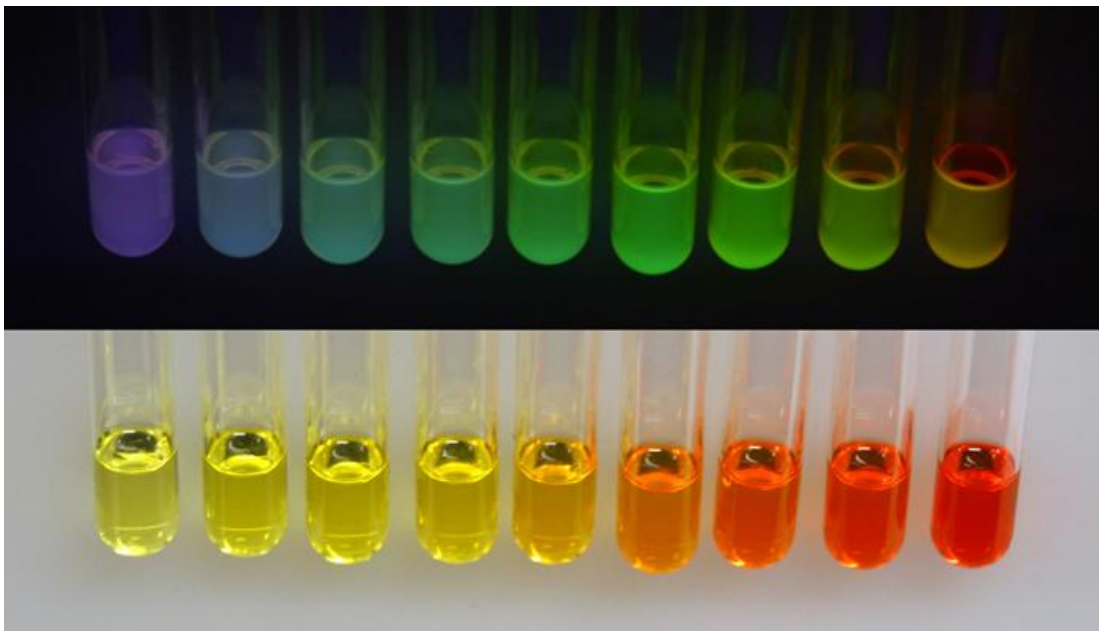


**Figure 2.1.** Fluorescence emission in different colors with UV illumination (top row) and ambient illumination (bottom row) with respect to the variation in the size of cadmium selenide quantum dots [2].

Magnetic properties of nanomaterials are also different than their bulk form. Superparamagnetism is a phenomenon that magnetic materials may exhibit a behavior similar to paramagnetism in which even at temperatures below the Curie or the Néel temperature. As a small length-scale phenomenon, the energy required to change the direction of the magnetic moment of a domain is comparable to the ambient thermal energy. At this point, the rate at which the domains will randomly

reverse direction becomes significant. Superparamagnetic behavior is observed when grain size of a material is in between 2 and 10 nanometers.

### 2.3. Properties of ZnO Nanowires

ZnO is a group II-VI compound semiconductor which can crystallize in hexagonal zinc-wurtzite structure, cubic zinc blende or cubic rock salt, in where each anion is surrounded by four cations at the corners of a tetrahedron as shown in Figure 1.2. Thermodynamically stable phase is zinc-wurtzite at ambient conditions. ZnO has a direct wide band gap of 3.3 eV at 300K which is very close to that of gallium nitride (GaN), another wide-band gap semiconductor ( $E_g \sim 3.4$  eV at 300K). GaN is widely used for the production of green, blue and white light emitting devices. ZnO can be used as a valid replacement for this material due to its abundancy, large exciton binding energy ( $\sim 60$  meV), simpler and more cost-effective crystal-growth methods compared to that of GaN. Simple and cost-effective crystal growth methods do also exist for the nanowire form of ZnO. In such crystal defects are much lower as compared to the bulk form. As a result, optoelectronic applications of ZnO nanowires have been reported by many researchers, which will be explained next.

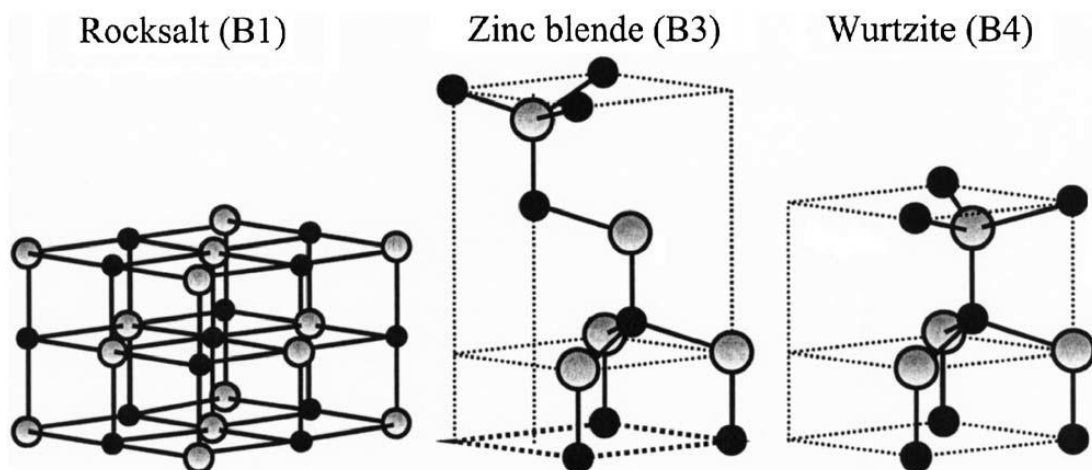


**Figure 1.2.** Stick and ball representation of ZnO structures. The shaded gray and black spheres denote Zn and O atoms, respectively.

## **2.4. Uses of ZnO Nanowires**

### **2.4.1. Light Emitting Diodes (LEDs)**

Lighting industry has a big challenge of meeting the demand of customers and society. 25% of all electricity is used for lighting in the world. Due to the environmental concerns, energy consumption must be reduced at all industrial and human activities. In lighting industry, incandescent light bulbs are being replaced with fluorescent light bulbs due their lower energy consumption. However, fluorescent light bulbs contain mercury and therefore, need to be disposed properly to avoid the environmental contamination. Solid state lighting technology is the next step for having environmentally friendly and low energy consuming lighting. LEDs seem to solve these issues, yet they have higher cost than fluorescent light bulbs. GaN is the main semiconductor material for the use in LEDs so far. Due to its remarkable optoelectronic properties, ZnO is a reliable replacement for LEDs made of bulk GaN crystals. ZnO nanowires have many advantages over GaN. First of all, manufacturing ZnO nanowires are 8-10 times cheaper compared to high-quality GaN bulk crystals due to its easy to implement manufacturing methods. Nanowire form of ZnO contains less crystallographic defects attributed to the single crystalline nature of the nanowires, leading to lower internal reflections, compared to its bulk counterpart. In addition to this ZnO nanowires have no grain boundaries.

LEDs are made of semiconducting material doped with impurities to form a p-n junction. Electrons and holes flow into the junction from n-side and p-side, respectively. Energy is emitted in the form of a photon, when an electron recombines with a hole and falls into a lower energy level, as shown in Figure 1.3.

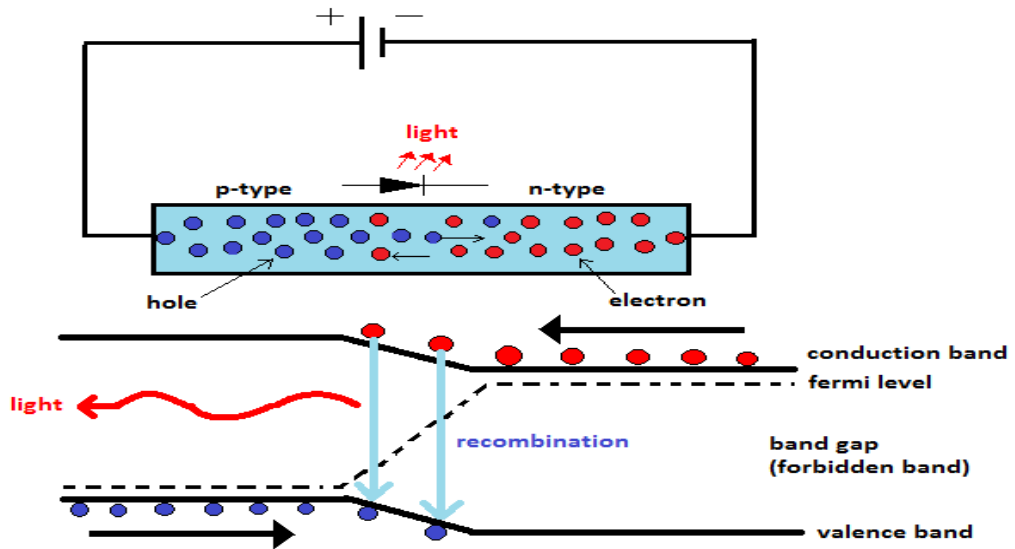


**Figure 1.3.** A schema the showing operating principle of a LED.

n-type ZnO nanowires can be synthesized easily, since making vacant O sites in the crystal structure has no difficulty. However, synthesis of p-type ZnO nanowires has problems due to low solubility of dopants in the lattice. p-type doping of ZnO necessitates group I elements substituting for Zn sites or group V elements substituting for O sites. Though it was reported that LEDs made of p-type and n-type ZnO nanowires was successful, having a detectable illumination requires high operating voltages [4]. So, studies are intensified on fabricating LEDs with n-type ZnO nanowires and p-type semiconducting polymers forming heterojunctions [8,9,10,11] as shown in Figure 1.4 (a), rather than developing LEDs with homojunctions, as shown in Figure 1.4 (b).

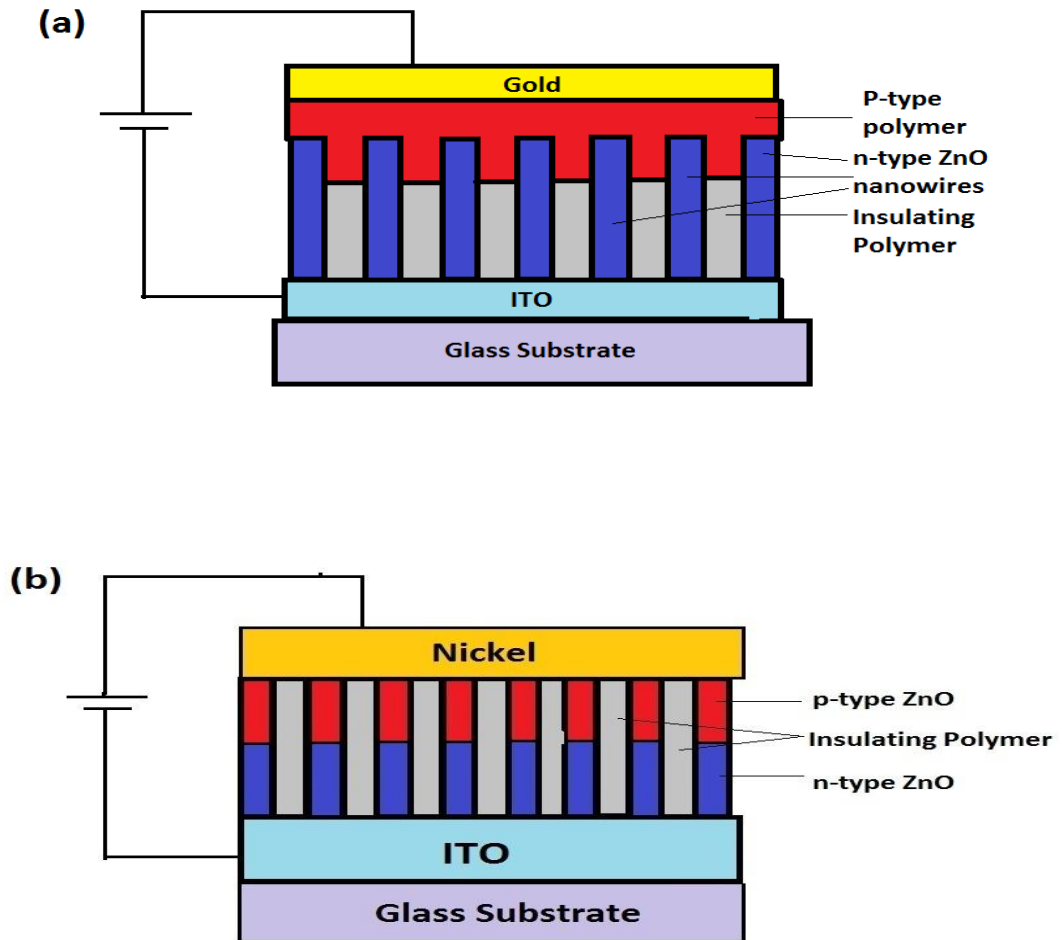


**Figure 2.4.** Schematics of (a) ZnO nanowire LEDs with heterojunctions (the interface that occurs between dissimilar semiconductors) and (b) ZnO nanowire LEDs with homojunctions (a semiconductor interface that occurs between layers of similar semiconductor material which are doped with different elements).

#### 2.4.2. Nanolasers

ZnO nanowires also lie in the field of interest of UV nanolasers. For having optical gain that is sufficient enough for lasing action in an electron-hole plasma (EHP) process, a high carrier concentration is essential. A more efficient radiative process in semiconductors is excitonic recombination. ZnO's exciton binding energy (~60 meV) compared to other alternate materials such as ZnSe (22 meV) and GaN (25 meV); makes it a viable material for short wavelength nanolaser devices. Also nanowire form enhances radiative recombination due to carrier confinement. In a



study, a device constituting of ZnO nanowires were synthesized with a vapor phase transport process, showed promising luminescence decay of 350 picoseconds compared to luminescence decay of 200 picoseconds of ZnO thin films [12]. Figure 1.5 shows the emission spectra from ZnO nanowire arrays on which 266 nm laser beam is focused. Optical pumping is demonstrated instead of electrical pumping since there is no p-n junction in ZnO nanowires. Base and tip of the ZnO nanowires act as cavities for stimulated emission corresponding to the band gap of ZnO (~380nm). The use of ZnO nanowires which have lower defect density instead of ZnO thin films are beneficial, since luminescence lifetime is closely related to the concentration of defects that trap the electrons and/or holes which is the cause of their non-radiative recombination.

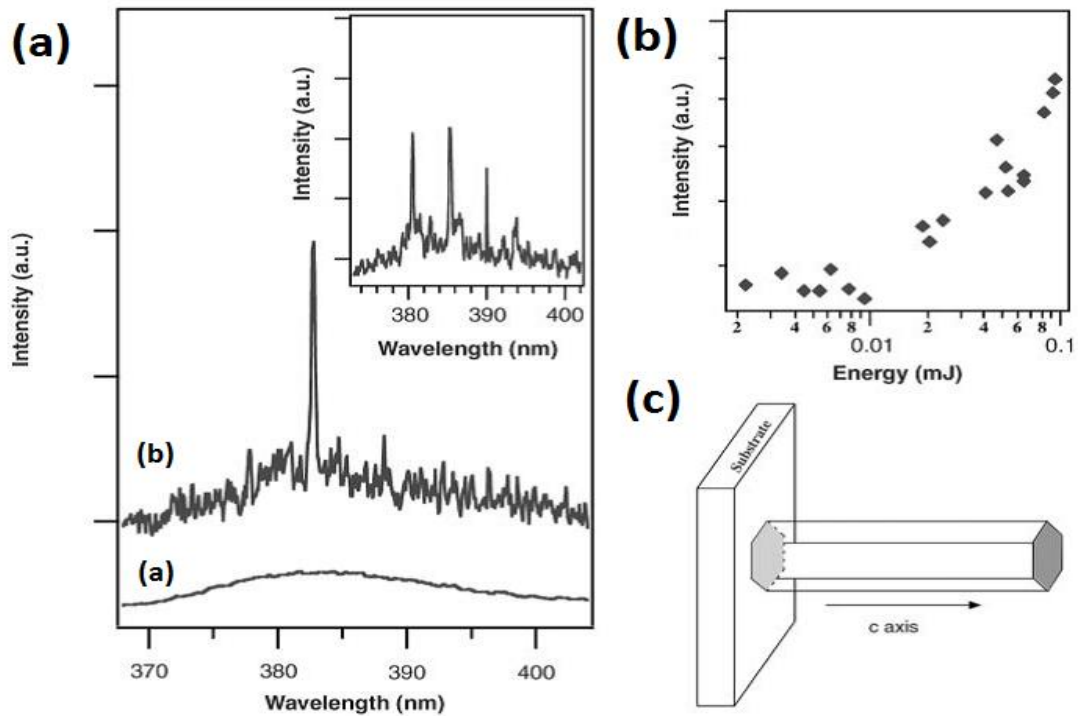


**Figure 2.5.** (a) Emission spectra from nanowire arrays below (line a) and above (line b and inset) the lasing threshold. The pump power for these spectra are 20, 100, and 150 kW/cm<sup>2</sup>, respectively. The spectra are offset for easy comparison. (b) Integrated emission intensity from nanowires as a function of optical pumping energy intensity. (c) Schematic illustration of a nanowire as a resonance cavity with two naturally faceted hexagonal end faces acting as reflecting mirrors [12].

### 2.4.3. Hydrophobic Surfaces

Water repellency is another important property of ZnO nanowires for the practical applications in microfluidics and protective coatings, as shown in Figure 1.6 [13]. It was reported that ZnO nanowire arrays deposited with electrochemical method and further surface modified with stearic acid show remarkable hydrophobicity with a contact angle of 176 degrees [14]. The hydrophobic surfaces made with ZnO nanowires is found to be stable over a wide pH range, at temperatures up to 250°C or long – term storage under ambient conditions.

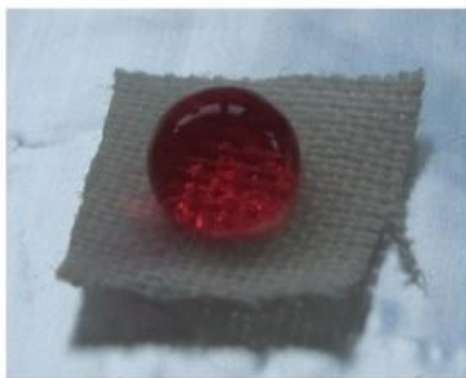


**Figure 1.6.** Hydrophobic behavior of cotton fabric with ZnO nanowires. [13].

### 2.4.4. Solar Cells

Solar cells directly convert sunlight into electricity. Great effort has been concentrated on improving the efficiency of different types of solar cells in recent years. Nanowires are in the center of interest for the solar cells; since their incorporation improves device efficiency due to enhanced absorption of light and stimulated transfer of charge carriers due to nanowires' three dimensional interface. Monocrystalline and polycrystalline silicon nanowire solar cells have remarkable light absorption capability due to their low light reflectivity [15]. Furthermore, the improvement of cost effective processing techniques could make these type of solar cells more common in the future. Likewise, the promise of ZnO nanowires have been revealed in dye sensitized solar cells [16], as shown in Figure 1.7 (a). A dye-

sensitized solar cell is based on a semiconductor formed between a photo-sensitized anode and an electrolyte, which is a photoelectrochemical system. During its operation, sunlight passes through the transparent electrode into the dye layer, where it can excite electrons that can then flow into the titanium dioxide nanoparticles. The electrons flow toward the transparent electrode, where they are collected for powering a load. After flowing through the external circuit, they are re-introduced into the cell on a metal electrode on the back, flowing into the electrolyte. The electrolyte then transports the electrons back to the dye molecules. The ZnO nanowire cells generate considerably higher currents than the ZnO particle cells over the accessible range of roughness factors which are defined as the total film area per unit substrate area of  $\sim 1000$  (55–75% higher at a roughness of 200) but they generate less current than TiO<sub>2</sub> particles due to conventional surface area since less dye is anchored to the ZnO nanowires, as shown in Figure 1.7 (b).

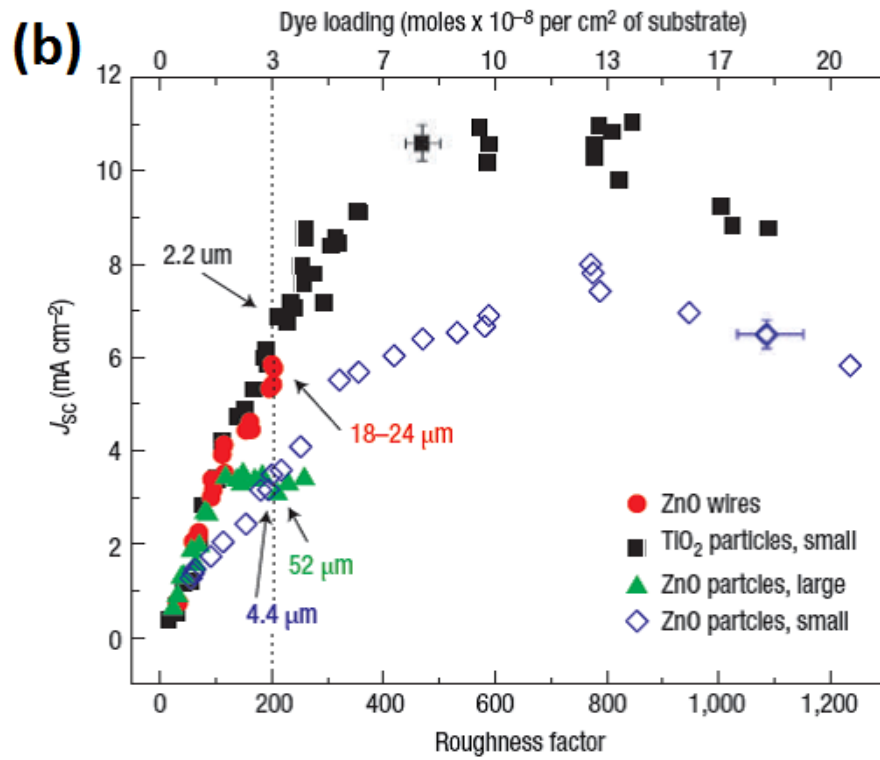
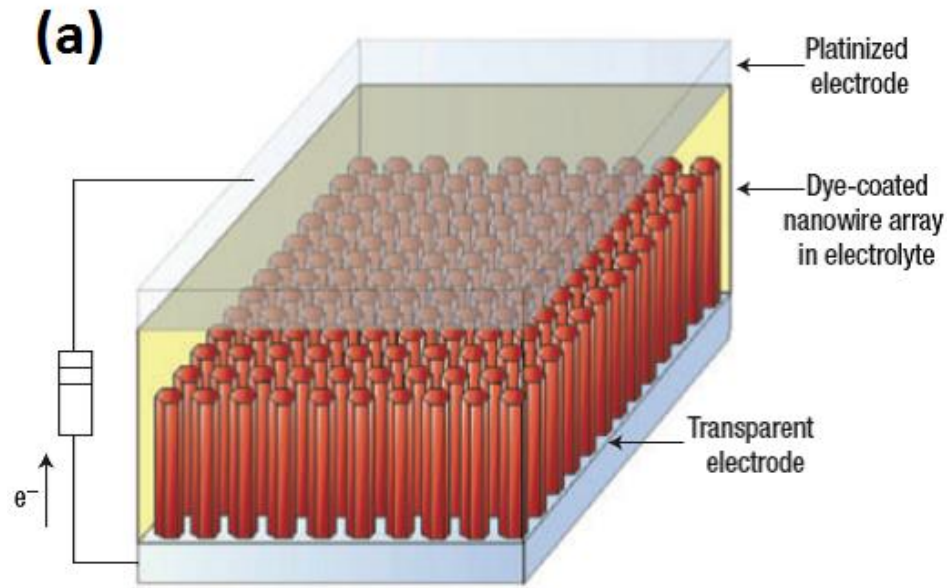


**Figure 2.7.** (a) Schematic of a dye-sensitized solar cell with ZnO nanowires. (b) Comparative performance of nanowire and nanoparticle cells. [16]

### 2.4.5. Field Effect Transistors

Transistors are fundamental components in almost all electronic devices. They are used for switching, voltage/current regulation and amplification of electrical signals. Traditional transistors are made of bulk silicon through doping them with group III or V elements for forming p-type and n-type zones, respectively. Bipolar junction and field effect transistors (FETs) are the two types of transistors that have been used in circuits. Bipolar junction transistors operate with diffusion of electrons and holes; whereas FETs operate with diffusion of one type charge carrier through the application of voltage to the gate to form a conducting channel between source and drain electrodes. ZnO nanowires can also be used for manufacturing FETs, as shown in Figure 1.8. [17]

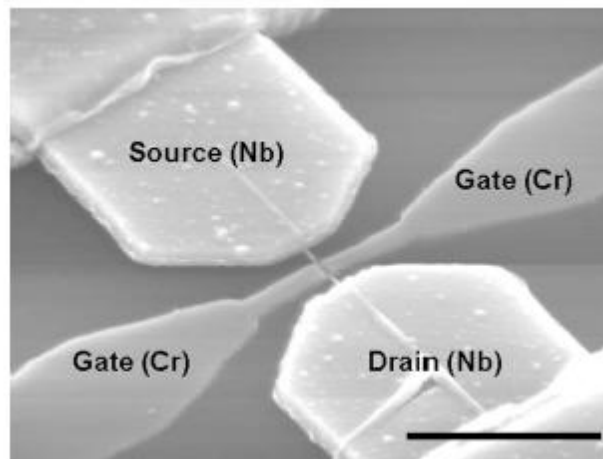


**Figure 2.8.** 45° tilted SEM image of fabricated ZnO nanowire FET with self-aligned gate electrodes and nanosize air gaps. Scale bar is 2.5  $\mu\text{m}$ . [17]

The fabricated FET exhibits excellent performance with a transconductance of 3.06  $\mu\text{S}$ , a field effect mobility of 928  $\text{cm}^2/\text{V}\cdot\text{s}$ , and an on/off current ratio of  $10^6$ , as shown in Figure 1.9. The electrical characteristics are the best obtained to date for a ZnO transistor without passivation [17].

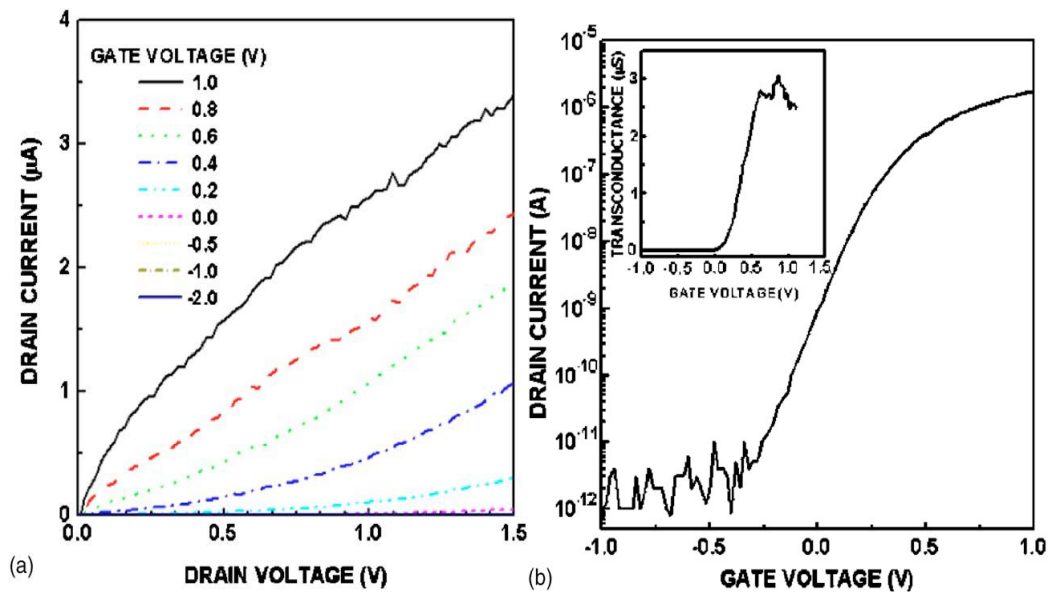


**Figure 2.9.** (a) Output characteristics of ZnO nanowire FET. The gate voltage range is from  $-2$  to  $1.0$  V. (b) Transfer characteristic of the device with  $0.8$  V of source-drain voltage. Insert is transconductance curve of the device. The saturation value is  $3.06 \mu\text{S}$ . [17]

#### 2.4.6. Gas Sensors

Gas sensors are used for detecting the presence and concentration of flammable, combustible or toxic gases in an environment. Semiconductor metal oxides have been studied and used for many decades as gas-sensing materials. In these devices, a sensitive film of metal oxide semiconductor reacts with gases and triggers the device when a certain threshold level is exceeded. ZnO is one of the earliest discovered and most widely applied oxide gas-sensing material. Thin-film form of ZnO has been used as gas sensors with its severely hampered performance due to its limited surface-to-volume ratio. Utilization of ZnO nanowires greatly enhances gas-sensing properties, reduces the operating temperature and shrinks down the size of the sensor as a result of its high surface-to-volume ratio. There are examples of sensors made of ZnO nanowires for different gases like ammonia ( $\text{NH}_3$ ), ethanol and liquefied petroleum gas (LPG) [18, 19, 20]. Figure 1.10 shows an ethanol gas sensor made of ZnO nanowires with its signal response to ethanol vapour in humid environments [19].

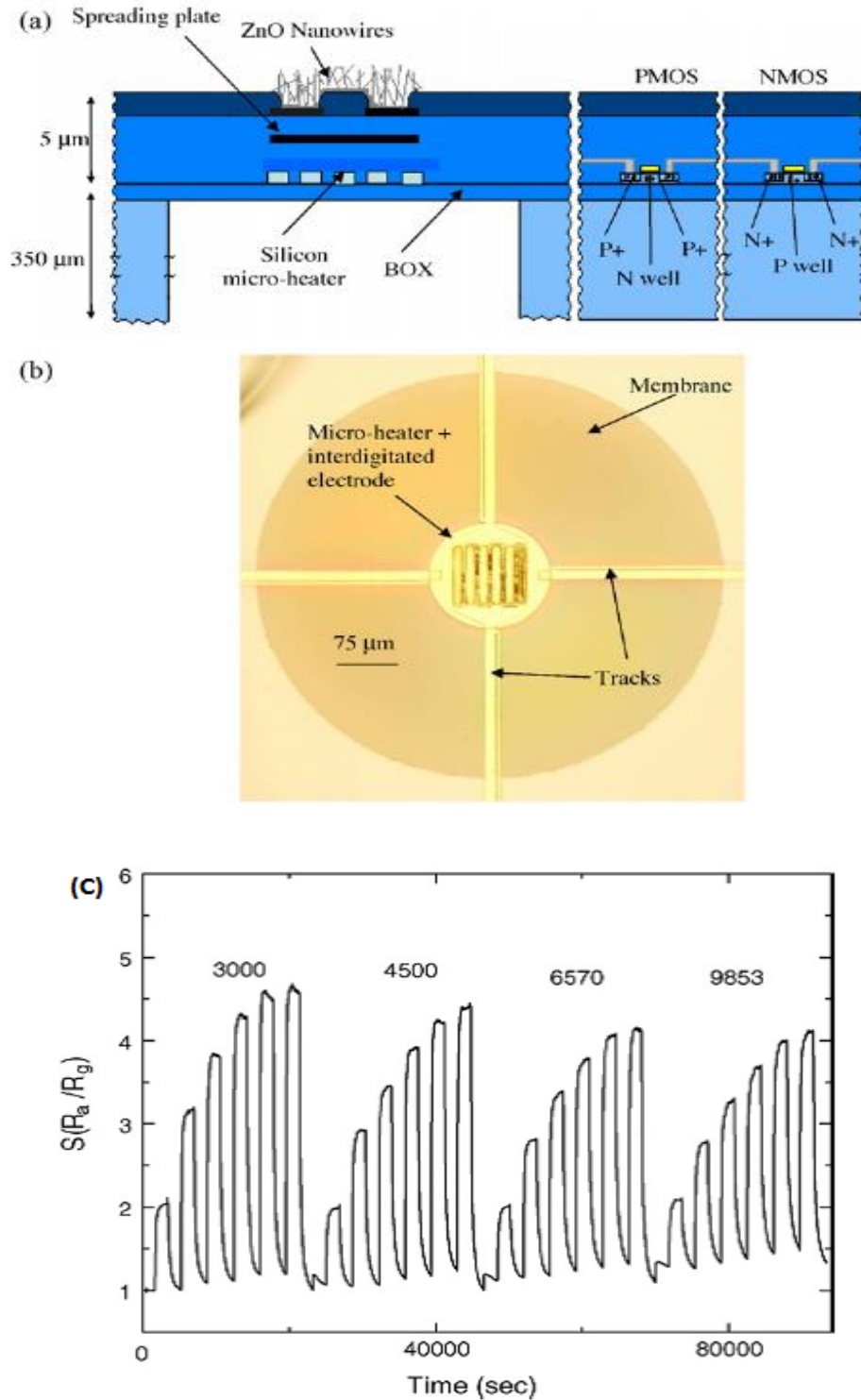


**Figure 2.10.** (a) Cross-sectional view of the ultrathin (5µm) silicon on insulator (SOI) micro-hotplate and the ceramic metal oxide semiconductor (CMOS) electronic cells. (b) An optical microscope picture of the fabricated micro hotplate with interdigitated electrode. (c) Response of the ZnO NWs measured at different humidities (3000 ppm, 4500 ppm, 6570ppm and 9853 ppm). [19].

### 2.4.7. Piezoelectrics

Another hot topic in nanotechnology is to provide power for the operation of devices made of nanostructures. Biosensors, for example, can be powered by natural movements of human body. The greatest challenge is to convert mechanical energy to electrical energy in an efficient manner to provide power for these nanosystems. Piezoelectricity is the electric charge that accumulates in certain solid materials when mechanical stress is applied to them. Nanowires made of materials having wurtzite crystal structures can be used to fabricate piezoelectric nanogenerators. When nanowires are deflected, they can generate polarization and form the current through schottky barrier, as shown in Figure 1.11. Corresponding output voltage image is shown in Figure 1.12. ZnO, GaN, CdS and ZnS are the most important candidates for nanogenerators in their nanowire form. Among them ZnO nanowires have key advantages. It exhibits both semiconducting and piezoelectric properties [22]. It is also relatively biosafe and biocompatible so that it can be used in biomedical applications.

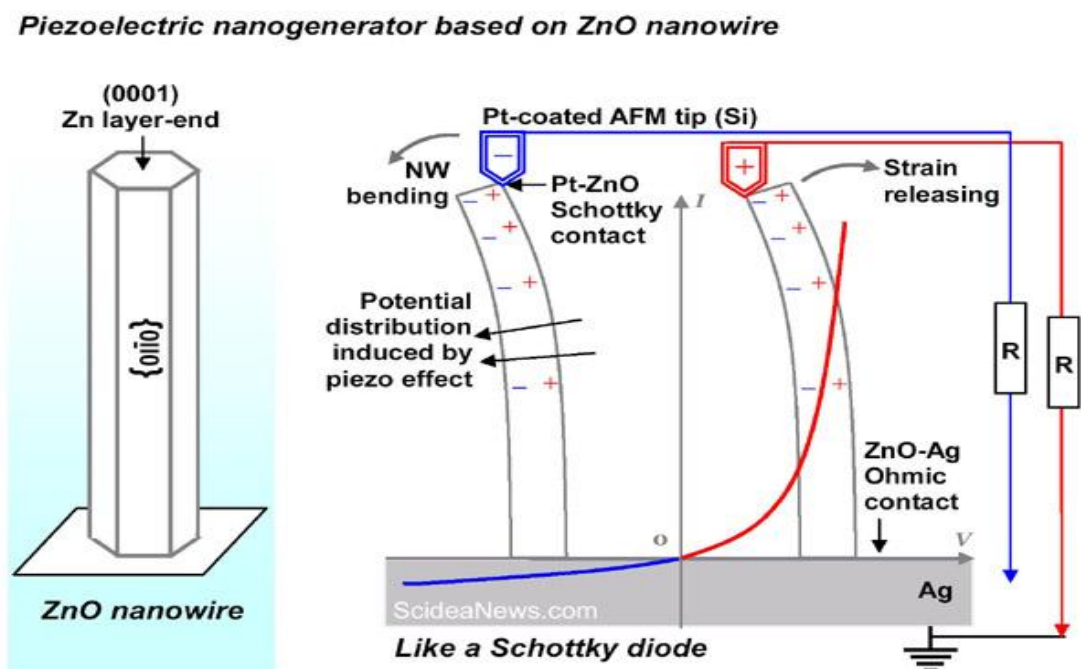


**Figure 2.11.** Schematic of a piezoelectric nanogenerator made of a ZnO nanowire working with vibrations caused by atomic force microscope tip [23].



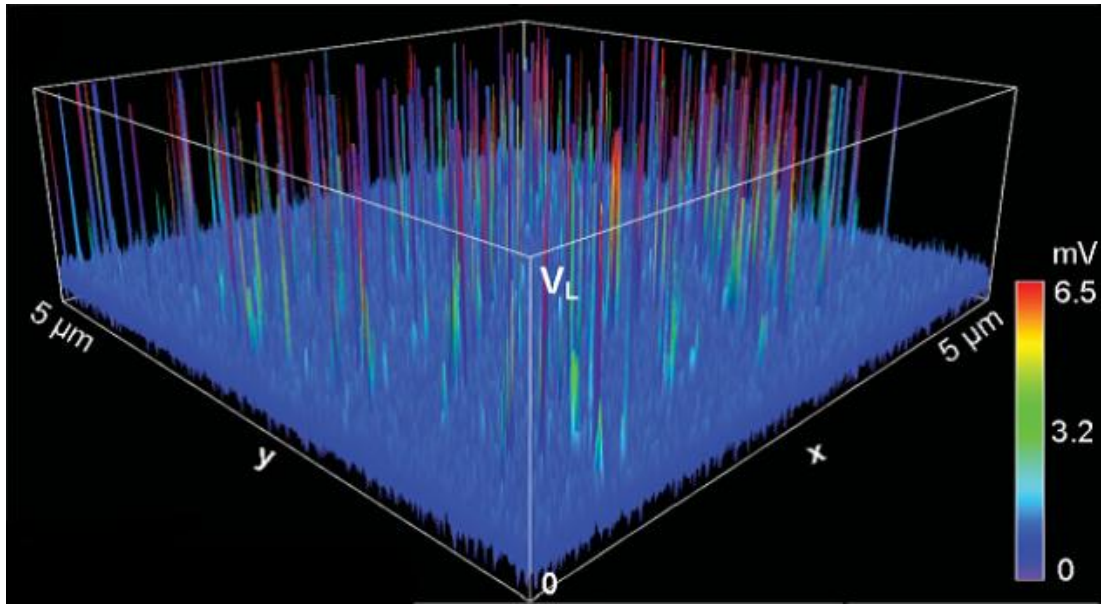


**Figure 1.12.** Corresponding output voltage image of the ZnO NW arrays. Most of the voltage peaks are ~6 to 9 mV in height [22].

## 2.5. Conventional Synthesis Methods for ZnO Structures

### 2.5.1. Synthesis of Bulk ZnO Crystals

Wide range of techniques have been developed for the synthesis of bulk ZnO crystals. Synthesis of high-quality ZnO crystals require homoepitaxial growth. In homoepitaxy, a crystalline film is grown on a substrate of the same material. The most widely used homoepitaxial growth method is Czochralski process for obtaining single crystalline semiconductors. For obtaining ZnO bulk crystals; hydrothermal, melt growth, vapor phase and vapor growth methods are used. Among these methods, vapor phase growth is very difficult to control due to the high vapor pressure of ZnO; however, very high-quality bulk ZnO wafers can be produced with this method. Hydrothermal growth has been used for many years due to its robustness and simple operation procedures compared to other methods. The crystal shapes depend on the precursor, solution basicity as well as on the shapes of seed crystals.

### **2.5.2. Deposition of ZnO Thin-Films**

The earlier studies were based on growing high quality ZnO thin-films for their use in optical and acoustic devices. ZnO thin-films have tendency to grow with strong (0001) preferential orientation on different kind of substrates such like sapphire [24], silicon carbide [25] and gallium arsenide [26]. Chemical vapor deposition (CVD) and magnetron sputtering were the earlier methods utilized for the deposition of ZnO thin films. Obtained thin films had polycrystalline nature. To obtain a fine monocrystalline structure in ZnO thin-films, other growth methods such as pulsed vapor deposition (PVD), molecular-beam epitaxy (MBE), metal-organic chemical vapor deposition (MOCVD) and hydride or halide vapor-phase epitaxy (HVPE), that have fine control over the deposition-procedure have been utilized.

### **2.6. Synthesis Methods of ZnO Nanowires**

A large number of methods have been developed for the synthesis of ZnO nanowires. These synthesis methods can be classified into two groups with respect to their mechanism as bottom-up and top-down methods. In bottom-up fabrication methods, atoms or molecules are placed one at a time to build desired nanostructure. In top-down fabrication methods, required material is protected by a mask and the exposed material is etched away. Among these, commonly used ZnO nanowire synthesis methods are shown in the Figure 1.13, within their respective classification. Vapor deposition and solution based synthesis methods are classified as bottom-up methods. Chemical vapor deposition (Vapor-Liquid-Solid mechanism) [27, 28], thermal evaporation [29], pulsed laser deposition [30], electron beam epitaxy [31] and metal organic chemical vapor deposition (MOCVD) [32, 33] are among vapor deposition methods. Hydrothermal method [34,45] and electrochemical deposition method [46,47] are among solution based synthesis methods. Lithography [48, 50], which is employed in template assisted fabrication is classified as a top-down process.

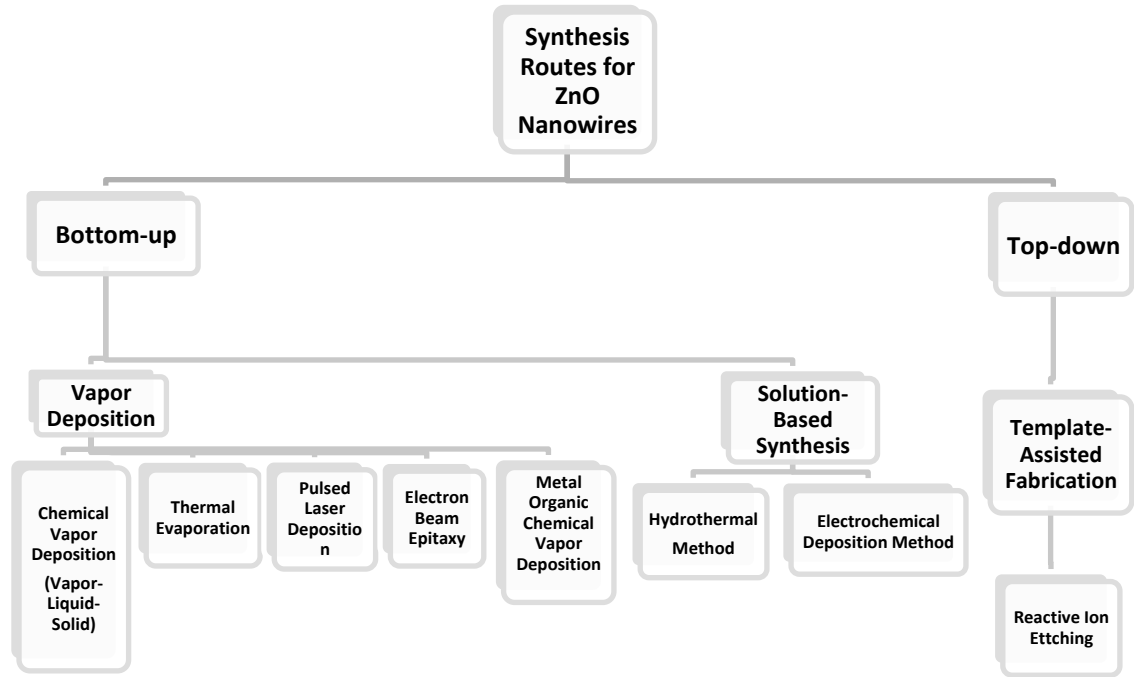


**Figure 2.13.** ZnO nanowire fabrication methods.

### 2.6.1. Vapor Deposition Methods

Growth of ZnO nanowires through vapor deposition includes different methods such as CVD, MOCVD, pulsed laser deposition and thermal evaporation. Basically, a vacuum system and a reactor through which the precursor gas flows are employed in these methods. In CVD method, precursor chemicals exposed to substrate will react or decompose on the substrate surface, as shown in Figure 1.14 [28]. The resulting reaction produces desired materials with distinctive nanostructures. MOCVD differs from CVD in such a way that surface reaction of organic compounds or metalorganics and metal hydrides yield desired nanomaterial's epitaxial growth on a substrate. In PVD, vaporized form of the precursor chemical is deposited on a surface of the substrate by condensation without the involvement of any chemical reactions. Thermal evaporation and pulsed laser deposition are two variations of PVD method.

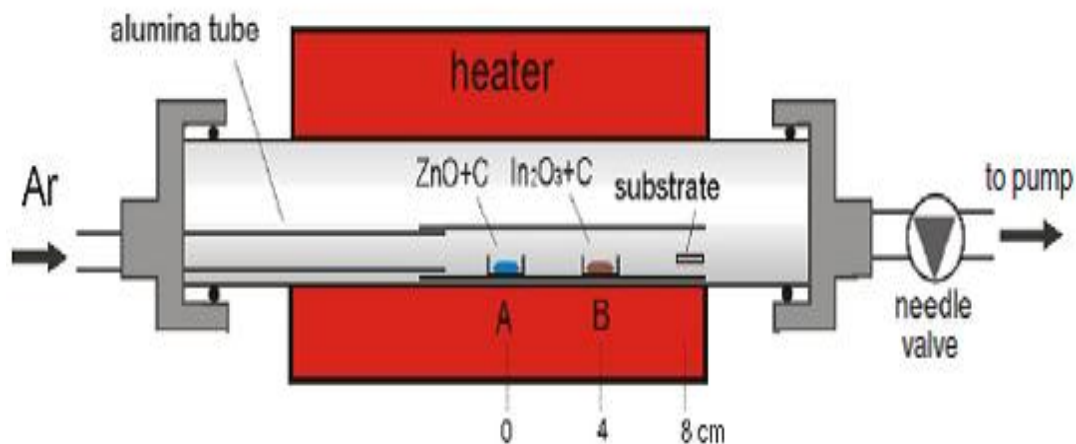


**Figure 2.14.** Schematic sketch of a CVD apparatus used for ZnO nanowire synthesis [28].

### 2.6.2. Vapor-Liquid-Solid (VLS) Mechanism

VLS mechanism involves growth of a crystal through direct adsorption of a gas phase on to a solid surface. In detail; a catalytic liquid metal or alloy rapidly absorbs a vapor to super-saturation level, then crystal growth initiates from nucleated seeds at the liquid solid interface. This method greatly lowers the reaction energy compared to normal vapor-solid growth and nanowires only grow in the areas activated by metal catalysts. Metal catalysts must form a liquid solution with the crystalline material to be grown and must be inert to the reaction products.

The growth mechanism in this method is schematically shown in Figure 1.15., functions in several stages [28]. Gold dot templates on GaN(0001)/Si (grown by metal organic vapour phase epitaxy) substrates were fabricated through a modified nanosphere lithography (NSL) technique. Growth of ZnO nanostructures was conducted inside a double tube furnace system through the Vapour Transport Deposition method.

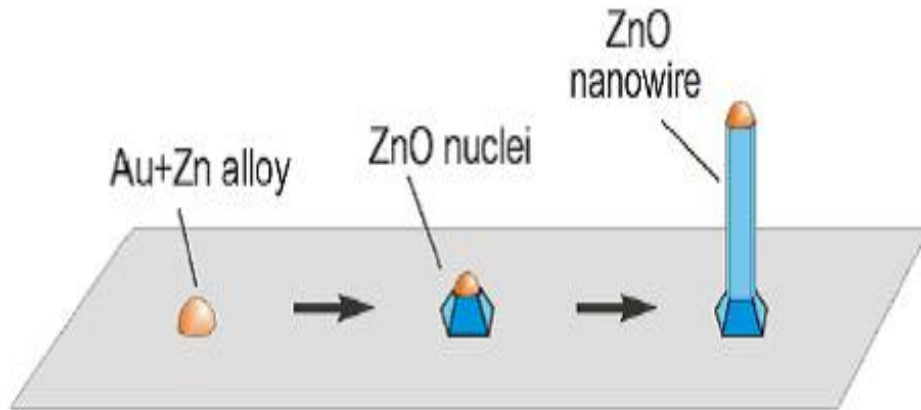


**Figure 2.15.** Schematic diagram of the VLS mechanism [28].

### 2.6.3. Template Assisted Fabrication

Lithography is the most widely used technique for forming templates to synthesize well-aligned ZnO nanowires on any substrate. Seeds like gold or ZnO nanoparticles which are the nucleation sites of ZnO nanowires can be patterned on a substrate with great precision by utilization of lithographic processes. After the lithographic process, etching of the base material can be done chemically using acids or mechanically using ultraviolet light, X-rays or electron beams depending upon the level of resolution required for features in the final product. Reactive Ion Etching (RIE) is used for fabricating ZnO nanowires [51]. In this method, chemically reactive plasma is used to remove excess material deposited on wafers. The precisely aligned ZnO nanowires increases the quality of devices manufactured with them, but using this technique is also increases the cost of ZnO nanowire growth process.

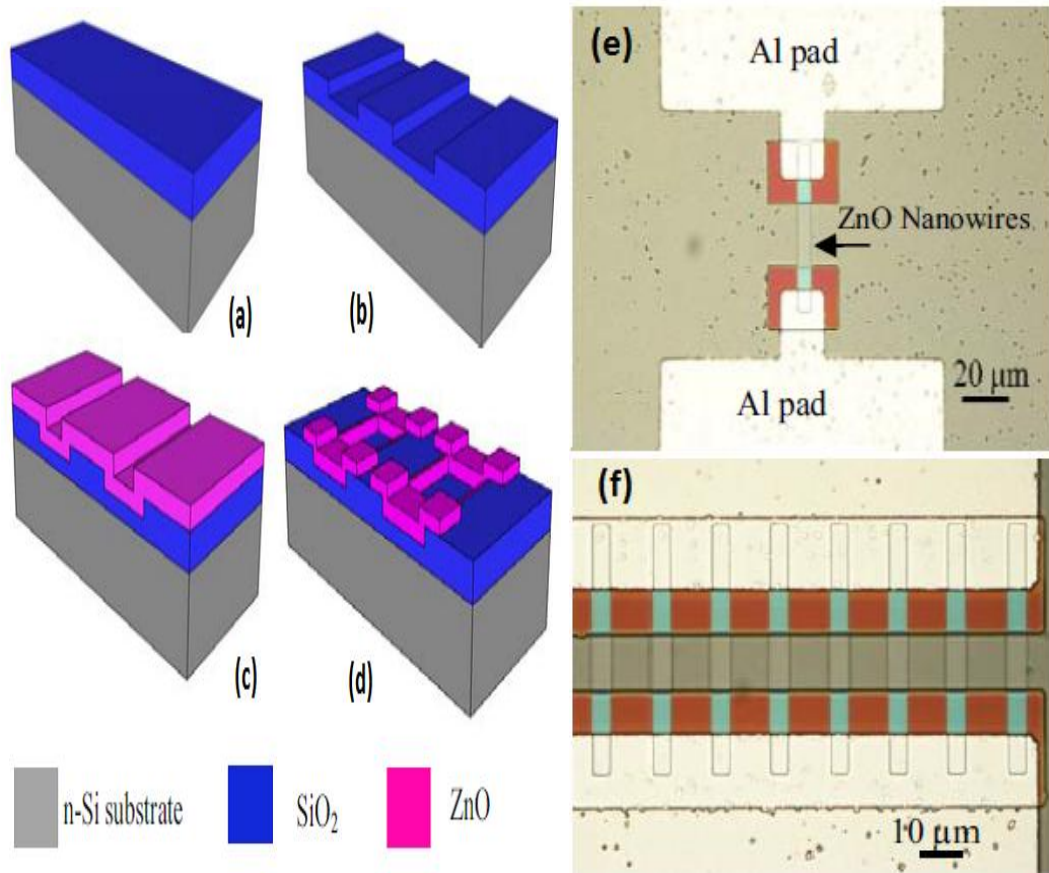
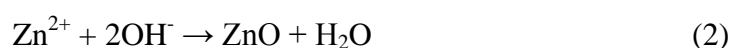
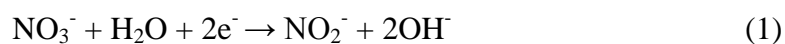


**Figure 2.16.** (a) Thermal Silicon dioxide( $\text{SiO}_2$ ) deposition, (b)  $\text{SiO}_2$  patterned and etched using reactive ion etching (RIE), (c) ZnO deposition with filtered cathodic vacuum arc (FCVA) method, (d) ZnO nanowire formed at the spacer after RIE etch, (e) Optical image of ZnO nanowires formed at the  $\text{SiO}_2$  spacer and (f) optical image of array of ZnO nanowires [51].

#### 2.6.4. Solution Based Synthesis

Electrochemical deposition method and hydrothermal method are among the solution based synthesis methods. To begin with; its cost-effective and easy to implement growth setup makes this process very favored. As a result, intense studies have been made on this synthesis method to improve the quality of ZnO nanowires obtained and to understand the factors influencing the growth of nanowires.

Among these two methods, electrochemical deposition method is more complex and costly, yet it yields ZnO nanowires with well-alignment on the substrates. Besides, dopant incorporation into the ZnO nanowires is easier and alignment of the ZnO nanowires perpendicularly on the substrate is possible without seeding the substrate and annealing them. In electrochemical deposition method, a typical experiment setup involves precursor chemicals dissolved preferentially in deionized water at room temperature, a hot plate to keep the temperature of the solution at desired level, a reference electrode made of a gold wire and a power source for applying potential difference between the substrate to be coated and reference electrode. Electrolytes can be prepared with zinc chloride and potassium chloride [47] or with zinc nitrate hexahydrate and hexamethylenetetramine (HMTA) [48]. The applied potential leads to the precipitation of ZnO and deposition on the surface of the cathode for the electrolyte that contains zinc chloride and potassium chloride via reaction (2) [47]. For the electrolyte containing zinc nitrate hexahydrate and HMTA, the applied potential initiates the reduction of nitrate ions to nitrite ions with the production of hydroxide ions and substrate surface which acts as cathode has high concentration of hydroxide ions. This enables the growth of ZnO nanowires, as shown in Figure 1.17. via the reactions (1) and (2) [48]:



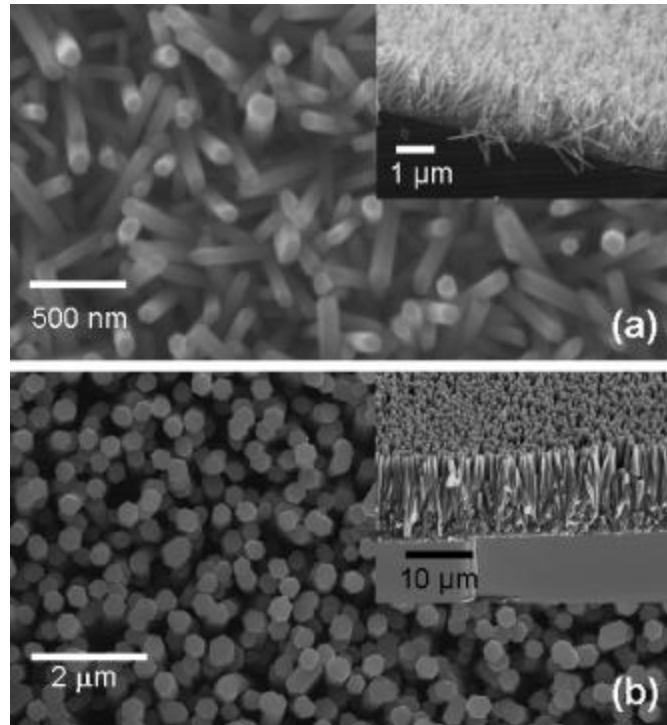


**Figure 2.17.** SEM images of ZnO nanowire arrays deposited on silicon substrate with applied potentials of 0 V for 8 h (a) and -1.2 V for 2 h. (b) ZnO nanocrystals which have a diameter of 10 nm were used as seeds for (a); the growth in (b) was unseeded [48].

In electrochemical deposition method, increasing the potential applied to the solution increases the growth rate and nucleation density of the ZnO nanowires on unseeded substrate.

The basics of hydrothermal method will be explained in detail the following chapter.



## CHAPTER 3

### HYDROTHERMAL SYNTHESIS OF ZnO NANOWIRES WITH THREE COMMON ZINC SALTS

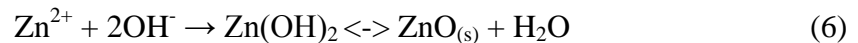
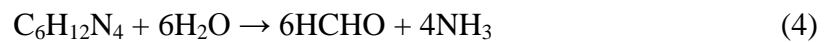
#### 3.1. History and Development of Hydrothermal Synthesis of ZnO Nanowires

A great effort has been made on understanding the factors influencing the hydrothermal synthesis of ZnO nanowires, since it is the most simple and low-cost method among the other methods mentioned. At 1986, Nishizawa et al. have decomposed aqueous solution of  $\text{Na}_2\text{Zn-EDTA}$  to obtain ZnO needle crystals at  $300^\circ\text{C}$  [52]. Decomposition experiments were conducted by heating 0.1 to 5.0 mL of aqueous  $\text{Na}_2\text{Zn-EDTA}$  in a microautoclave. The hydrothermal synthesis which employs use of zinc nitrate hexahydrate and HMTA was first introduced by Lionel Vayssieres et al. in 2003 [53]. The arrayed ZnO nanorods and nanowires were synthesized on single crystalline sapphire, glass, silicon wafers, polycrystalline fluoride doped  $\text{SnO}_2$  glass and ZnO nanostructured thin films at  $95^\circ\text{C}$ . Since then, intense studies were focused on determining the factors affecting the growth of ZnO nanowires and their implementation on various optoelectronic devices. Zhang et al. shown the effect of  $\text{Zn}^{2+}/\text{OH}^-$  concentration ratios on the aspect ratio of ZnO nanowires [38]. Another remarkable advancement on growth rate of ZnO nanowires has been realized by Ünalán et al. in 2008 [40]. A method to synthesize ZnO nanowires rapidly by heating the growth solution in a microwave oven was reported. Apart from that, the effect of concentration ratios of zinc nitrate hexahydrate and HMTA, solution concentration values, reaction time and mechanical stirring were studied. The addition of acetic ions into the growth solution containing zinc nitrate hexahydrate and HMTA leading to high aspect ratio ZnO nanowires was shown by Wang et al. in 2009 [37].

### 3.2. ZnO Nanowire Growth Reactions and Mechanism

ZnO nanowire growth is affected by many factors. The temperature and pH of the solution, zinc source used, the ratio of concentrations of zinc source and HTMA, conditions during seeding of substrates and the cooling rate of the growth solution in which the ZnO nanowires are immersed after the growth process [47] are among these factors which are influencing the morphology and dimensions of ZnO nanowires.

The reactions occurring during the growth of ZnO nanowires can be summarized as:



The net reaction is:



$\text{Zn}^{2+}$  ions can be supplied from common zinc salts such like zinc chloride ( $\text{ZnCl}_2$ ), zinc nitrate hexahydrate ( $\text{Zn}(\text{NO}_3)_2(\text{H}_2\text{O})_6$ ), zinc acetate dihydrate ( $\text{Zn}(\text{O}_2\text{CCH}_3)_2(\text{H}_2\text{O})_2$ ); which are dissolved in deionized water. Among these salts, growth of ZnO nanowires with zinc nitrate hexahydrate salt as a zinc source with HMTA has been well studied. Zinc acetate dihydrate was also used for the growth of ZnO nanowires in a nonaqueous solvent, trioctylamine, which is a coordinating tertiary amine [34]. Zinc chloride has been used in both electrochemical deposition [46] and hydrothermal method [38].

HMTA is used as a buffer to keep the solution pH values at a steady level during the growth of ZnO nanowires. At first, it hasn't been well-understood whether HMTA is adsorbed onto and capping {10-10} faces as well as it also acts as buffer for keeping the pH of the solution during the growth reactions. Recently, it was shown that HMTA only acts as a source of  $\text{OH}^-$  ions which are consumed during the reactions in the growth solution. ZnO nanowires are grown using the pH buffer 2-(N-morpholino)ethanesulfonic acid (MES) and applying continuous titration with

potassium hydroxide to providing the same pH conditions, where growth with HMTA occurs [55].

Other chemicals can also be added to the reaction solution for changing the morphology of the nanowires and pH of the solution. A high pH leads to an increase in absolute deposition rate on (001) surface of the ZnO nanowires. Aspect ratio of the ZnO nanowires can be increased by the addition of chemicals like ethylenediamine, sodium dodecyl sulfate or acetic ions which impedes the growth on side planes of the ZnO nanowires [37]. The crystal morphology can also be controlled by the addition of various chemicals. Dimethyleneborane (DMBA) and sodium citrate can form ZnO platelets upon their addition to the growth solution [34].

Strong bases like NaOH can also be added to growth solution increase the pH [43]. It is reported that highly basic solutions are essential for the growth of ZnO nanowires with high aspect ratio.

Temperature of the growth solution is also an important factor that influences nanowire morphology and growth rate. In the past studies, it has been seen that increase in the temperature of the growth solution increases the growth rate of ZnO nanowires.

Application of mechanical stirring to the growth solution during the reaction increases the growth rate of ZnO nanowires [36].

Seeding the substrate for the ease of ZnO nanowire nucleation and growth is beneficial for enabling the use of different type of substrates. Interestingly, relative humidity during the seeding process affects the packing and alignment of nanowires [42]. Also annealing the seeded substrates lead to growth of perpendicularly aligned ZnO nanowires [42].

The morphology of ZnO nanowires depend on the growth mechanism. ZnO is a classic polar crystal with its wurtzite structure.  $\text{Zn}^{2+}$  and  $\text{O}^{2-}$  ion layers are arranged on the top of each other at (001) planes. Side planes of ZnO nanowires are neutral so, growth of the ZnO crystal is favored along [0001] direction. (001) planes may be positively or negatively charged depending on Zn-atom or O-atom surface termination. The top of the ZnO nanowires may exhibit a tapered or a flat hexagonal

shaped morphology depending on the pH of the solution near the vicinity of nanowires at the moment. Nanowires that have Zn-atom terminated surfaces is expected to be longer than their O-atom surface terminated counterparts. When all the ZnO is nucleated and precipitated in the solution, the majority of nanowires have Zn-atom surface terminations with Zn polar surfaces. Hence, majority of (001) top planes of nanowires are positively charged.

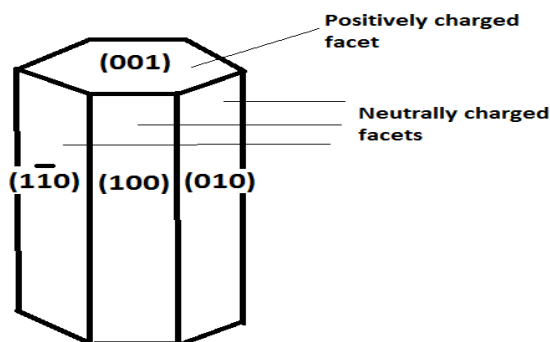


**Figure 3.1.** Schematic representation of an individual ZnO nanowire with Zn-terminated surface.

### 3.3. Experimental Details

In this part of the study, ZnO nanowires were grown on p-type Si (001) substrates with zinc acetate dihydrate ( $\text{Zn}(\text{O}_2\text{CCH}_3)_2(\text{H}_2\text{O})_2$ , 99.0%), zinc chloride ( $\text{ZnCl}_2$ , 98.0%) and zinc nitrate hexahydrate ( $\text{Zn}(\text{NO}_3)_2(\text{H}_2\text{O})_6$ , 98.0%) salts and HMTA ( $(\text{CH}_2)_6\text{N}_4$ , 99.0 %) with the same parameters. All chemicals were purchased from Sigma-Aldrich and used without further purification. Si (001) substrates were first ultrasonically cleaned, in consecutive acetone (99.8%), isopropanol (99.8) and deionised (DI) water baths (18.3 megaohm) for 10 minutes. Then, the substrates were dried with nitrogen gas for removal of water from the surface. Before the application of hydrothermal growth process, Si (001) substrates were seeded. A 5 mM solution of zinc acetate dihydrate in 1-propanol was prepared and used for the deposition of the seed layer through spin coating. Spin coating is applied for 3 times at 2000 rev/min.

After each coating step the substrates were dried on a hot plate set at 120°C, then cooled on a cold metal surface for next spin coating step. Seeded substrates were dipped into aqueous solutions containing 80 ml of 0.02 M zinc acetate dihydrate, 0.02 M zinc chloride and 0.02 M zinc nitrate hexahydrate with 0.02 M HMTA prepared with deionized water (18.3 megaohm). The growth solutions was sonicated for 15 minutes then placed into silicon oil bath which is kept at the desired growth temperature for 10 minutes to initiate the precipitation of ZnO. Afterwards, substrates were placed and suspended vertically inside these growth solutions. After desired amount of time, substrates were taken out of the growth solution and rinsed with deionized water. In order to monitor the temperature and pH change of the each growth solution prepared with different zinc salt sources, a pH probe was placed through the tightly capped solution bottles. A photograph of the growth setup used in this thesis is shown in Figure 2.2.

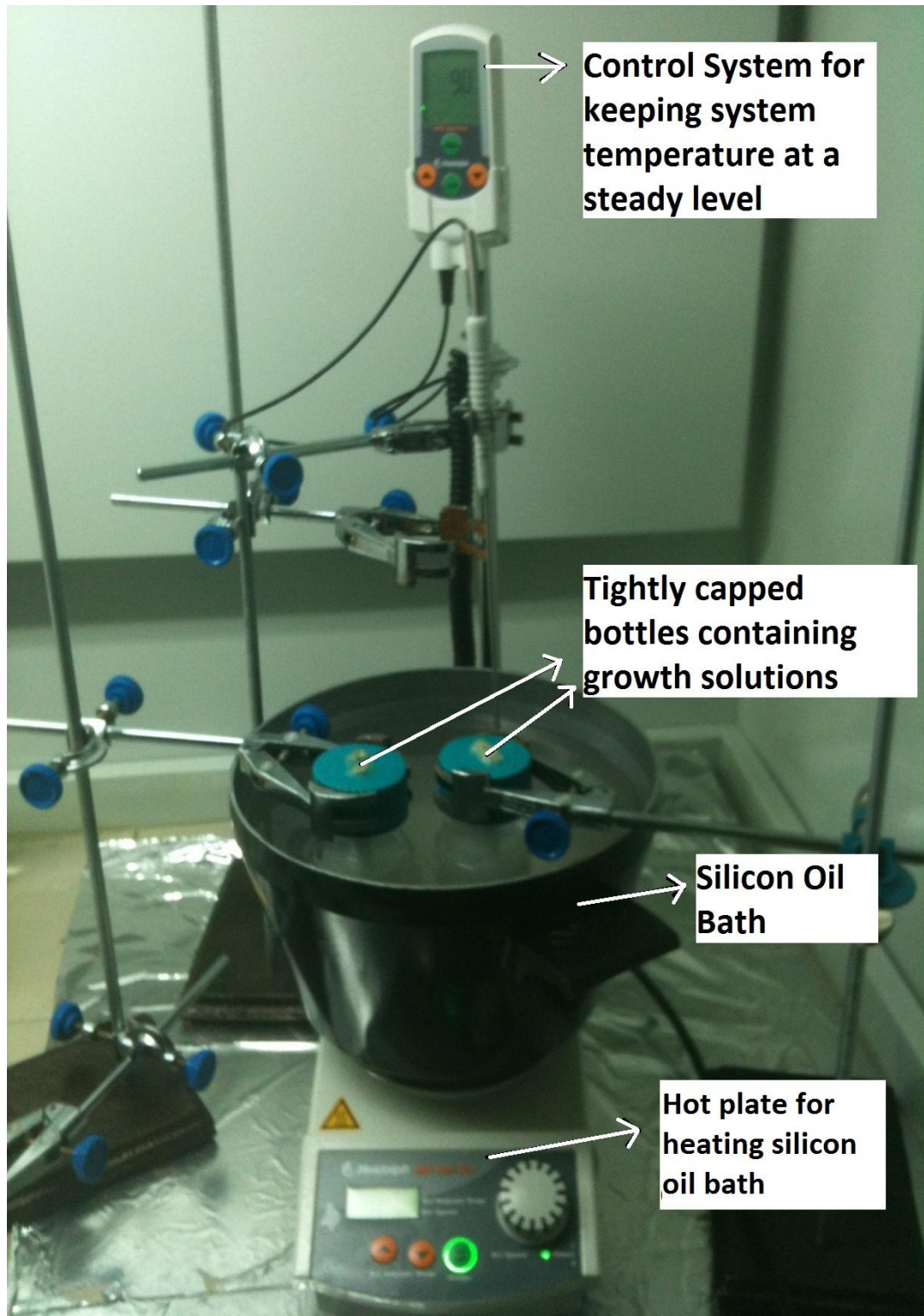


**Figure 3.2.** Photograph of the hydrothermal growth setup used in experiments.

The effect of microwave heating on the growth of ZnO nanowires was also studied. Aqueous solutions containing each of 0.02 M zinc acetate dihydrate, 0.02 M zinc chloride and 0.02 M zinc acetate hexahydrate mixed with 0.02 M HMTA and deionized water (18.3 megaohm) were prepared. Substrates were spin coated with the described procedure. One set of substrates were used in microwave heating process without any treatment after spin coating. The other set of substrates were annealed in a lab furnace at 350°C for 20 minutes to have the ZnO seeds oriented along (001) direction in order to obtain aligned ZnO nanowires. Annealing process leads to formation of zinc oxide seeds by decomposition of zinc acetate dihydrate at 350°C, which is shown in thermogravimetric analysis at the plot in Figure 2.3.

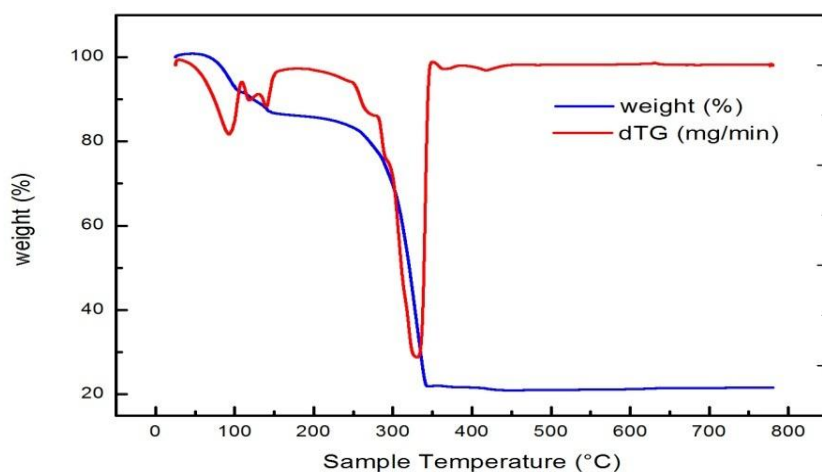


**Figure 3.3.** Change of the weight of zinc acetate dihydrate compound temperature obtained from thermogravimetric analysis.

The substrates were suspended in a beaker containing 30 ml growth solution and were kept in a commercially available microwave oven (2.45 GHz) operated at 700W for 1 minute. The hot growth solution was changed with a fresh one after its removal from the microwave oven; then it was put back again for another minute. This process was repeated for three times. Then, substrates were rinsed and sonicated with deionized water.

## **3.4. ZnO Nanowire Characterization Methods**

### **3.4.1. Scanning Electron Microscopy (SEM)**

The lengths and diameters of ZnO nanowires were analyzed by FE-SEM (Nova NanoSEM 430) operated at 15 kV voltage. Cross sectional SEM images were obtained from cleaved edges of the substrates. Both cross-sectional and top view SEM images were examined following each parametric change in the experimental procedure. No gold or carbon coating was utilized.

### **3.4.2. Transmission Electron Microscopy (TEM)**

Transmission Electron Microscope (TEM) was used to observe the surface morphology in atomic scale and obtain crystallographic data. The ZnO nanowire arrays were scraped off from silicon substrates, dispersed in isopropanol and drop casted on holey carbon coated 400 mesh copper grids. A JEOL 2010 high-resolution transmission electron microscope (HRTEM) operated at 200 kV was used for characterization.

### **3.4.3 XRD Measurements**

The crystal structure of the ZnO nanowires was investigated using X-ray diffraction (XRD) using a vertical goniometer axis Rigaku Cu K $\alpha$  X-ray diffractometer with the Bragg-Brentano focusing geometry.

### **3.4.4. UV-VIS Spectroscopy**

Optical absorption measurements (UV-VIS) were taken using VARIAN CARY 100 BIO UV-Visible Spectrometer in normal incidence mode from ZnO nanowires grown on quartz substrates and solutions containing each of three salts in quartz sample cuvettes with reference quartz and deionized water in quartz cuvettes. UV-vis spectroscopy is the measurement of the wavelength and intensity of absorption of near-ultraviolet and visible light by a sample. The UV-VIS spectrometer setup for measuring the near-ultraviolet and visible light absorptivity of solutions in quartz cuvettes is schematically shown in figure 2.4.



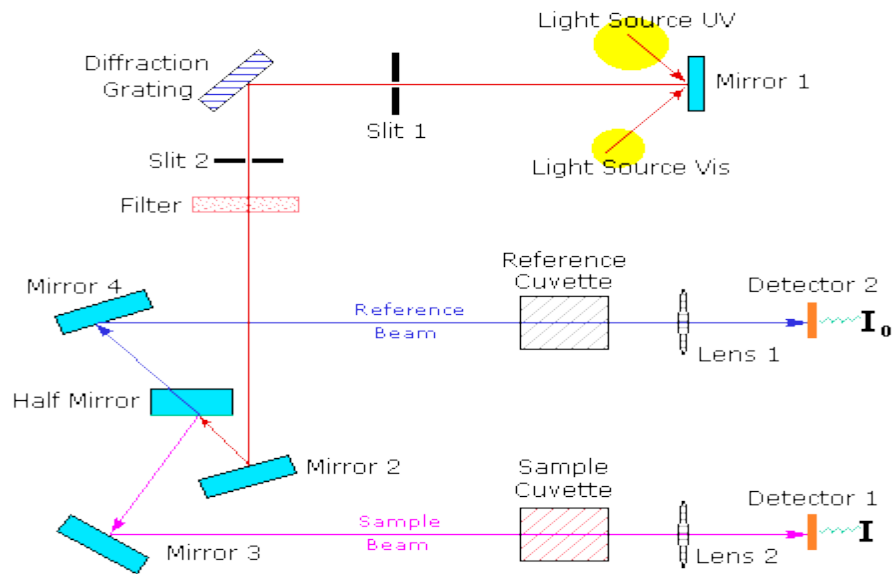


**Figure 3.4.** Schematic of UV-VIS spectroscopy system.

### 3.4.5. Photoluminescence Measurements

Photoluminescence measurements were performed using HORIBA Jobin Yvon PL system at a wavelength of 325 nm. Photoluminescence spectroscopy is a nondestructive method for probing the electronic structure of materials. In this method, light at a certain wavelength is directed on a sample, as shown in Figure 2.5. After its absorption, excess energy of absorbed light is transferred to the sample which is also called photo-excitation. Photo-excitation leads to the movement of electrons within the sample to permissible excited states. The excess energy is released when the excited electrons return to their equilibrium states and an emission of light may occur which is also known as radiative transition. The most common radiative transition in semiconductors is between states in the conduction and valence bands, with the energy difference being known as the band gap. Band gap determination is essential for characterizing semiconductors.

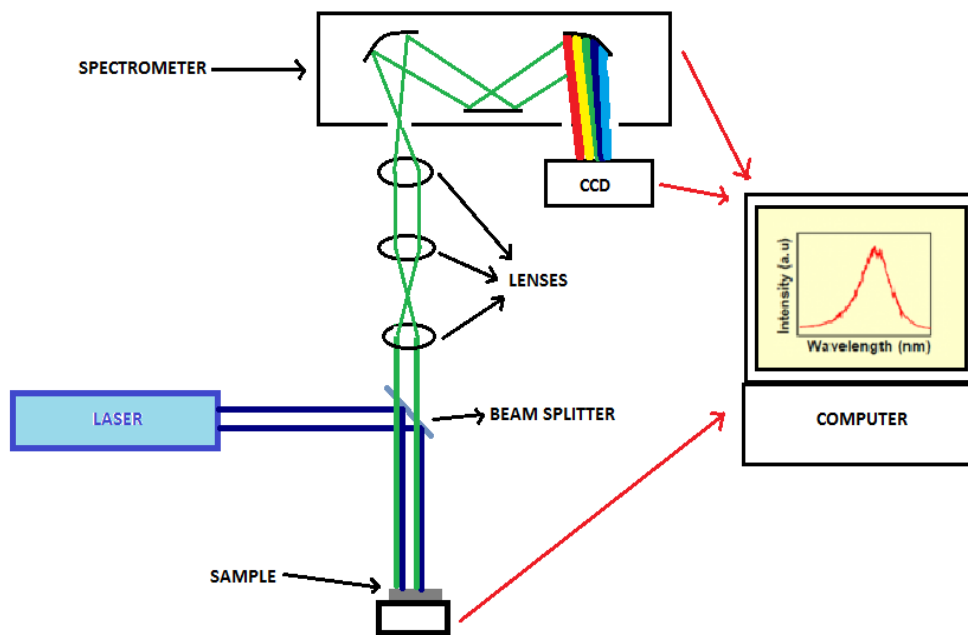


**Figure 3.5.** Schematic of photoluminescence measurement system.

### 3.4.6. Thermogravimetric Analysis (TGA)

Setaram Setsys – 16/18 Differential Scanning Calorimetry system is used for the determination of the rate of change of weight of zinc acetate dihydrate salt with heating rate of  $10^{\circ}\text{K}/\text{min}$ . at atmospheric conditions by putting zinc acetate dihydrate powder in an alumina crucible.

### 3.5. Hydrothermal Synthesis of ZnO Nanowires with Conventional Heating

#### 3.5.1. Zinc Acetate Dihydrate as Zinc Source

XRD spectrum from ZnO nanowires grown at 85°C, for 120 minutes within an equimolar 0.02 M zinc acetate dihydrate and HTMA solution is shown in Figure 2.6. The strong peak at 34.8° (2θ) corresponding to (002) spacing of the wurtzite structure (JCPDS Card No: 36 – 1451) revealed the preferential alignment of the nanowires on the substrate in their c – axis direction.

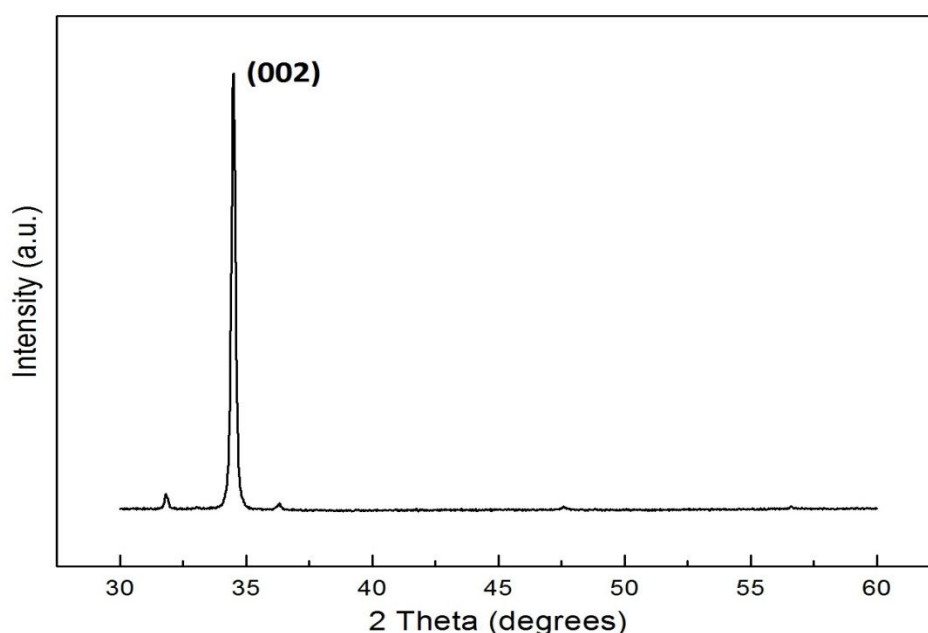


**Figure 3.6.** X-Ray diffraction pattern for ZnO nanowires grown on silicon substrate in an equimolar 0.02M solution of zinc acetate dihydrate and HMTA for 120 minutes.

The effect of growth time up to 3 hours is investigated. Cross-sectional SEM images of ZnO nanowires grown using zinc acetate dihydrate salt for 30, 60, 90, 120, 150 and 180 minutes are given in Figure 2.7 (a)-(f), respectively. From the figure the features of ZnO nanowires are visible at every time interval and their length have almost increased with a steady rate, as shown in Figure 2.8. Their diameter seems to be constant between 60 and 150 minutes. A slight deviation is observed in the diameter of ZnO nanowires at the end of 180 minutes.

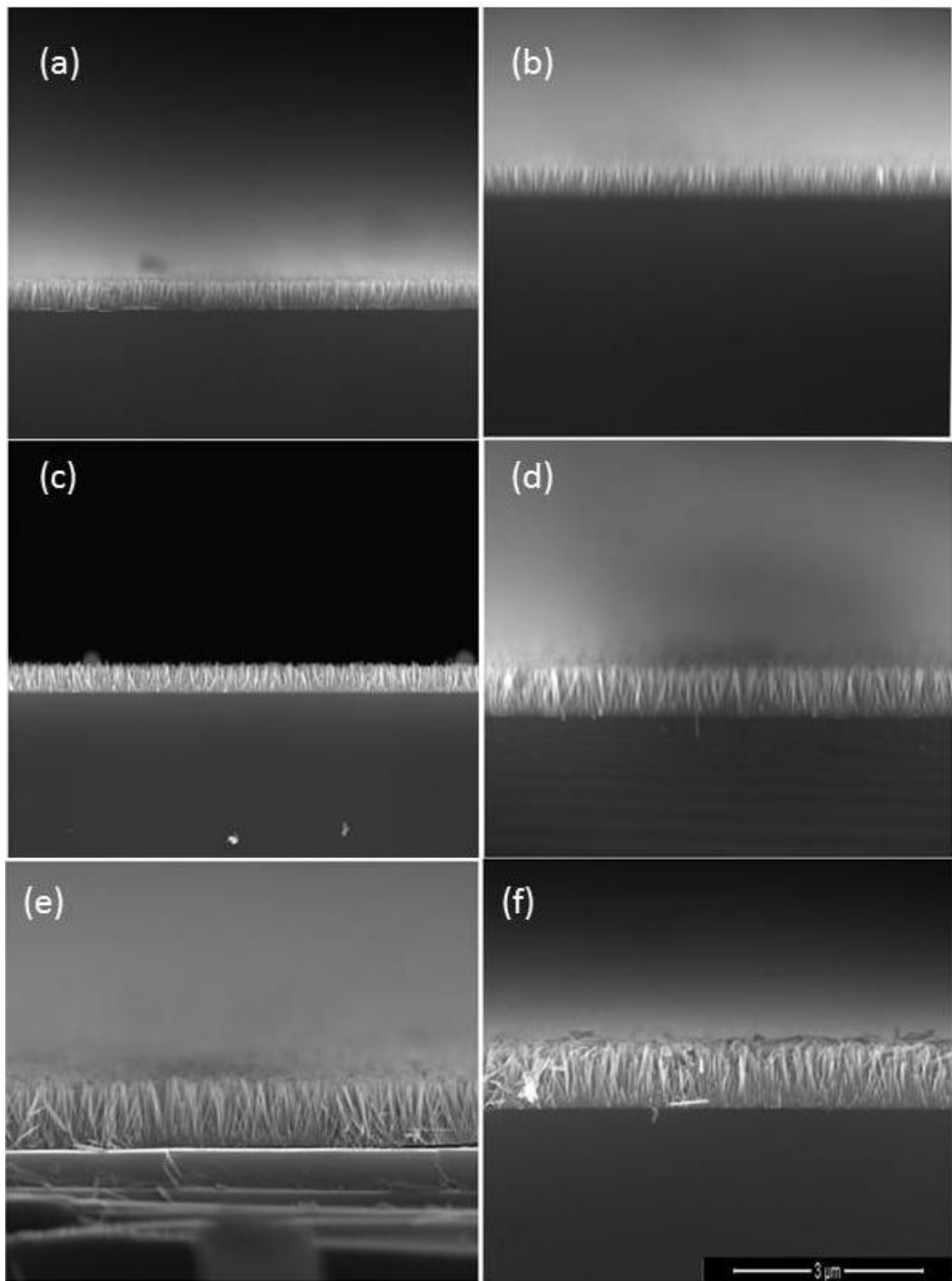


**Figure 3.7.** Cross-sectional SEM images of ZnO nanowires that are grown for (a) 30, (b) 60, (d) 120, (e) 150 and (f) 180 minutes. All scales are the same. Magnifications are 40000x.

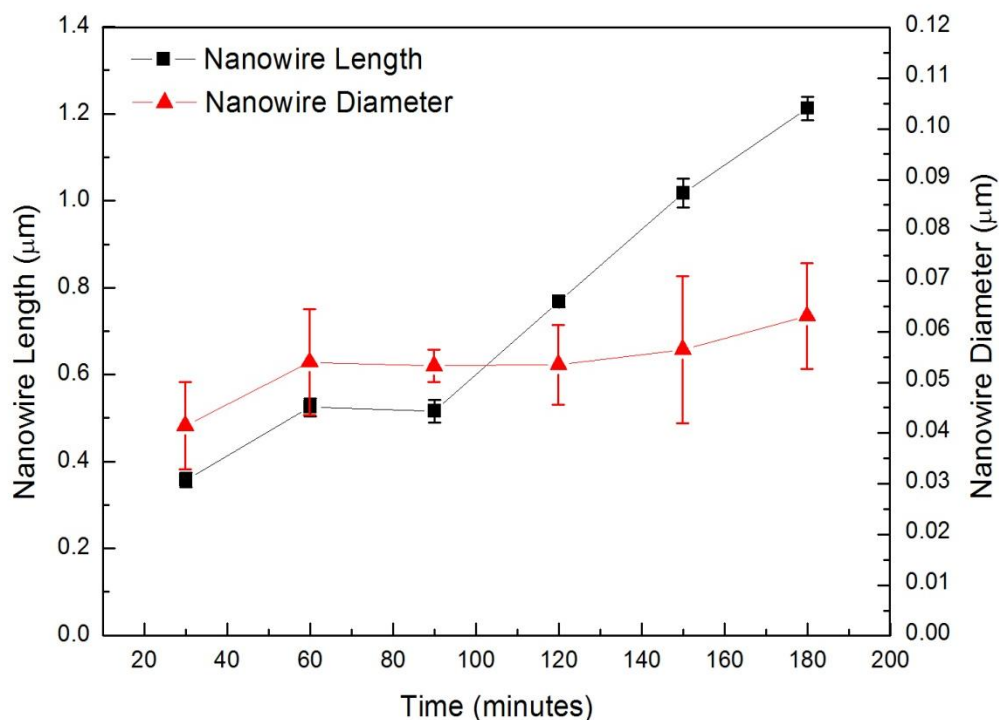


**Figure 3.8.** Variation of diameter and length of nanowires with growth time using zinc acetate dihydrate salt. Lines are for visual aid.

### 3.5.2. Zinc Nitrate Hexahydrate as Zinc Source

XRD spectrum from ZnO nanowires grown at 85°C for 120 minutes within an equimolar 0.02 M zinc nitrate hexahydrate and HTMA is shown in Figure 2.9. The strong peak at 34.8° (2θ) corresponding to (002) spacing of the wurtzite structure (JCPDS Card No: 36 – 1451) revealed the preferential alignment of the nanowires on the substrate in their c – axis direction. The peak at 34.8° (2θ) has weaker intensity compared to the ZnO nanowires grown in the solution containing zinc acetate dihydrate.

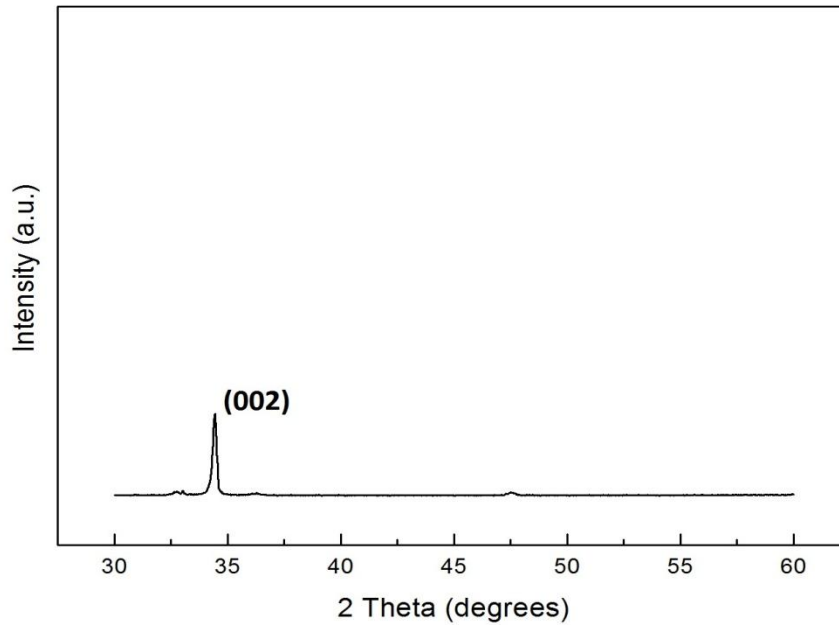


**Figure 3.9.** X-Ray diffraction pattern for ZnO nanowires grown on silicon substrates within an equimolar 0.02 M zinc nitrate hexahydrate and HMTA solution for 120 minutes.

The effect of growth time up to 3 hours is investigated. Cross-sectional SEM images of ZnO nanowires growth with zinc nitrate hexahydrate salt for 30, 60, 90, 120, 150 and 180 minutes are given in Figure 2.10 (a)-(f), respectively. Both length and diameter of the ZnO nanowires increase with time, as shown in Figure 2.11. This result is valid since other studies have also indicated that both ZnO nanowire length and diameter increase steadily. Nanowire morphology is clearly visible on each sample.

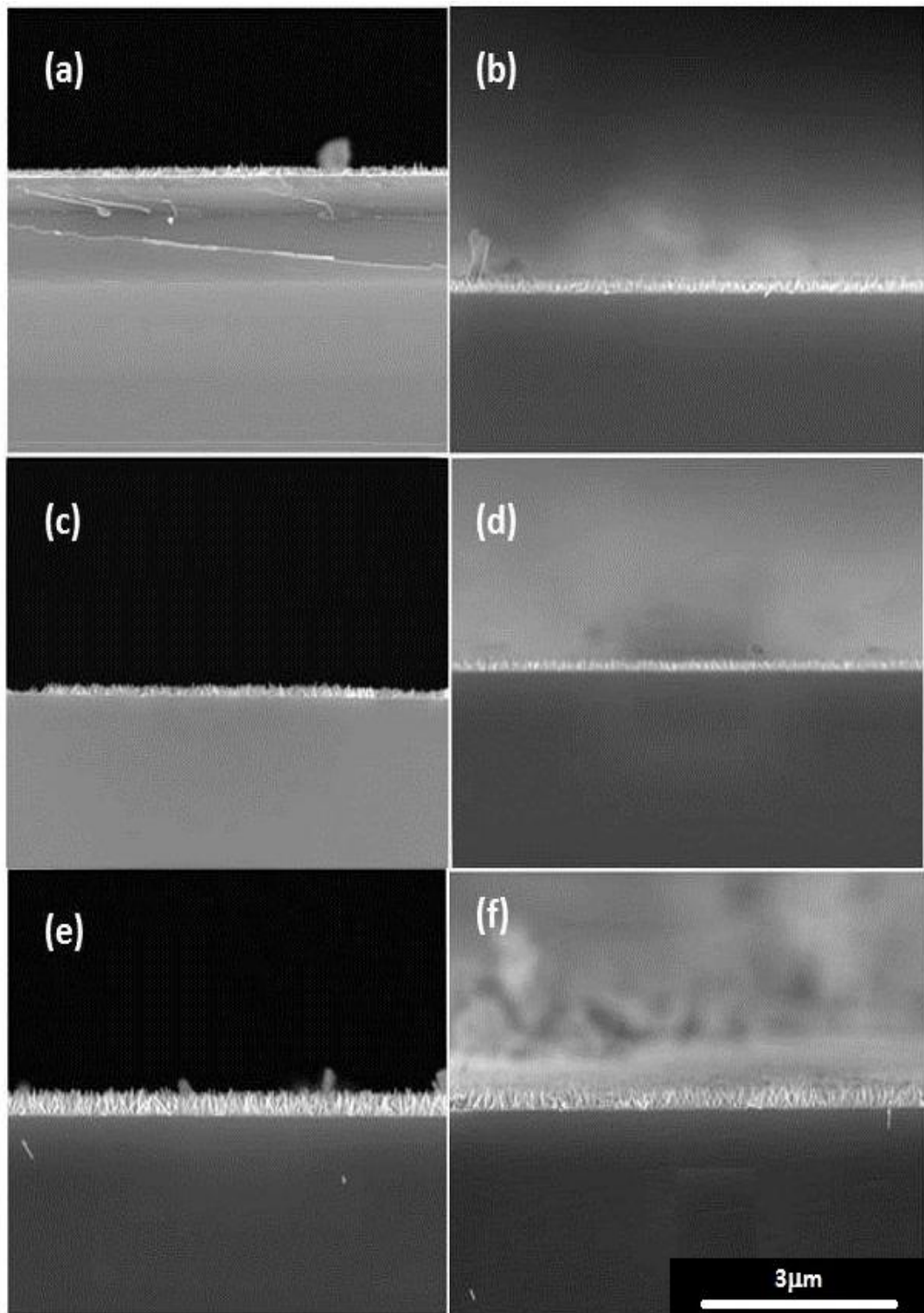


**Figure 3.10.** Cross-sectional SEM images of ZnO nanowires that are grown for (a) 30, (b) 60, (c) 90, (d) 120, (e) 150 and (f) 180 minutes. All scales are the same. Magnifications are 40000x.

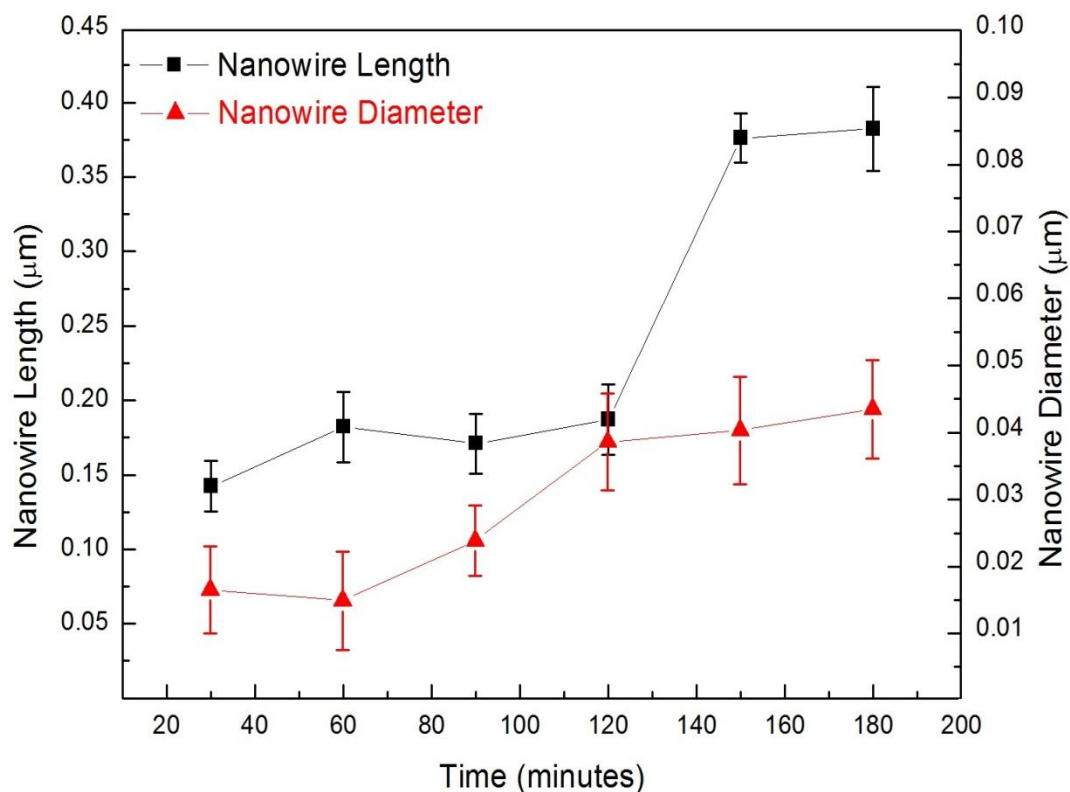


**Figure 3.11.** Variation of diameter and length of nanowires with growth time using zinc nitrate hexahydrate salt. Lines are for visual aid.

### 3.5.3 Zinc Chloride as Zinc Source

XRD spectrum from ZnO nanowires grown at 85°C for 2 hours within an equimolar 0.02 M zinc chloride and HTMA solution is shown in Figure 2.12. The strong peak at 34.8° (2θ) corresponding to (002) spacing of the wurtzite structure (JCPDS Card No: 36 – 1451) revealed the alignment of the nanowires on the substrate in their c – axis direction. The peak at 34.8° (2θ) has weaker intensity compared to the ZnO nanowires grown in the solution containing zinc acetate dihydrate and almost have the same intensity with ZnO nanowires grown in the solution containing zinc nitrate hexahydrate.



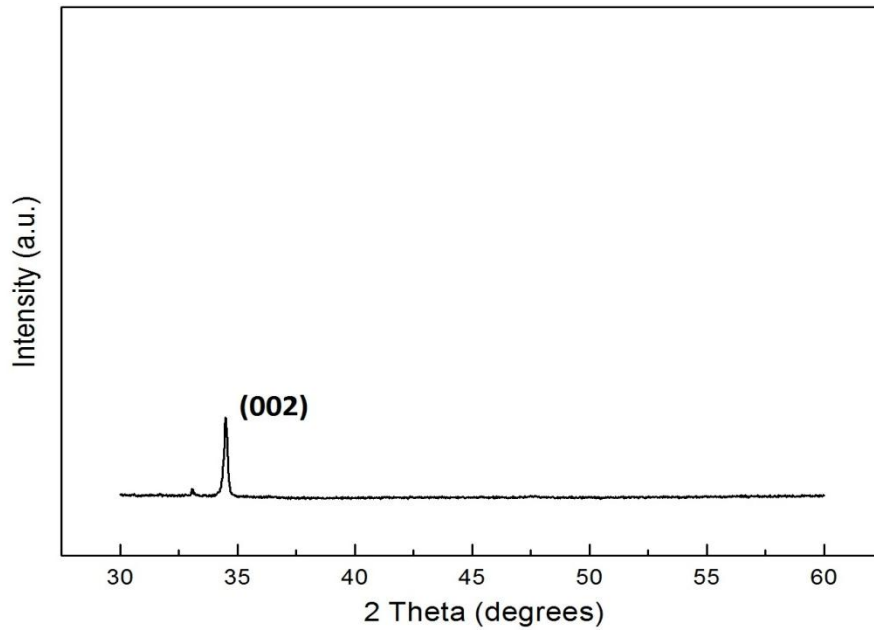


**Figure 3.12.** X-Ray diffraction pattern for ZnO nanowires grown on silicon substrate in an equimolar 0.02M zinc chloride and HMTA solution for 120 minutes.

The effect of growth time up to 3 hours is investigated. Cross-sectional SEM images of ZnO nanowires grown with zinc chloride salt for 30, 60, 90, 120, 150 and 180 minutes are given in Figure 2.13(a)-(f), respectively. In first 30 and 60 minutes, no nanowire like features are visible. At the end of 3 hours, a thin film like formation is observed on the substrate with tips of some of the nanowires visible. The length and diameter of ZnO nanowires is also increasing with time, as shown in Figure 2.14.

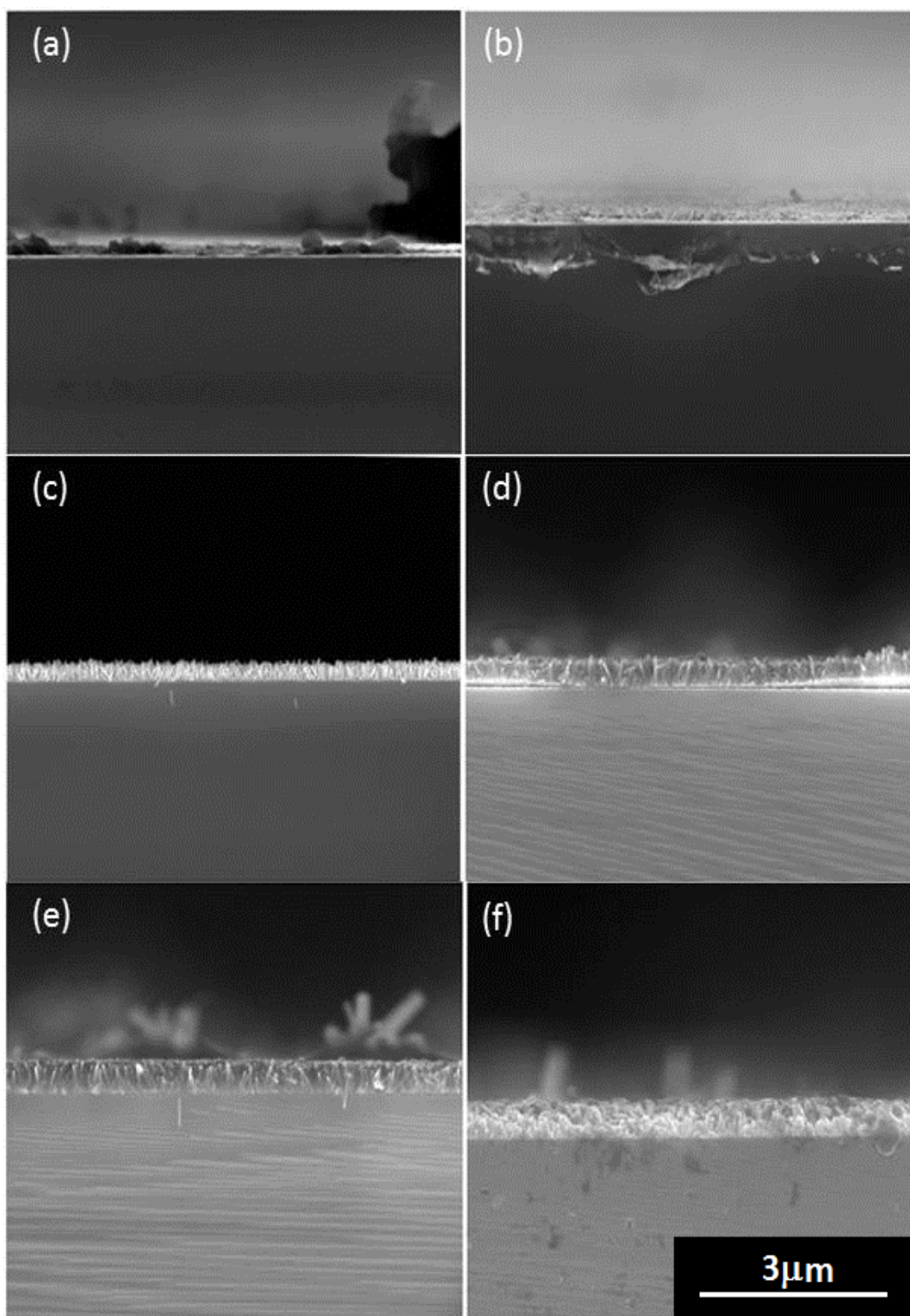


**Figure 3.13.** Cross-sectional SEM images of ZnO nanowires that are grown for (a) 30, (b) 60, (c) 90, (d) 120, (e) 150 and (f) 180 minutes. All scales are the same. Magnifications are 40000x.

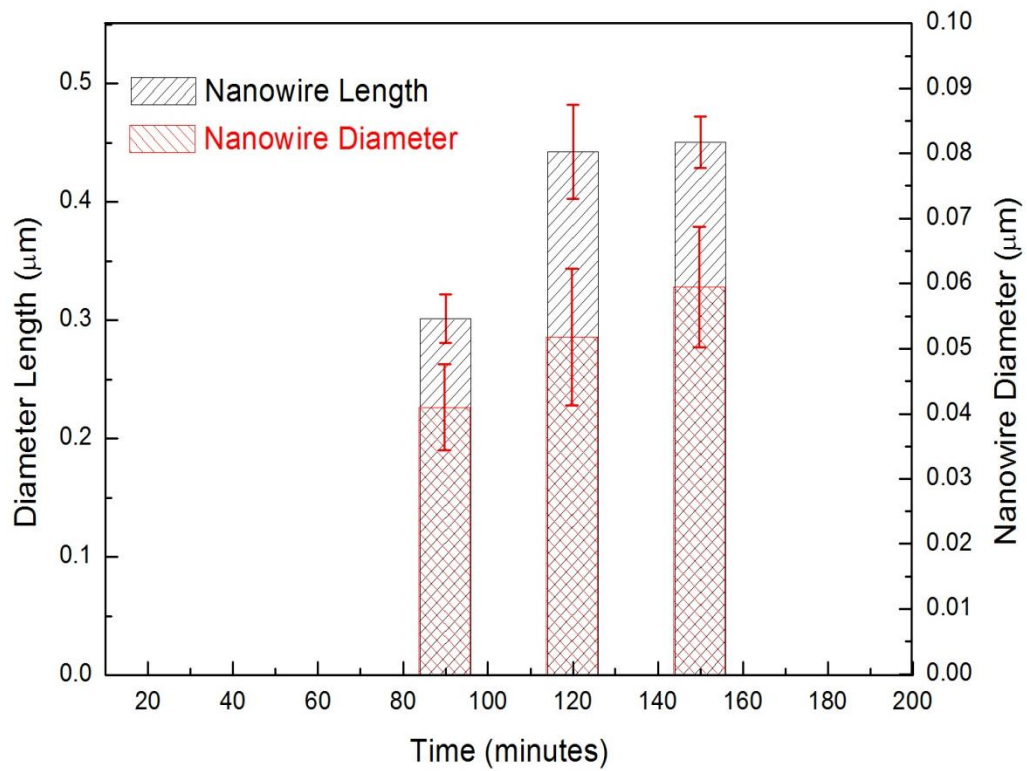


**Figure 3.14.** Variation of diameter and length of nanowires with growth time using zinc chloride salt. Bar charts for 30, 60 and 180 minutes have not been drawn since nanowire features have not been observed.

### 3.5.4 Comparison of Zinc Salts Used in Hydrothermal Method

All the zinc salts that are used for the growth of ZnO nanowires is giving different results. It is evident that counterion of zinc salts has profound effect on ZnO nanowire morphology and growth rate. The temperature and pH of each growth solution is monitored for understanding why these different characteristics emerge. Figure 2.15 shows the change in temperature of each growth solution containing three different zinc salts with time. It is seen that solutions warm up with an identical rate, showing the uniformity of the growth setup employed ( $\pm 1^\circ\text{C}$ ) for the experiments.

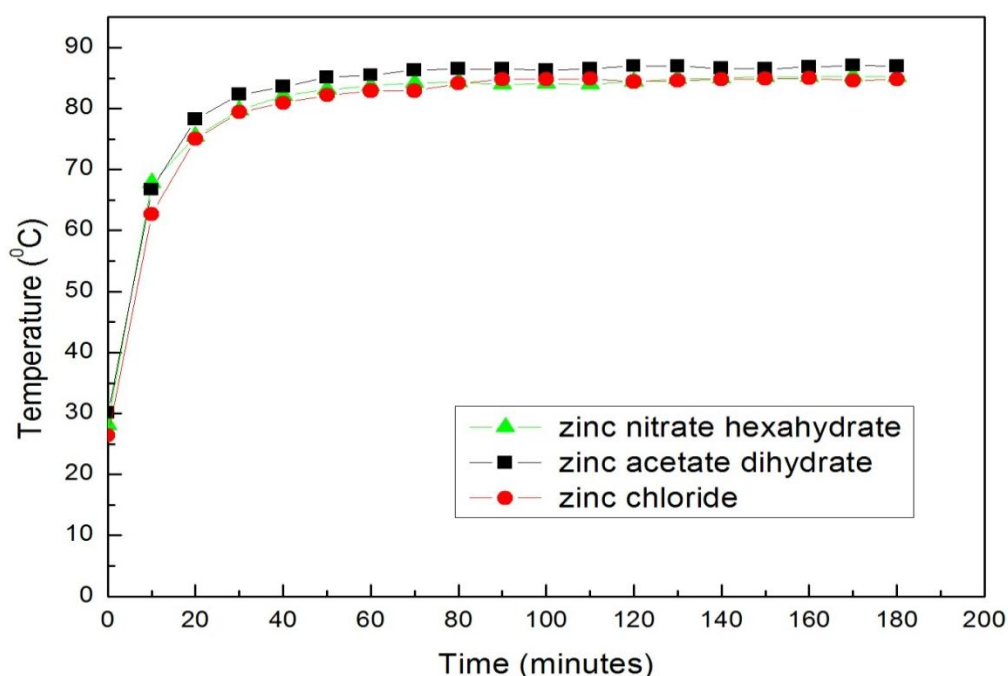


**Figure 3.15.** Variation of the temperature of the growth solutions with time.

Figure 2.16, shows the change in pH of each growth solution with respect to time. It is observed that each solution has a different pH level at room temperature. Furthermore, the decrease rate of the pH values is almost identical, whereas stabilized pH values towards the end of the growth period is different. The growth solution containing zinc acetate dihydrate has a pH value of 6.34, which is closest to neutral among other salts, before it was put into the silicon oil bath for heating. During ZnO nanowire growth, it also has a fixed pH value of 5.74, which is also closest to neutral compared to other solutions. These close to neutral values may

explain why ZnO nanowires those are grown in the solution containing zinc acetate dihydrate have higher aspect ratio compared to ZnO nanowires grown with other zinc salts. Concurrently, zinc chloride solution has a pH value of 6.31 before the reaction and a fixed pH value of 5.67 during the reaction period. These values are close to neutral than the ones for zinc nitrate hexahydrate solution. Higher pH values in growth solution may lead to higher growth rate, thus this result may also explain why ZnO nanowires grown with zinc chloride has slightly longer than ZnO nanowires grown with zinc nitrate hexahydrate.

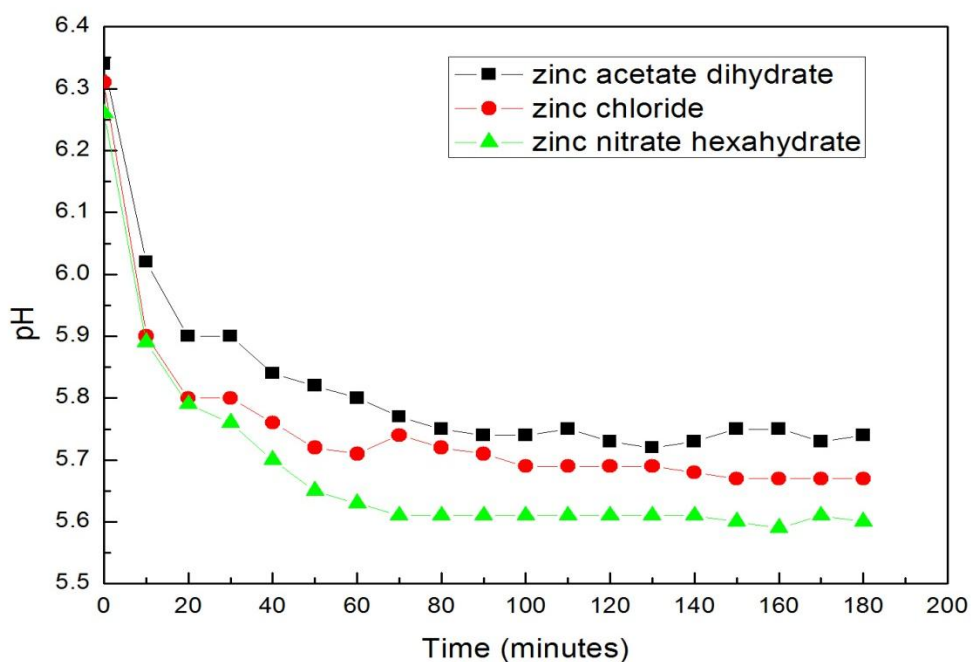


**Figure 3.16.** Variation of the pH of the growth solutions with time.

Figure 2.17 shows the transmittance of each solution at 550 nm containing three different salts. According to the graph at any time, the solution containing zinc acetate dihydrate salt has the lowest rate of ZnO formation at the beginning of the heating and throughout the growth period. As a result,  $Zn^{+2}/OH^{-}$  ratio has the lowest value at any time during the reaction. This should also lead to the formation of high aspect ratio ZnO nanowires. Besides, capping effect of acetic ions also contribute to this condition. The presence of acetic ions suppresses the growth of the ZnO nanowires along  $\langle 10-10 \rangle$ ; thus, increasing the length of ZnO nanowires.

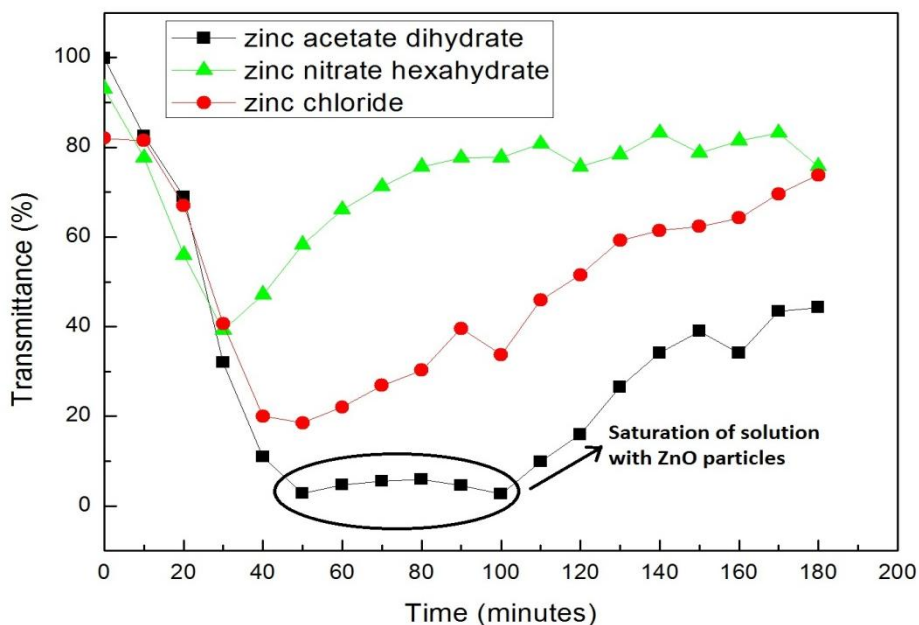


**Figure 3.17.** Variation of the transmittance of each growth solution with time containing different zinc salts.

Solubilities of zinc chloride (432 g/100 ml) and zinc nitrate hexahydrate (184.3 g/100 ml) in water is excessive compared to zinc acetate dihydrate (43 g/100 ml). However, the important factor is the ionization of zinc in these solutions, which is influenced by their counterions. Both chloride and nitrate ions form relatively highly acidic solutions compared to acetate ions which form weakly acidic solutions. As a result, zinc highly ionizes in solutions prepared with zinc chloride and zinc nitrate hexahydrate; whereas, ionization of zinc is less in the solution containing zinc acetate dihydrate. Thus,  $Zn^{+2}/OH^{-}$  ratio in solutions containing zinc chloride and zinc nitrate hexahydrate is higher compared to solutions containing zinc acetate dihydrate.

Also, there are more zinc ions in the solution containing zinc chloride salt than the solution containing zinc nitrate hexahydrate, which is because of higher ionization of zinc in the solution containing zinc chloride salt. As a result, the solution containing zinc chloride has less transmittance at 550 nm compared to the solution containing zinc nitrate hexahydrate.

## 3.6. Hydrothermal Synthesis of ZnO Nanowires with Microwave Heating

### 3.6.1. Microwave Heating with Annealed Substrates

Figure 2.17 shows the length and diameter of ZnO nanowires grown with different zinc salts. Figure 2.18 shows cross-sectional and top-view SEM images of ZnO nanowires grown on annealed (at 350°C for 20 minutes) substrates with different zinc salts by microwave heating. Zinc acetate dihydrate salt, similar to conventional heating, leads to the formation of ZnO nanowires with the longest length compared to other salts, as shown in the Figure 2.17. Top view SEM images show that ZnO nanowires grown in the solution containing zinc acetate dihydrate salt has flat tips and they are very densely nucleated compared to counterparts grown in solutions containing other salts. ZnO nanowires grown in the solutions containing zinc nitrate hexahydrate and zinc chloride salt has almost the same length and diameter. Cross-sectional SEM images reveal that ZnO nanowires grown with zinc chloride and zinc nitrate hexahydrate have tapered tips.

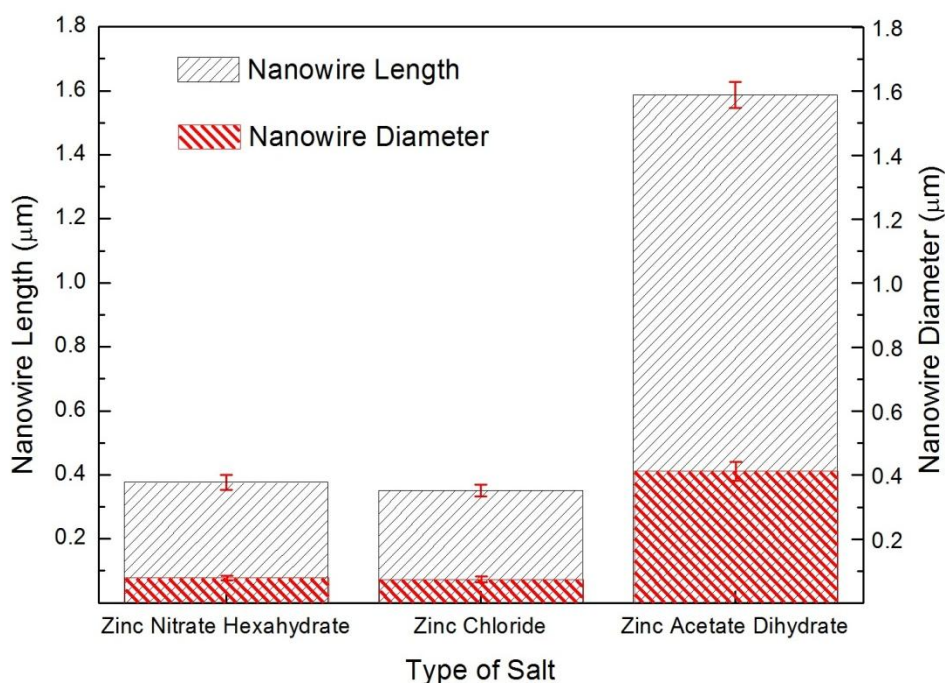


**Figure 3.17.** Variation of length and diameter of ZnO nanowires grown with different zinc salts.

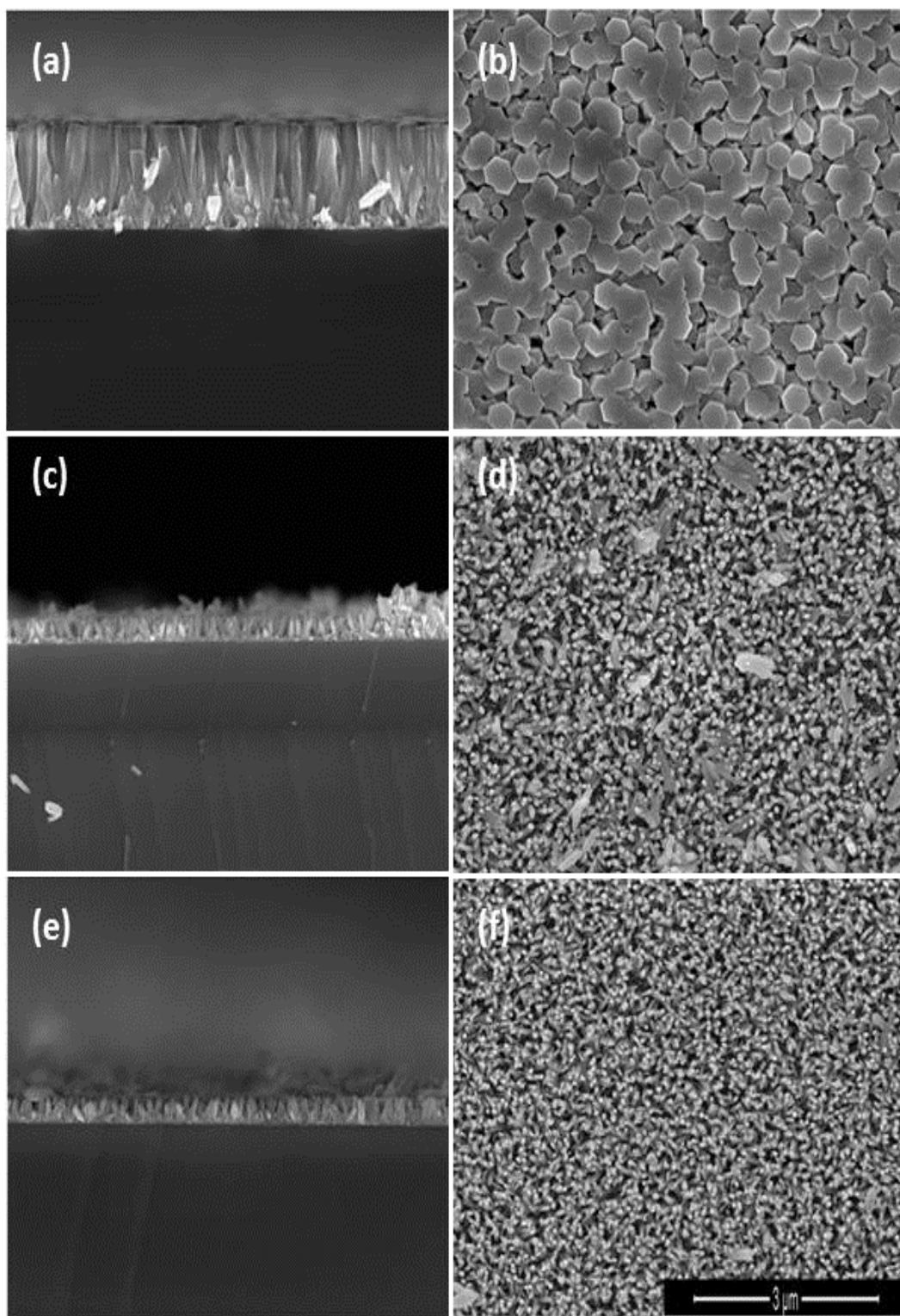


**Figure 3.18.** Cross-sectional SEM images of the annealed samples grown with (a) zinc acetate dihydrate salt, (c) zinc chloride salt, (e) zinc nitrate hexahydrate salt. Top view SEM images of the samples grown with (b) zinc acetate dihydrate salt, (d) zinc chloride salt and (f) zinc nitrate hexahydrate salt. Magnifications are 40000x.



### 3.6.2. Microwave Heating with Non-annealed Substrates

Figure 2.19 shows the length and diameter of ZnO nanowires grown with different zinc salts. Figure 2.20 shows cross-sectional and top-view SEM images of ZnO nanowires grown on non-annealed substrates within solutions containing different zinc salts by applying microwave heating. Similar to the use of annealed substrates, top view SEM images show that ZnO nanowires grown with zinc acetate dihydrate salt have flat tips. They seem to be nucleated very densely due to higher diameter of ZnO nanowires compared to others grown other salts, as shown in the Figure 2.20. The ZnO nanowires grown with zinc nitrate hexahydrate have slightly longer length and almost the same diameter compared to the ones grown with zinc chloride salt. Similar to the use of annealed substrates, cross-sectional SEM images reveal that ZnO nanowires grown with zinc chloride and zinc nitrate hexahydrate salts have tapered tips.

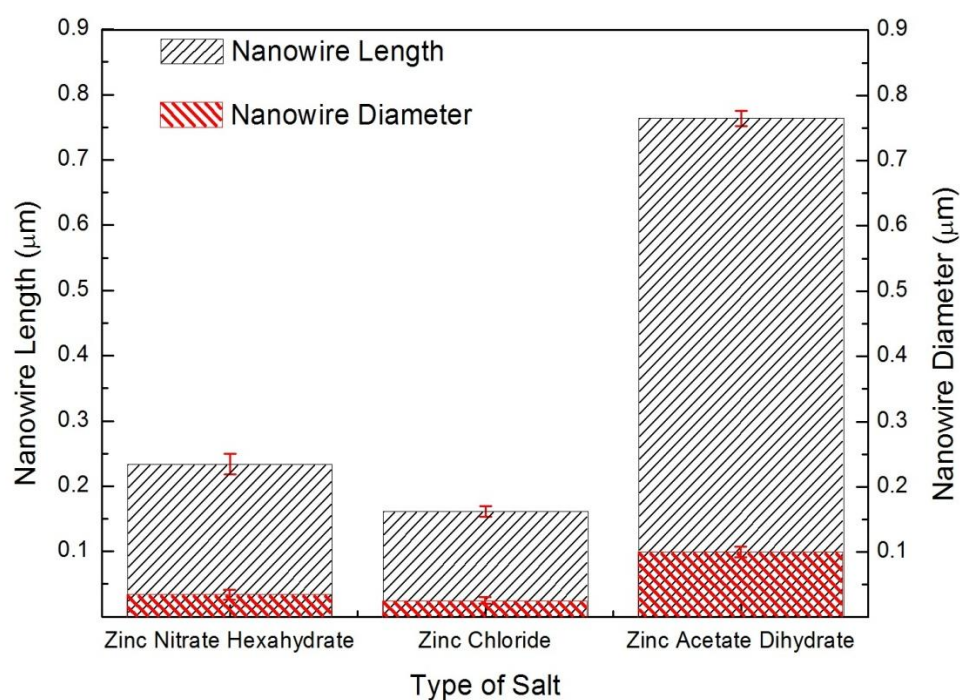


**Figure 3.19.** Variation of length and diameter of ZnO nanowires grown with different salts using non-annealed substrates.

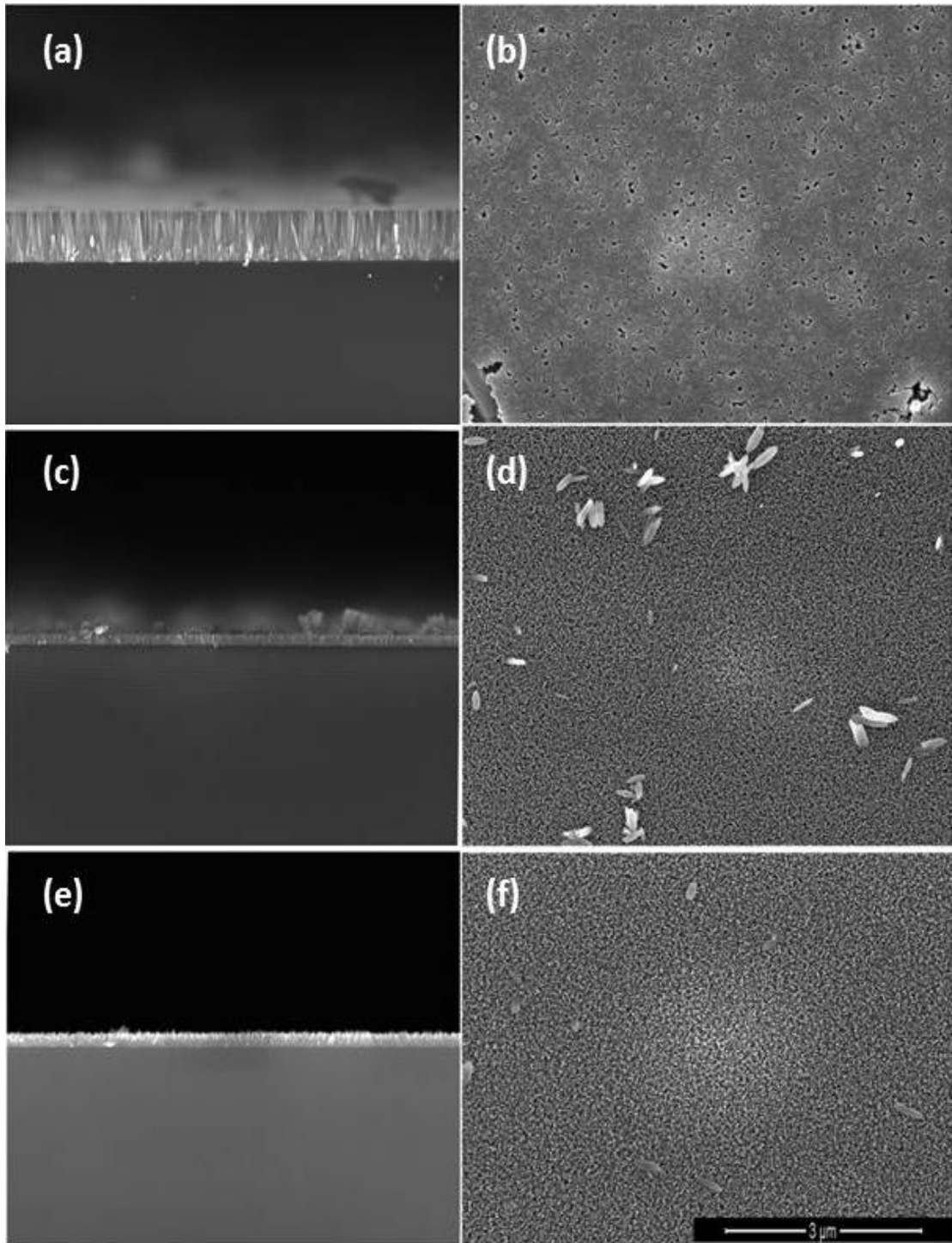


**Figure 3.20.** Cross-sectional SEM images of the non-annealed samples grown with (a) zinc acetate dihydrate, (c) zinc chloride and (e) zinc nitrate hexahydrate salt. Top view SEM images of the samples grown with (b) zinc acetate dihydrate (d) zinc chloride and (f) zinc nitrate hexahydrate salt. Magnifications are 40000x.

### 3.6.3. Comparison of Microwave Heating with Conventional Heating

Microwave heating has some advantages compared to conventional heating. Hydrothermal synthesis of ZnO nanowires can be carried out with microwave heating in 3 minutes (with renewing growth solution after every one minute) in a 2.45 GHz kitchen microwave oven compared to the 2 to 3 hour conventional heating of the growth solutions for obtaining ZnO nanowires with similar lengths. Interestingly, microwave heating leads to ZnO nanowires with tapered tips in solutions containing zinc chloride and zinc nitrate hexahydrate solutions while ZnO nanowires grown in the solution containing zinc acetate dihydrate have flat tips. It was reported by Sun et al. [41] that ZnO nanowires with tapered tips tend to form when overall reduction of  $\text{Zn}^{+2}/\text{OH}^-$  ratio with the increasing time for the growth of ZnO nanowires. In our case, reaction time for the growth of ZnO nanowires is equal for each solution containing different zinc salts. The very fast formation of ZnO in the solutions containing zinc chloride and zinc nitrate hexahydrate leads to sudden decrease in  $\text{Zn}^{+2}/\text{OH}^-$  ratio compared to the solution containing zinc acetate dihydrate, close to the end of each one minute long microwave heating period. This condition is also related to existence of higher amount of  $\text{Zn}^{+2}$  ions in the solution containing zinc acetate dihydrate compared to solutions containing zinc chloride and zinc nitrate hexahydrate. Thus, higher  $\text{Zn}^{+2}/\text{OH}^-$  ratio close to the end of each one minute long microwave heating period leads to formation of ZnO nanowires with flat tips with zinc acetate dihydrate. In addition, annealing of seeds leads to the formation of longer and larger diameter ZnO nanowires.

## CHAPTER 4

### DETERMINATION of HYDROTHERMAL GROWTH PARAMETERS USING ZINC ACETATE DIHYDRATE SALT

#### 4.1. Introduction

Three different zinc salts for the hydrothermal growth of ZnO nanowires were investigated and compared. It has been seen that using zinc acetate dihydrate as zinc source leads to formation of ZnO nanowires with highest aspect ratio among all zinc sources. In past studies, zinc acetate dihydrate has been used for seeding substrates but it hasn't been used extensively for growth of ZnO nanowires in the hydrothermal method. A parametric study regarding the use zinc acetate dihydrate as zinc source has been made for determining optimum growth parameters.

#### 4.2. Experimental Details

In this work, silicon (Si) (001) substrates were used to grow ZnO nanowires. All chemicals were purchased from Sigma-Aldrich and Merck and used without further purification. Before the application of hydrothermal growth process, pieces of Si substrates were first ultrasonically cleaned, in consecutive acetone (99.8%), isopropanol (99.8) and deionised (DI) water baths (18.3 megaohm) for 10 minutes. Substrates were dried with nitrogen gas. A 5 mM solution of zinc acetate dihydrate in 1-propanol was prepared and used for the deposition of seed layer through spin coating. Right after spin-coating, substrates were annealed at 350°C for 20 minutes to have the ZnO seeds oriented along (002) direction in order to obtain aligned ZnO nanowires. Seeded substrates were then dipped into aqueous solutions of zinc acetate dihydrate ( $\text{Zn}(\text{O}_2\text{CCH}_3)_2(\text{H}_2\text{O})_2$ , 99.0%) and HMTA ( $(\text{CH}_2)_6\text{N}_4$ , 99.0 %) at the set growth temperature and kept for the desired amount of time for the nanowire growth

after heating the growth solutions at oil bath for 20 minutes. The effect of solution concentrations (0.01 – 0.1M) with zinc acetate dihydrate/HMTA concentration ratios of 3:1, 2:1, 1:1, 1:2 and 1:3 were investigated. Growth times up to 3 hours at growth temperatures in the range of (50 to 100°C) were elaborated. At the end of the growth process, substrates were rinsed with DI water and dried with nitrogen gas to remove any residual salts and organic material.

### 4.3. Characterization of Nanowires

XRD spectrum of ZnO nanowires grown at 85°C, for 3 hours at an equimolar zinc acetate dihydrate and HTMA concentration of 0,02 M is shown in Figure 3.1. A strong peak at 34.8° corresponding to (0.002) spacing of the wurtzite structure (JCPDS Card No: 36 – 1451) revealed the preferential alignment of the nanowires on the substrate in their c – axis direction. Figure 3.2 shows the transmittance of the ZnO nanowires grown at 85°C, for 180 minutes at an equimolar zinc acetate dihydrate and HTMA concentration of 0.02 M. In the 3.17 – 6.2 eV photon energy range, almost constant and high transparency in the visible range and a sharp absorption onset at 374 nm is observed. The bandgap of the ZnO nanowires are estimated to be 3.27 eV from the Tauc plot considering the direct bandgap, as shown at the inset of the graph in Figure 3.2. Photoluminescence measurement which is shown in Figure 3.3. revealed strong band edge emission at 3.3 eV without any detectable defect related emission. TEM analysis revealed further structural information. Figure 3.4 shows low resolution TEM image of ZnO nanowires grown using the same growth conditions. HRTEM image is shown in Figure 3.5. with a selected area electron diffraction (SAED) pattern given in the inset. SAED pattern in the zone axis, reveals the single crystalline nature of the wires and their growth in [0001] direction. Furthermore, the labeled lattice spacing of 0.52 nm corresponds to the interlayer spacing of the (0001) planes in the ZnO lattice, as shown in Figure 3.6.

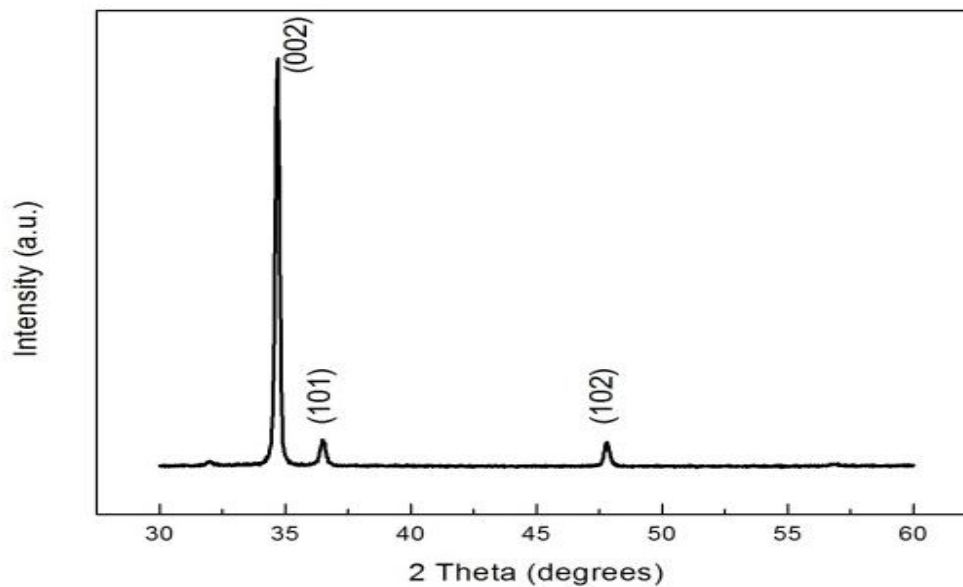


**Figure 4.1.** XRD spectrum from ZnO nanowires grown on silicon substrates.

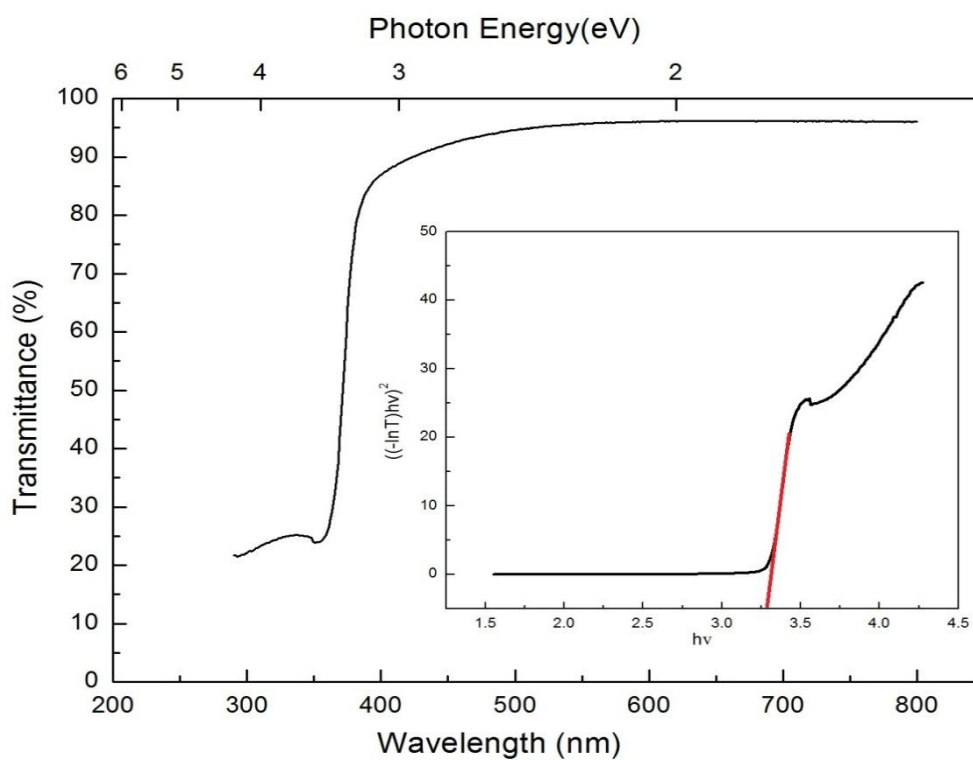


**Figure 4.2.** UV-VIS transmission pattern of ZnO nanowires grown on quartz substrates. Inset shows the Tauc plot showing the change in  $(\alpha h\nu)^2$  with respect to energy.

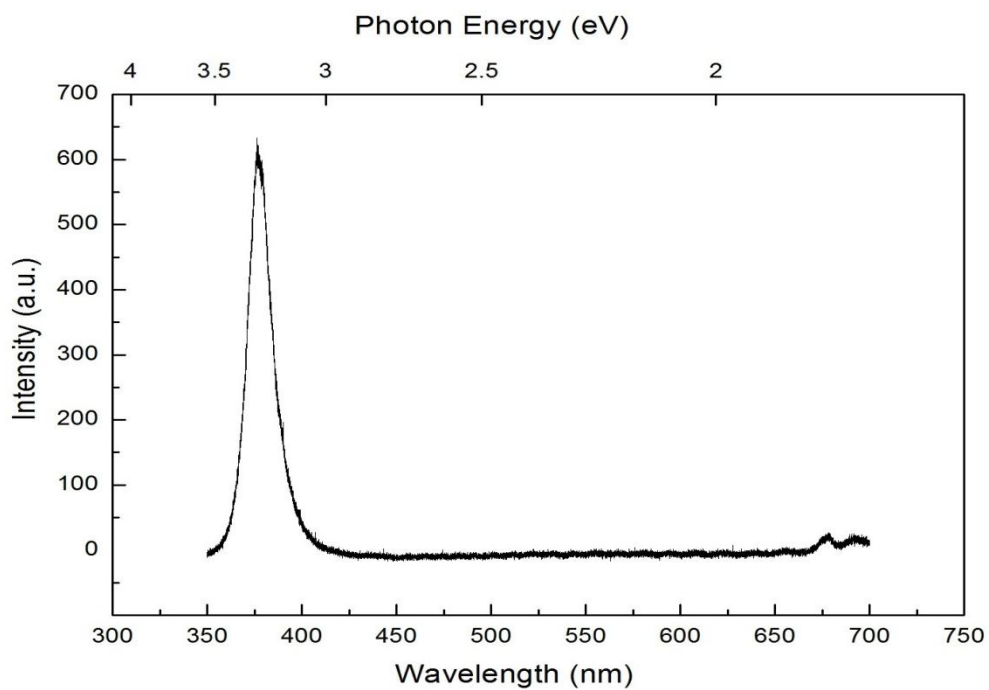


**Figure 4.3.** Photoluminescence spectra from ZnO nanowires grown on silicon substrates.

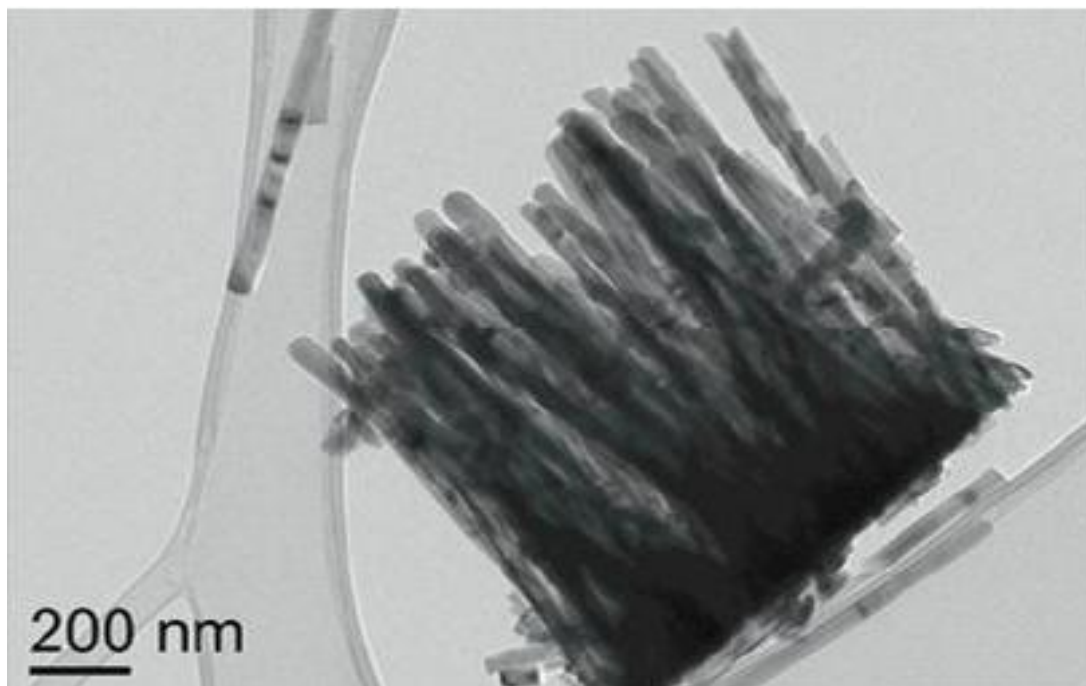


**Figure 4.4.** Bright Field TEM image showing a group of ZnO nanowires at relatively low magnification.

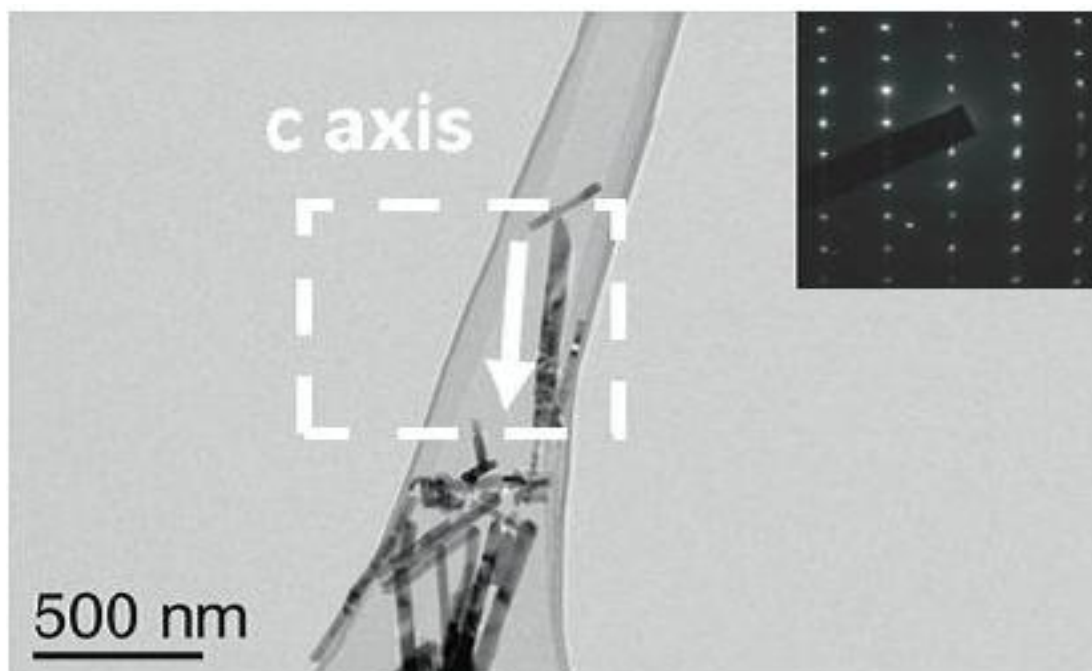


**Figure 4.5.** Bright field TEM image and corresponding SAED pattern (inset) taken from single ZnO nanowire.

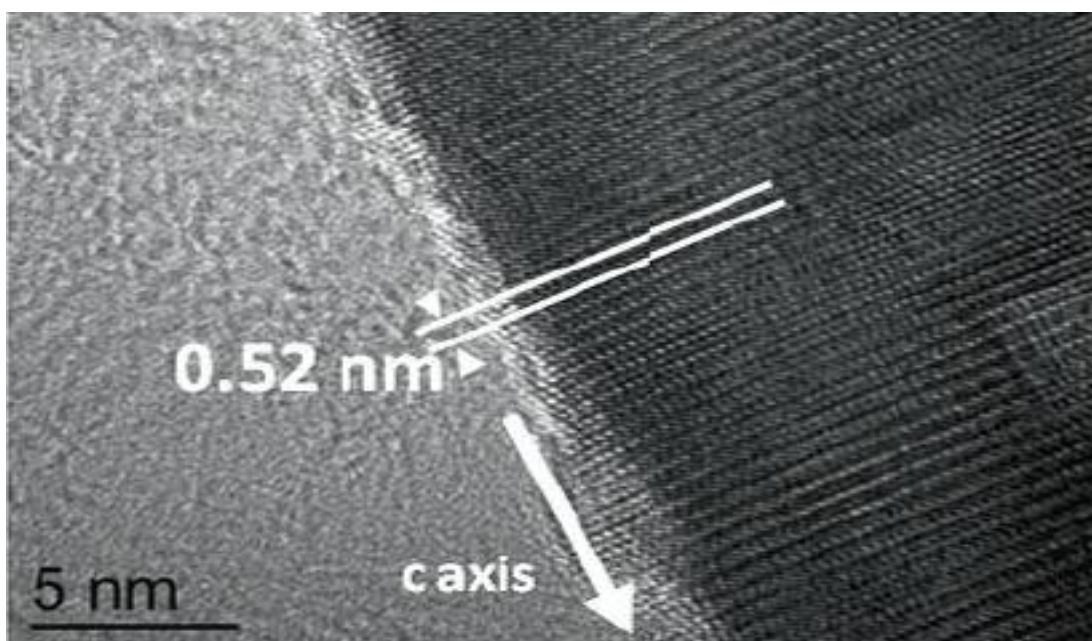


**Figure 4.6.** High resolution TEM image of a single ZnO nanowire showing the lattice fringes along the [0001] growth direction.



## 4.4. Investigation of ZnO Nanowire Hydrothermal Growth Parameters

### 4.4.1. Effect of the Time

Figure 3.7.(a)-(d) shows the cross-sectional SEM images of ZnO nanowires that are grown at 100°C for 40, 80, 160 and 180 minutes respectively. Plot in Figure 3.8, on the other hand shows change in diameter and length of the nanowires with time. The graph at the inset shows change in aspect ratio of the nanowires with time. An equimolar solution for 0,02M zinc acetate dihydrate and HMTA was used to determine the effect of growth time. As shown in Figure 3.8, lengths of the nanowires increase steadily during the reaction period, while their diameter is found to be almost constant. At the end of 180 minutes, perpendicularly aligned nanowires with high aspect ratios (up to 35) were obtained. It has been seen that the use of annealing of seeded substrates leads to formation of ZnO nanowires with higher aspect ratios compared to the use of non-annealed ones. As it is known, adding acetic ions to a solution of zinc nitrate hexahydrate and HMTA lead to highly effective capping effect for growing nanowires with high aspect ratios compared to other capping agents, such as sodium dodecyl sulfate and ethylenediamine [37]. Furthermore, low  $Zn^{+2}/OH^-$  ratios throughout the growth process, as explained in Chapter 2, contributes to formation of ZnO nanowires with high aspect ratio.

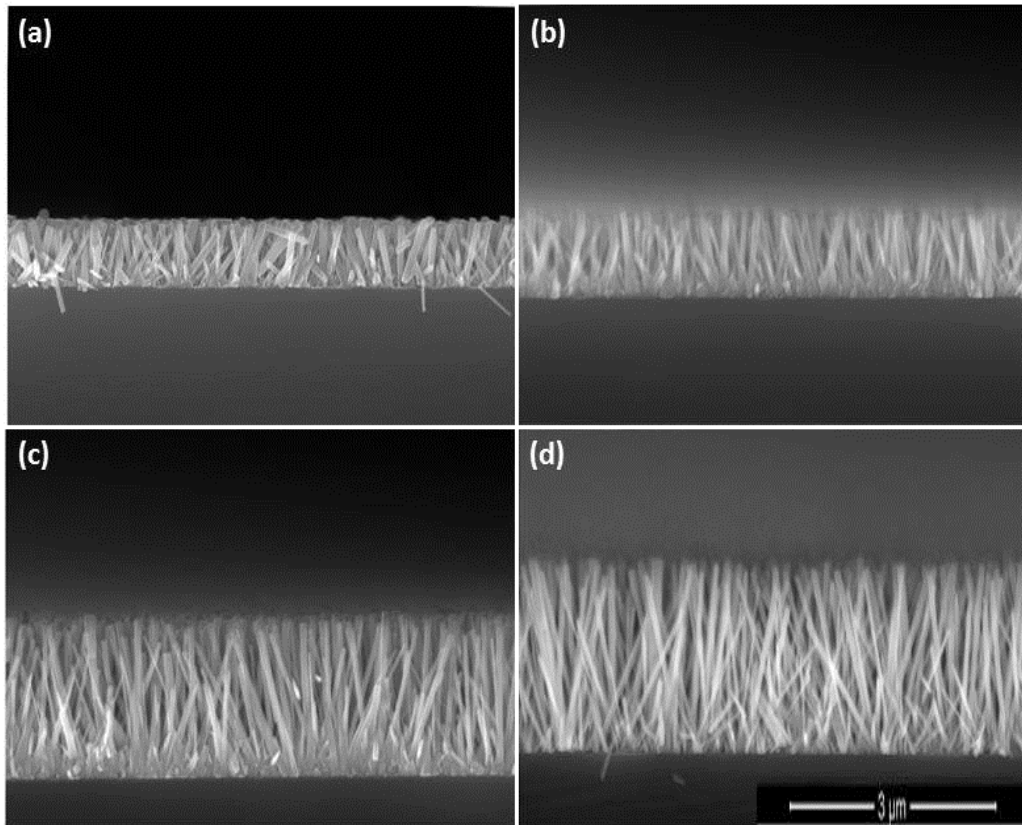


**Figure 4.7.** Cross-sectional SEM images of ZnO nanowires that are grown for (a) 40, (b) 80, (c) 160 and (d) 180 minutes. Magnifications are 40000x.

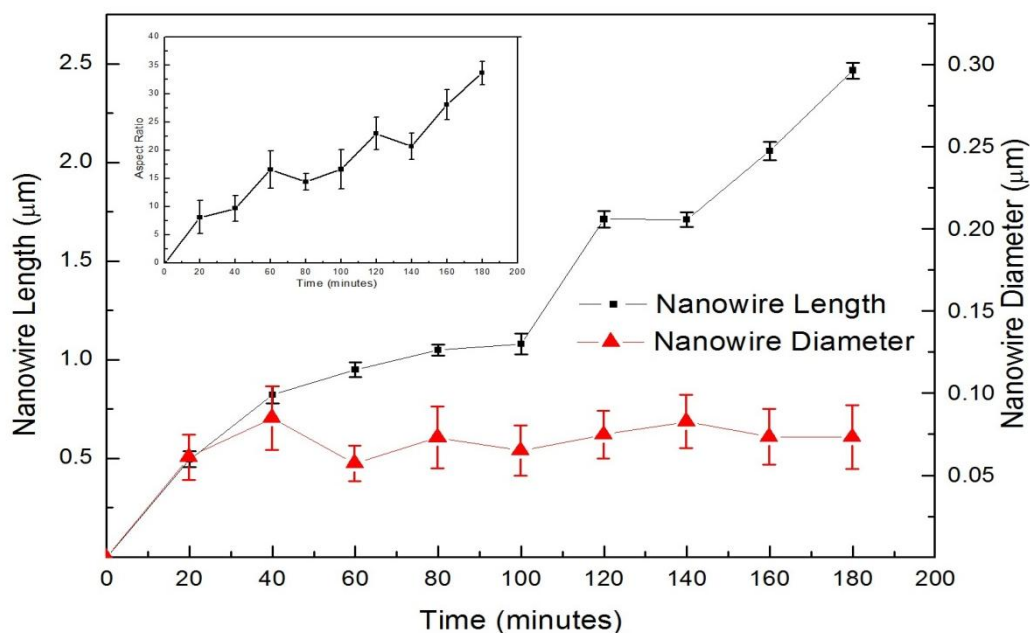


**Figure 4.8.** Variation of the diameter and length of ZnO nanowires with reaction time. Inset shows the variation of aspect ratio of the same samples. Lines are for visual aid.

#### 4.4.2. Effect of the Temperature

Temperature of the growth solution is another factor that has a direct influence on nanowire length and diameter. Figures 3.9 (a)-(f) show the cross-sectional SEM images of ZnO nanowires that are grown at 50, 60, 70, 80, 90 and 100°C, respectively. These nanowires were grown for 3 hours. Plot in figure 3.10. shows the change in the diameter and length of ZnO nanowires as a function of temperature. Lengths of the nanowires increase steadily with temperature, while their diameters are found to be almost constant around 80 nm. Nanowire growth was not observed for the sample kept at 50°C. Short ZnO nanowires were observed, when growth process was conducted at 60°C. This indicates that a temperature in between 50 and 60°C initiates the growth of ZnO nanowires in this method. It is evident that higher temperatures increase the kinetics of the reaction favoring the quick precipitation of ZnO; therefore, resulting in longer and high aspect ratio (up to 55) for nanowires grown at 100°C for 180 minutes) nanowires. This means that as temperature of the reaction increases, the capping effect of acetic ions is getting more prominent. In

addition, the resulting decrease in the  $Zn^{+2}$  concentration and the  $Zn^{+2}/OH^-$  ratio in the solution due to increase in reaction kinetics might also contribute keeping the diameters of the nanowires constant.

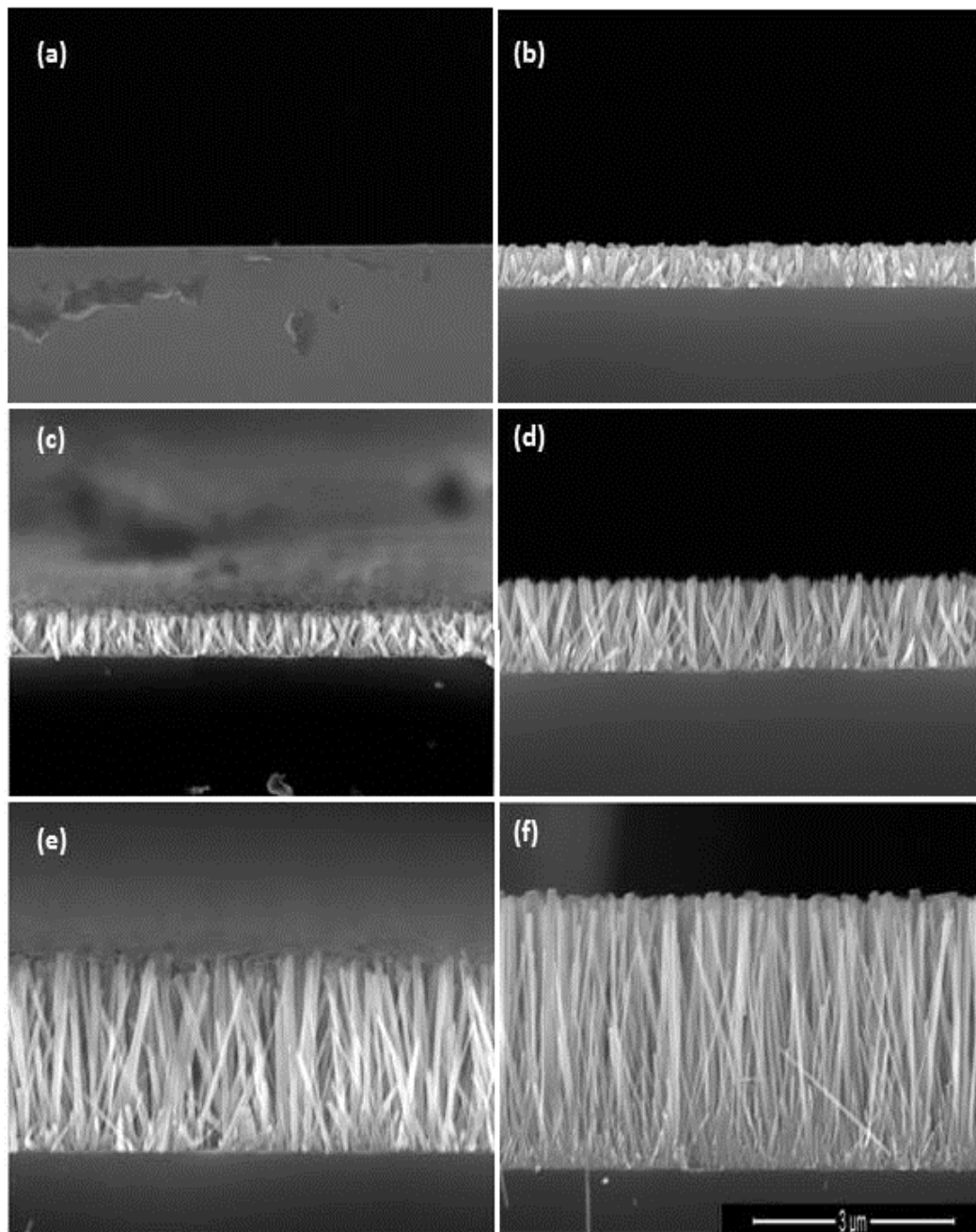


**Figure 4.9** Cross-sectional SEM images of ZnO nanowires that are grown at (a) 50°C, (b) 60°C, (c) 70°C, (d) 80°C, (e) 90°C and (f) 100°C. Magnifications are 40000x.

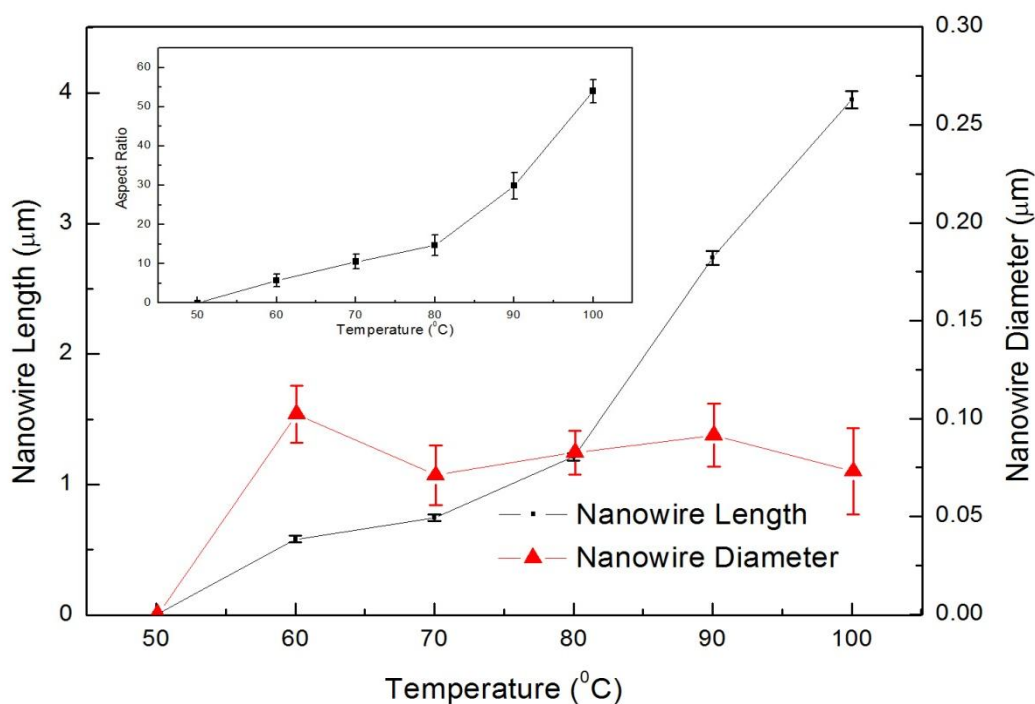
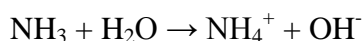
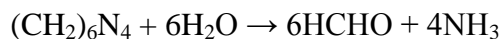


**Figure 4.10.** Variation of diameter and length of ZnO nanowires with temperature. Inset shows the aspect ratio of the samples. Lines are for visual aid.

#### 4.4.3. Effect of the Concentration Ratios on the Growth Process

The effect of different concentration ratios on the diameter and length of ZnO nanowires is plotted at in figure 3.11. Figures 3.12.(a)-(e) show the cross-sectional SEM images of ZnO nanowires that are grown with HMTA and zinc acetate dihydrate solution concentration ratio of 3:1, 2:1, 1:1, 1:2 and 1:3, respectively. Nanowires were grown for 3 hours.. The reactions that are taking place during the ZnO nanowire growth are [37]:



From these reactions, it appears that formation of 1 mol of ZnO product requires a half mole of  $(\text{CH}_2)_6\text{N}_4$  and 1 mole of  $(\text{Zn}(\text{O}_2\text{CCH}_3)_2(\text{H}_2\text{O})_2)$ , which is equivalent to  $[(\text{CH}_2)_6\text{N}_4] / [(\text{Zn}(\text{O}_2\text{CCH}_3)_2(\text{H}_2\text{O})_2)]$  ratio of 1/2. So, we may expect to obtain longest

ZnO nanowires using this ratio. However in our study, longest ZnO nanowires were obtained when [HMTA/Zinc Acetate Dihydrate] ratio was 1. Excess amount of  $(\text{CH}_2)_6\text{N}_4$  provides sufficient amount of  $\text{OH}^-$  ions for the growth of ZnO nanowires in the solution where actual concentration of  $\text{NH}_3$  is less than the nominal concentration. When the ratio of the concentration of Zinc acetate dehydrate is higher, the structure of ZnO deviates from nanowires to a thin film-like form. This condition is related to increase in  $\text{Zn}^{+2}/\text{OH}^-$  concentration ratio which in turn decreases the length and aspect ratio of ZnO nanowires yet increases their diameter. On the other hand, higher HMTA ratios compared to zinc acetate dihydrate led to an increase in the aspect ratio of ZnO nanowires. This is due to the higher availability of  $\text{OH}^-$  ions that leads to formation of more ZnO compared to other concentration ratios.

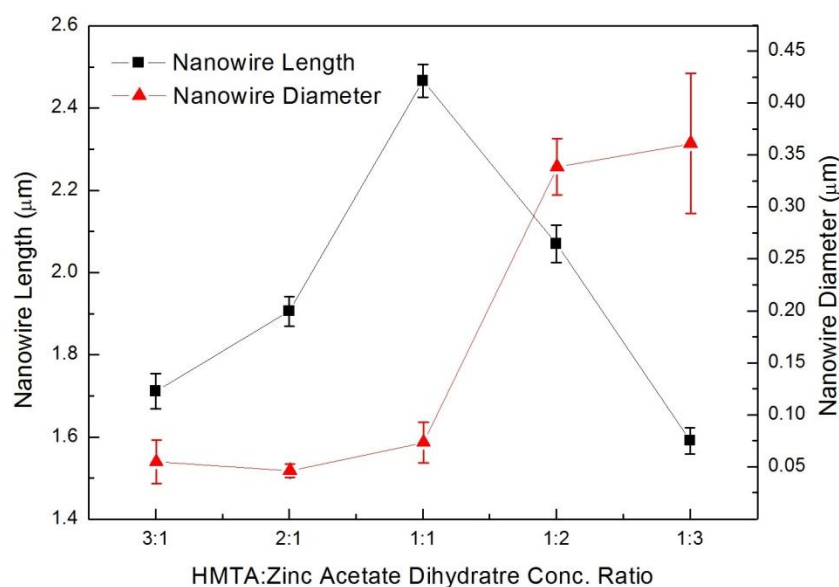


**Figure 4.11.** Graph showing the effect of different solution concentration ratios of HMTA and zinc acetate hexahydrate on the diameter and length of ZnO nanowires. Lines are for visual aid.

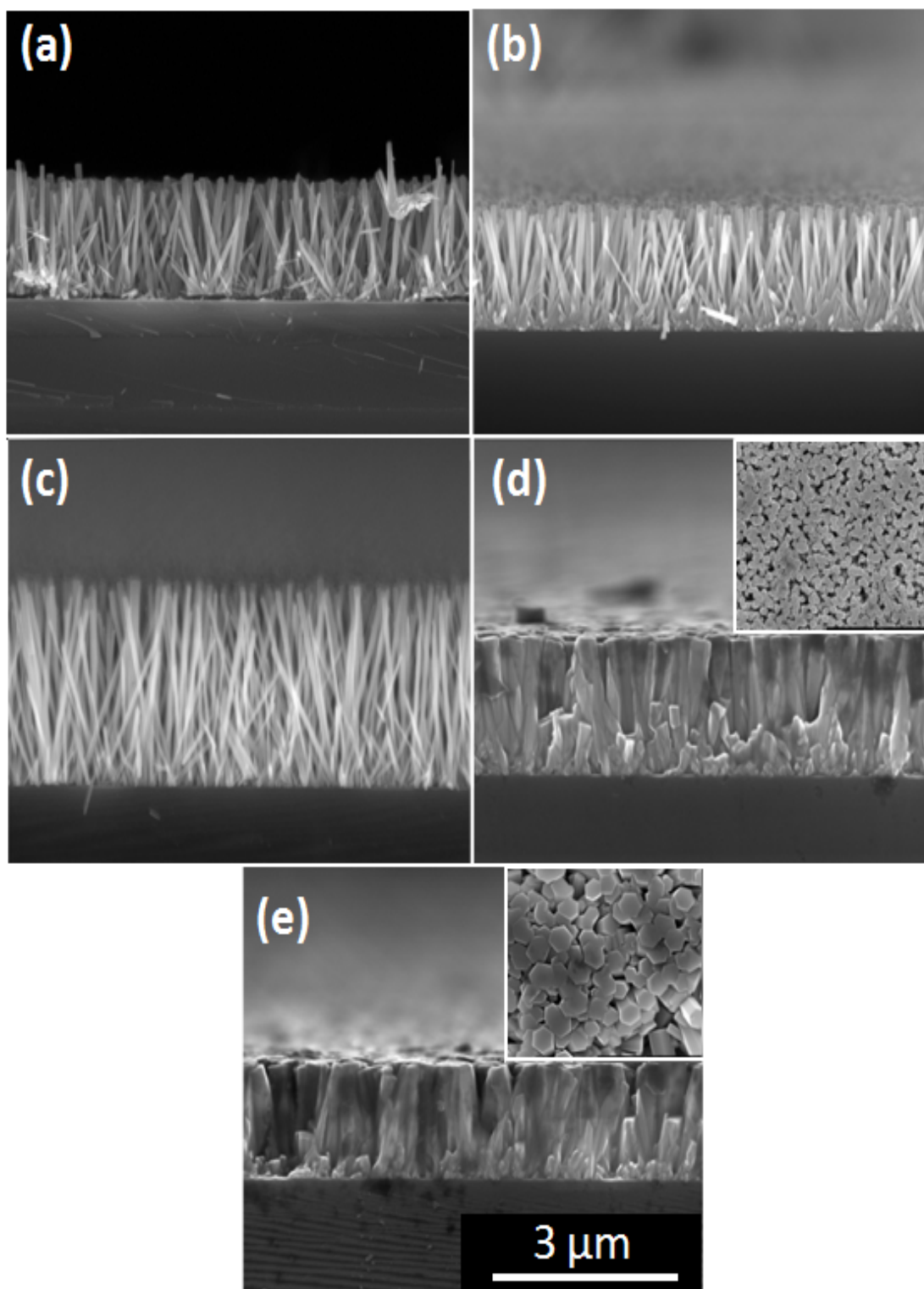


**Figure 4.12.** Cross-sectional SEM images of ZnO nanowires grown with solution concentration ratios of ([HMTA]/[Zinc Acetate Dihydrate]) (a) 3:1, (b) 2:1, (c) 1:1, (d) 1:2 and (e) 1:3. Magnifications are 40000x.

#### 4.4.4. Effect of the Solution Concentration on the Growth Process

Figures 3.13 (a)-(f) shows the cross-sectional SEM images of ZnO nanowires grown in an equimolar ratio of zinc acetate dihydrate and HMTA with concentrations of 0.01M, 0.02M, 0.03M, 0.04M, 0.05M and 0.1M, respectively. The effect of different concentrations on the diameter and length of ZnO nanowires as a function of equimolar concentrations of HMTA and zinc acetate dihydrate is plotted in Figure 3.14. Nanowires were grown at 85 °C. Only a few nanowires are observed on the substrates for the sample grown at a solution concentration of 0.01M. It is clear that the growth of these nanowires was not originated from the seeds on the substrates and they get attached to the substrate during precipitation. Thin and long nanowires with high aspect ratio were observed for a solution concentration of 0.02M. With the increase in solution concentration to 0.05M, an evident increase in the nanowire diameter was observed. This is a result of existence of more  $Zn^{+2}$  ions compared to  $OH^-$  ions in the growth solution which influences the growth of the nanowires from the side planes. A film like morphology was observed for the nanowires grown at a solution concentration of 0.1M. Nanowire features and more prominent hexagonal facets of ZnO can still be seen within the thin film morphology, which clearly indicates the capping effect of acetate ions have been impeded. Optimum concentration was then determined to be 0.02M leading to the growth of high aspect ratio ZnO nanowires.



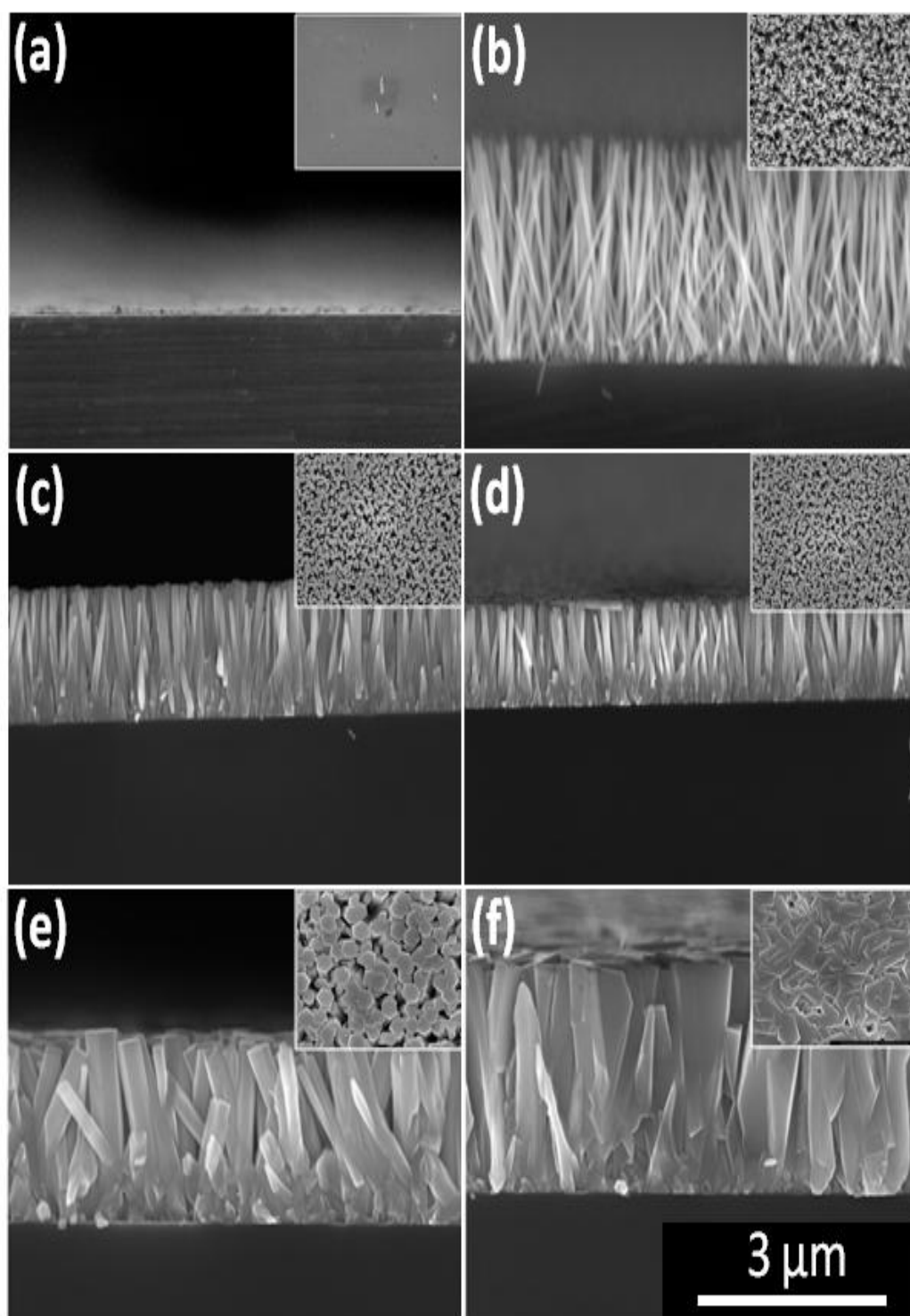


**Figure 4.13.** Cross-sectional SEM images of ZnO nanowires grown in solutions for 180 minutes containing (a) 0.01 M, (b) 0.02 M, (c) 0.03 M, (d) 0.04 M, (e) 0.05 M, and (f) 0.1 M. Inset shows top view SEM images of the samples grown at indicated concentrations. Magnifications are 40000x.

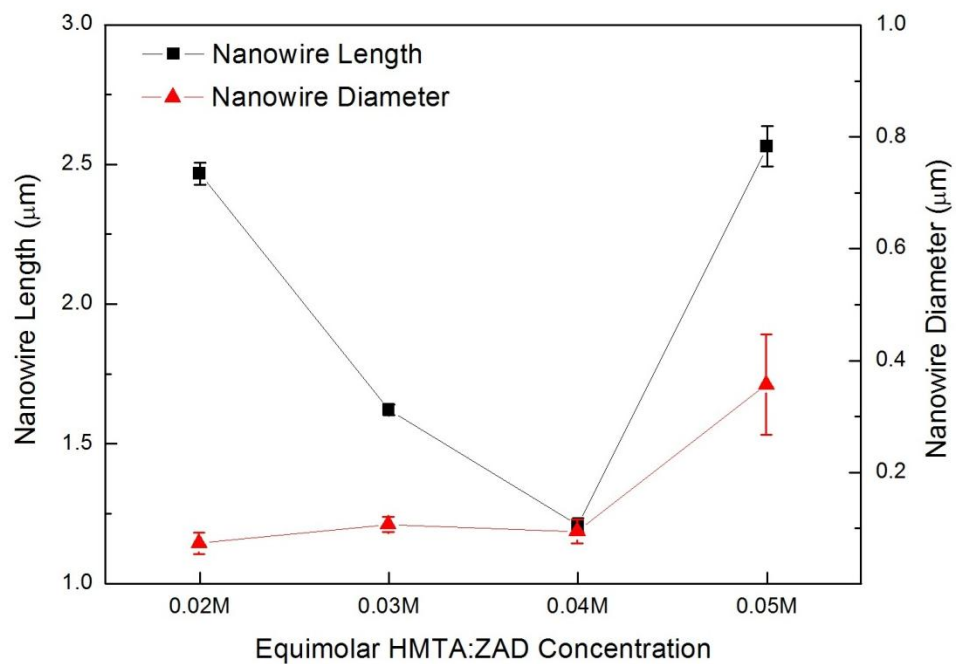


**Figure 4.14.** Graph showing the effect of different equimolar solution concentrations of HMTA and zinc acetate hexahydrate on the diameter and length of ZnO nanowires. Lines are for visual aid.

## CHAPTER 5

### CONCLUSIONS AND FUTURE RECOMMENDATIONS

#### 5.1. Conclusions

This thesis consists of a detailed study on the synthesis of vertically aligned ZnO nanowire arrays with hydrothermal method utilizing three different zinc salts. In addition, a detailed parametric study on hydrothermal synthesis of vertically aligned ZnO nanowires using zinc acetate dihydrate salt is provided.

In the first part; zinc acetate dihydrate, zinc nitrate hexahydrate and zinc chloride salts are used for the synthesis of ZnO nanowires with conventional and microwave heating. Temperature, pH and transmittance of the solution to visible light is monitored for detailed analysis of the growth of ZnO nanowires for hydrothermal synthesis with conventional heating. The results revealed that ZnO nanowires with highest aspect ratio can be synthesized by using zinc acetate dihydrate salt as zinc source. Application of microwave heating to three different zinc salt containing solutions shows the existence of complete precipitation of ZnO in solutions containing zinc chloride and zinc nitrate hexahydrate. For the solution containing zinc acetate dihydrate salt, ZnO nanowires with lower aspect ratio compared to the ZnO nanowires synthesized with conventional heating.

In the second part; ZnO nanowires have been grown using zinc acetate dihydrate as the zinc salt and the effect of growth parameters such as time, temperature, solution concentration and concentration ratios of the precursor chemicals have been determined. The use of zinc acetate dihydrate, which has acetic ions enhances the capping effect and leads to the growth of high aspect ratio nanowires. The length of the nanowires can be controlled through the growth time and solution concentration. On the other hand, the diameter of the nanowires can be controlled by the precursor concentration ratio and solution concentration. A thin film morphology was obtained

through the growth conducted with a high zinc acetate dihydrate concentration as compared to HMTA and at high solution concentrations. Zinc acetate dihydrate salt can be preferred for the hydrothermal synthesis of ZnO NWs, due to its potential for providing high-aspect ratio and high growth rate.

## **5.2. Future Work**

In this thesis, it is proven that ZnO nanowires with desired lengths can be synthesized through hydrothermal growth method. Future work involving growth can be based on application oriented growth which includes template assisted growth, extra-long nanowire growth, morphology control and nanotube growth.

## REFERENCES

- [1] Optical Characterization of interband and intersubband transitions, <http://www.matsceng.ohio-state.edu/~myers/OCL.htm> (Last visited on 23.12.2012)
- [2] Nanomaterials, Nanotechnologies and Design, Nanomaterials: Properties, Elsevier Ltd., 2009.
- [3] “Light emitting diode”, [en.wikipedia.org/wiki/LED](http://en.wikipedia.org/wiki/LED) (Last visited on 23.12.2011)
- [4] M.-T. Chen, “Near UV LEDs made with in situ doped p-n homojunction ZnO nanowire arrays,” *Nano Letters*, **vol. 10**, (Nov. 2010), no. 11, pp. 4387-93,.
- [5] S. J. Jiao, “ZnO p-n junction light-emitting diodes fabricated on sapphire substrates,” *Applied Physics Letters*, **vol. 88**, (2006), no. 3, p. 031911.
- [6] A. Tsukazaki, “Repeated temperature modulation epitaxy for p-type doping and light-emitting diode based on ZnO”, *Nature Materials*, **vol. 4**, (Dec. 2004), no. 1, pp. 42-46.
- [7] Z. P. Wei, “Room temperature p-n ZnO blue-violet light-emitting diodes”, *Applied Physics Letters*, **vol. 90**, (2007), no. 4, p. 042113.
- [8] M.-C. Jeong, B.-Y. Oh, M.-H. Ham, and J.-M. Myoung, “Electroluminescence from ZnO nanowires in n-ZnO film/ZnO nanowire array/p-GaN film heterojunction light-emitting diodes,” *Applied Physics Letters*, **vol. 88**, (2006), no. 20, p. 202105.
- [9] R. Könenkamp, R. C. Word, and M. Godinez, “Ultraviolet electroluminescence from ZnO/polymer heterojunction light-emitting diodes,” *Nano Letters*, **vol. 5**, (Oct. 2005), no. 10, pp. 2005-8.
- [10] X. W. Sun, J. Z. Huang, J. X. Wang, and Z. Xu, “A ZnO Nanorod Inorganic / Organic Heterostructure Light-Emitting Diode Emitting at 342 nm” , *Nano Letters*, **vol. 8**, (2008), pp 1219–1223.
- [11] C.-Y. Chang, “Electroluminescence from ZnO nanowire/polymer composite p-n junction”, *Applied Physics Letters*, **vol. 88**, (2006), no. 17, p. 173503.
- [12] M. H. Huang, “Room-temperature ultraviolet nanowire nanolasers”, *Science* (New York, N.Y.), **vol. 292**, (Jun. 2001), no. 5523, pp. 1897-9.

- [13] “superhydrophobic textile surfaces using zinc oxide nanowires”, <http://www.mete.metu.edu.tr/announcements/news/39/> (Last visited on 01.02.2012)
- [14] G. He and K. Wang, “Applied Surface Science The super hydrophobicity of ZnO nanorods fabricated by electrochemical deposition method”, *Applied Surface Science*, **vol. 257**, (2011), no. 15, pp. 6590-6594.
- [15] E. Garnett and P. Yang, “Light trapping in silicon nanowire solar cells”, *Nano Letters*, **vol. 10**, (Mar. 2010), no. 3, pp. 1082-7.
- [16] M. Law, L. E. Greene, J. C. Johnson, R. Saykally, and P. Yang, “Nanowire dye-sensitized solar cells.” *Nature Materials*, **vol. 4**, (Jun. 2005), no. 6, pp. 455-9.
- [17] S. N. Cha, J. E. Jang, Y. Choi, and G. A. J. Amaratunga, “High performance ZnO nanowire field effect transistor using self-aligned nanogap gate electrodes”, **vol. 89**, (2006), pp. 9-11.
- [18] J. B. K. Law and J. T. L. Thong, “Improving the NH<sub>3</sub> gas sensitivity of ZnO nanowire sensors by reducing the carrier concentration”, *Nanotechnology*, **vol. 19**, (May 2008), no. 20, p. 205502.
- [19] S. Santra, “ZnO nanowires grown on SOI CMOS substrate for ethanol sensing”, *Sensors and Actuators B: Chemical*, **vol. 146**, (Apr. 2010), no. 2, pp. 559-565.
- [20] K. V. Gurav, P. R. Deshmukh, and C. D. Lokhande, “Sensors and Actuators B : Chemical LPG sensing properties of Pd-sensitized vertically aligned ZnO nanorods”, *Sensors & Actuators: B. Chemical*, **vol. 151**, (2011), no. 2, pp. 365-369.
- [22] Z. L. Wang and J. Song, “Piezoelectric nanogenerators based on zinc oxide nanowire arrays” *Science (New York, N.Y.)*, **vol. 312**, (Apr. 2006), no. 5771, pp. 242-6.
- [23] “ZnO nano/piezo-generator: harvesting electricity from Zhonglin's field of nanowires”, [www.scideanews.com](http://www.scideanews.com) (Last visited on 24.12.2011)
- [24] X. W. Sun and H. S. Kwok, “Optical properties of epitaxially grown zinc oxide films on sapphire by pulsed laser deposition”, *Journal of Applied Physics*, **vol. 86**, (1999), no. 1, pp. 408-411.
- [25] M. A. L. Johnson, S. Fujita, W. H. Rowland, Jr., W. C. Hughes, J. W., Cook, Jr., and J. F. Schetzina, “MBE growth and properties of ZnO on sapphire and SiC substrates”, *Journal of Electronic Materials*, **vol. 25**, (1996), pp. 855-862.

- [26] W. Shih and M. Wu, "Growth of ZnO films on GaAs Substrate with a SiO<sub>2</sub> buffer layer by RF planar magnetron sputtering for surface acoustic wave applications", *Journal of Crystal Growth*, **vol. 137**, (1994), pp. 319-325.
- [27] S. Y. Li, C. Y. Lee, and T. Y. Tseng, "Copper-catalyzed ZnO nanowires on silicon (1 0 0) grown by vapor – liquid – solid process", *Journal of Crystal Growth*, **vol. 247**, (2003), pp. 357-362.
- [28] H. J. Fan, "Vapour-transport-deposition growth of ZnO nanostructures : switch between c -axial wires and a -axial belts by indium doping", *Nanotechnology*, **vol. 231**, (2006), pp. 231-239.
- [29] A. Umar, H. W. Ra, J. P. Jeong, E. K. Suh and Y. B. Hahn, "Synthesis of ZnO nanowires on Si substrate by thermal evaporation method without catalyst: Structural and optical properties", *Korean Journal of Chemical Engineering*, **vol. 23**, (2006), pp. 499-504.
- [30] A. Rahm, M. Lorenz, T. Nobis, G. Zimmermann, M. Grundmann, B. Fuhrmann and F. Syrowatka, "Pulsed-laser deposition and characterization of ZnO nanowires with regular lateral arrangement", *Applied Physics A: Materials Science & Processing*, **vol. 88**, (April 2007), pp. 31-34.
- [31] Y. W. Heo, V. Varadarajan, M. Kaufman, K. Kim, D. P. Norton, F. Ren, and P. H. Fleming, "Site-specific growth of ZnO nanorods using catalysis-driven molecular-beam epitaxy", *Applied Physics Letters*, **vol. 81**, (2002), pp. 3046-3049.
- [32] H. Yuan and Y. Zhang, "Preparation of well-aligned ZnO whiskers on glass substrate by atmospheric MOCVD", *Journal of Crystal Growth*, **vol. 263**, (Mar. 2004), pp. 119-124.
- [33] Z. Ye, J. Huang, W. Xu, J. Zhou, and Z. Wang, "Catalyst-free MOCVD growth of aligned ZnO nanotip arrays on silicon substrate with controlled tip shape", *Solid State Communications*, **vol. 141**, (Feb. 2007), pp. 464-466.
- [34] L.E. Greene, M. Law, D.H. Tan, M. Montano, J. Goldberger, G. Somorjai, and P. Yang, "General route to vertical ZnO nanowire arrays using textured ZnO seeds", *Nano Letters*, **vol. 5**, (Jul. 2005), pp. 1231-6.
- [35] S. Xu, C. Lao, B. Weintraub, and Z. Lin, "Density-controlled growth of aligned ZnO nanowire arrays", *Journal of Materials Research*, **vol. 23**, (2008), pp. 2072-2077.
- [36] S.-F. Wang, T.-Y. Tseng, Y.-R. Wang, C.-Y. Wang, H.-C. Lu, and W.-L. Shih, "Effects of Preparation Conditions on the Growth of ZnO Nanorod Arrays Using Aqueous Solution Method", *International Journal of Applied Ceramic Technology*, **vol. 5**, (Sep. 2008), pp. 419-429.

- [37] S. Xu, N. Adiga, S. Ba, T. Dasgupta, C.F.J. Wu, and Z.L. Wang, "Optimizing and Improving the Growth Quality of ZnO Nanowire Arrays Guided by Statistical Design of Experiments.," *ACS Nano*, **vol. 3**, (Jun. 2009), pp. 1803-1812.
- [38] W. Zhang and K. Yanagisawa, "Hydrothermal Synthesis of ZnO Long Fibers", *Chemistry Letters*, **vol. 34**, (2005), pp. 1170-1171.
- [39] L. Li, H. Yang, J. Yu, Y. Chen, J. Ma, J. Zhang, Y. Song, and F. Gao, "Controllable growth of ZnO nanowires with different aspect ratios and microstructures and their photoluminescence and photosensitive properties" *Journal of Crystal Growth*, **vol. 311**, (Aug. 2009), pp. 4199-4206.
- [40] H.E. Unalan, P. Hiralal, N. Rupesinghe, S. Dalal, W.I. Milne, and G. a J. Amaratunga, "Rapid synthesis of aligned zinc oxide nanowires" *Nanotechnology*, **vol. 19**, (Jun. 2008), 5 pages.
- [41] Y. Sun, D.J. Riley, and M.N.R. Ashfold, "Mechanism of ZnO nanotube growth by hydrothermal methods on ZnO film-coated Si substrates", *The journal of physical chemistry. B*, **vol. 110**, (Aug. 2006), pp. 15186-92.
- [42] Y. Lee, T. Sounart, D. Scrymgeour, J. Voigt, and J. Hsu, "Control of ZnO nanorod array alignment synthesized via seeded solution growth", *Journal of Crystal Growth*, **vol. 304**, (Jun. 2007), pp. 80-85.
- [43] Y.-J. Lee, T.L. Sounart, J. Liu, E.D. Spoeke, B.B. McKenzie, J.W.P. Hsu, and J. a Voigt, "Tunable Arrays of ZnO Nanorods and Nanoneedles via Seed Layer and Solution Chemistry", *Crystal Growth & Design*, **vol. 8**, (Jun. 2008), pp. 2036-2040.
- [44] Y. Qin, R. Yang, and Z.L. Wang, "Growth of Horizontal ZnO Nanowire Arrays on Any Substrate Growth of Horizontal ZnO Nanowire Arrays on Any Substrate", *Journal of Physical Chemistry C*, **vol. 112**, (2008), pp. 18734-18736.
- [45] Y.-J. Kim, C.-H. Lee, Y.J. Hong, G.-C. Yi, S.S. Kim, and H. Cheong, "Controlled selective growth of ZnO nanorod and microrod arrays on Si substrates by a wet chemical method", *Applied Physics Letters*, **vol. 89**, (2006), p. 163128-3.
- [46] J. Elias, R. Tena-Zaera, and C. Lévy-Clément, "Electrochemical deposition of ZnO nanowire arrays with tailored dimensions", *Journal of Electroanalytical Chemistry*, **vol. 621**, (Sep. 2008), pp. 171-177.
- [47] J. Cui and U. J. Gibson, "Enhanced nucleation, growth rate, and dopant incorporation in ZnO nanowires", *The Journal of Physical Chemistry B*, **vol. 109**, (Nov. 2005), pp. 22074-7.



- [48] S. K. Sharma, A. Rammohan, and A. Sharma, "Templated one step electrodeposition of high aspect ratio n-type ZnO nanowire arrays", *Journal of Colloid And Interface Science*, **vol. 344**, (2010), pp. 1-9.
- [49] H. Fan, "Well-ordered ZnO nanowire arrays on GaN substrate fabricated via nanosphere lithography", *Journal of Crystal Growth*, **vol. 287**, (Jan. 2006), pp. 34-38.
- [50] S. H. Lee, "Control of the ZnO nanowires nucleation site using microfluidic channels", *The Journal of Physical Chemistry B*, **vol. 110**, (Mar. 2006), pp. 3856-9.
- [51] S. M. Sultan, K. Sun, J. Partridge, M. Allen, P. Ashburn, and H. M. H. Chong, "Fabrication of ZnO Nanowire Device Using Top-Down Approach", *12th International Conference on Ultimate Integration on Silicon (ULIS)*, **vol. 2**, (2011), pp. 4-6.
- [52] H. Nishizawa, T. Tani And K. Matsuoka, "Crystal Growth of ZnO by Hydrothermal Decomposition of Zn-EDTA", *Communication of American Chemical Society*, **vol. 67**, (1984), pp. 98-100.
- [53] L. Vayssieres, "Growth of Arrayed Nanorods and Nanowires of ZnO from Aqueous Solutions", *Advanced Materials*, **vol. 15**, (Mar. 2003), pp. 464-466.
- [54] R. Savu, R. Parra, E. Joanni, B. Jancjar, S. A.Elizariario, R. Camargo, P. R. Bueno, J. A.Varela, E. Longo and M. A. Zaghete, "The effect of cooling rate during hydrothermal synthesis of ZnO nanorods", *Journal of Crystal Growth*, **vol. 311**, (Aug. 2009), pp. 4102-4108.
- [55] K. M. Mcpeak, T. P. Le, N. G. Britton, Z. S. Nickolov, Y. A. Elabd, and J. B. Baxter, "Chemical Bath Deposition of ZnO Nanowires at Near-Neutral pH Conditions without Hexamethylenetetramine ( HMTA ): Understanding the Role of HMTA in ZnO Nanowire Growth", *Langmuir*, **vol. 27**, (2011), pp. 3672-3677.
- [56] J.-Y. Kim, J. W. Cho, and S. H. Kim, "The characteristic of the ZnO nanowire morphology grown by the hydrothermal method on various surface-treated seed layers", *Materials Letters*, **vol. 65**, (Apr. 2011), pp. 1161-1164.
- [57] S. Cho, H. Jeong, D.-H. Park, S.-H. Jung, H.-J. Kim, and K.-H. Lee, "The effects of vitamin C on ZnO crystal formation", *Crystal Engineering Communications*, **vol. 12**, (2010), p. 968.
- [58] J. Hu, Z. Chen, J. Xie, and Y. Yu, "A shortcut hydrothermal strategy for the synthesis of zinc nanowires", *Journal of Physics D: Applied Physics*, **vol. 41**, (Feb. 2008), p. 032004.
- [59] P. K. Sharma, R. K. Dutta, M. Kumar, P. K. Singh, A. C. Pandey, and V. N. Singh, "Highly Stabilized Monodispersed Citric Acid Capped ZnO : Cu<sup>2+</sup>

Nanoparticles : Synthesis and Characterization for their Applications in White Light Generation from UV LEDs”, IEEE Transactions on Nanotechnology, **vol.10**, (2009), pp. 163-169.

- [60] C.-Y. Lee, “Enhanced ultraviolet electroluminescence from ZnO nanowires in TiO<sub>2</sub>/ZnO coaxial nanowires/poly(3,4-ethylenedioxythiophene)-poly(styrene-sulfonate) heterojunction”, Journal of Applied Physics, **vol. 107**, (2010), no. 3, 5 pages.
- [61] C. Pacholski, A. Kornowski, and H. Weller, “Self-assembly of ZnO: from nanodots to nanorods”, *Angewandte Chemie (International ed. in English)*, **vol. 41**, (Apr. 2002), pp. 1188-91.
- [62] L. Wang, K. Chen, and L. Dong, “Synthesis of Exotic Zigzag ZnO Nanoribbons and Their Optical, Electrical Properties”, *Journal of Physical Chemistry C*, **vol. 114**, (2010), pp. 17358-17361.
- [63] C. Badre, T. Pauporté, M. Turmine, and D. Lincot, “A ZnO nanowire array film with stable highly water-repellent properties”, *Nanotechnology*, **vol. 18**, (Sep. 2007), pp. 365705-4.
- [64] J. Nause, “ZnO broadens the spectrum”, *III-Vs Review*, **vol. 12**, (1999), p.28.